Study on Maximum Power Control System for Small Wind Turbine Using Wind Speed Prediction

March 2014

Takahiro Kitajima

◇ ◇ ◇ CONTENTS ◇ ◇ ◇

1 Introduction **1**

2 Maximum Power Control System of Wind Turbine **5**

2.1 Introduction to wind turbine 5

2.2 Mathematical model of wind turbine 8

2.3 Maximum power control system 26

2.4 Proposed maximum power control algorithm 26

2.4.1 Configuration of control system 27

2.4.2 Control algorithm 28

3 Simulation Results of Proposed Control System **31**

3.1 Wind speed data used in simulation 31

3.2 Comparison objects for proposed control system 31

3.3 Control results with precise prediction of wind speed 33

3.4 Discussion for the influence of wind speed prediction error 41

3.5 Control results with persistent model prediction 43

4 Long Term Prediction System of Wind Speed **47**

4.1 Definition of wind speed and direction 49

4.2 Complex-valued neural network 50

4.2.1 Complex-valued neuron of complex-valued neural network . . . 50

4.3 Long-term prediction system of wind speed 51

4.3.1 Complex-BP algorithm 54

4.3.2 Comparison object for proposed wind speed prediction system . 58

4.4 Wind speed prediction results of long term 59

5 Extremely Short Term Prediction System of Wind Speed 77

5.1 Extremely short-term prediction system of wind speed 77

5.2 Wind speed prediction results of extremely short-term 79

6 Conclusions and Future Works 89

6.1 Conclusions 89

6.2 Future works 90

References 93

Publications 99

Acknowledgments 103

CHAPTER 1

Introduction

In recent years, renewable and clean natural energy has attracted much attention as a solution to depletion of fossil fuels and global warming due to the emission of carbon dioxide. Therefore, wind turbines are being rapidly introduced as alternative electric power generation systems using renewable energy worldwide [1]. However, the output of wind turbines fluctuates widely depending on the cube of the wind speed. In particular, the output of small wind turbines located at urban area including houses, apartments, and office buildings is apt to fluctuate because of turbulence [2–4] as well as remote areas [5]. It is said that the wind is usually blowing up to 6 m/s in city area [6]. In such area, it is desired that wind turbines efficiently convert wind energy to electrical energy [3], [7–9]. Variable speed wind turbines are generally characterized as having higher efficiency than fixed speed wind turbines. Moreover fixed pitch with variable speed wind turbines are becoming more popular for lower installation cost [10].

There are mainly two types of approaches for energy conversion method of wind turbines, efficiently. One method is research works approaching from a structure design of a wind turbine [2], [11], [12]. In the one of the researches, Y. Ohya *et al.* propose a wind turbine with flanged diffuser [13]. Since the diffuser concentrates the wind flow to the wind turbine, the wind turbine can generate more electrical power about four times to five times compared to without the diffuser.

The other method is approached from a control field of a wind turbine. And there are a variety of maximum power control method to improve power generation efficiency. In those preceding researches, hill climbing methods are usually used [14]. A maximum power point tracking control with hill climbing of variable step for rotational speed is proposed to track ramp variation of wind speed from 0 m/s to 12 m/s [15]. As other

hill climbing methods, variable step of load resistance and duty cycle are presented in [16], [17] respectively. In those methods, there are two serious problems with hill climbing method which significantly decreases performances under rapidly changing wind speed [18]. The one is that a large step size causes oscillations around a maximum power point for fast tracking. The second is misleading of hill climbing by wind speed changing, because the direction of the climbing is decided only by the increase or decrease of generating power. Therefore [18] proposed a control algorithm based on searching the nonunique optimal power curve in online depending on the wind speed, and use it as a reference for control to improve those problems. Here, a fast tracking control is desired because of the large inertia moment of wind turbines compared with photovoltaic systems. Reference [19] focuses on reduction the influence of the inertia moment of the wind turbines by employing a proportional controller for fast control performance. Also, J. Chen *et al.* proposed fasten maximum power point tracking method by using aerodynamic power observer [20]. In those preceding researches, the control systems use only current information such as wind speed, rotational speed, current, and voltage, and operate wind turbines.

Until now, the wind speed prediction systems from 10 minutes to several hours ahead for applying to operation of power system and wind turbine control have been studied. Those prediction system are consisted by using a complex-valued neural network (called here, CVNN) [21], a real-valued neural network (called here, RVNN) [22], or self-tuning fuzzy reasoning [23]. And the effectiveness of the proposed systems is confirmed. The prediction system consisting of the CVNN can take into account wind dynamics in two dimensional space by expressing wind data as a vector, which has both magnitude and direction, because the CVNN has a good ability for treating a complex-value. Due to that kind of the capability of the CVNN, improvement of prediction accuracy was seen comparing with a prediction system using the RVNN.

In this dissertation, a novel approach of maximum power control system for small wind turbines in wind variability environment by using predicted wind speed data is proposed. After confirming the validity of the proposed wind turbine control system, a wind speed prediction system by using a CVNN is proposed. To extract maximum power from wind turbines, it is necessary that the rotational speed of wind turbines should be adjusted at optimal point in the real time [15]. However wind turbines have a large inertia compared to the inertia of the generator [24]. Therefore the time lag of the

rotational speed control will occur in environment with turbulence. The features of the proposed control system are to use future information which is predicted wind speed and to set a reference trajectory of the rotational speed of the wind turbine based on both the predicted wind speed ahead of a few seconds and the mechanical time constant of the wind turbine. The effect of using the predicted data is that the controller can operate the wind turbine efficiently and stably so that the rotational speed of the wind turbine catches up with the reference speed at maximum power point. Then, variable speed control of wind turbine is realized by using power converter control technique. The effectiveness of the proposed control system and the wind speed prediction system are demonstrated by computer simulations in the rest of the dissertation.

The rest of this dissertation is organized as follows. Chapter 2 describes the proposed maximum power control system of wind turbine. The control system is mainly consisted of three parts, which are wind turbine, controller, electronic load which in this case is a battery. The mathematic model of wind turbine, including torque equation and voltage equation is derived. Then the basic schema of maximum power control, the configuration of control system and control algorithm are introduced. And the simulation results of the proposed control system are shown in chapter 3. In simulation results, there are three comparison objects for the proposed control system to evaluate its performance by using observed real wind speed data.

Chapter 4 describes wind speed prediction system for long-term by using a hierarchical complex-valued neural network. Then the definition of wind data in complex number is introduced. After that, the configuration of a complex-valued neural network and its learning algorithm are explained. Moreover as a comparison object of the proposed wind speed prediction system, a real-valued neural network is shown. Simulation results of proposed and conventional prediction systems are compared to show usefulness and advantage of the proposed prediction system clearly. And then t-test is conducted which is a method to ensure the validity of difference between proposed prediction system and conventional prediction system.

A wind speed prediction system for extremely short-term based on a recurrent complex-valued neural network is introduced in chapter 5. Simulation results of proposed and comparison prediction systems are compared to show usefulness and advantage of the proposed prediction system. Conclusions and perspective to future works are given in the last chapter.

CHAPTER 2

Maximum Power Control System of Wind Turbine

2.1 Introduction to wind turbine

Recently, renewable energy has attracted much attention as a solution to depletion of fossil fuels and global warming such as wind turbines, photovoltaics, and so on. Especially, wind turbines are being rapidly introduced as alternative electric power generation systems using renewable energy worldwide. Figure 2.1 shows cumulative installed wind turbine capacity in the world from 1996 to 2012. From this figure, the total capacity of installed wind turbine quickly increasing is shown in recent years. The total at the end of 2012 was 282.5 GW in the world, nearly 45 GW of new wind turbine installed. Therefore compared 2011 with 2012, annual increasing rate of wind turbine capacity is about 19 %. Figure 2.2 indicates the shares of annual installed wind turbine represented by individual countries in the world 2012. The country with the greatest percentage of installation was USA, and the second country was China. And the two countries accounts for about 60 % of new installed capacity, followed by Germany, India, UK, and Italy, and so on. Thus USA, China, EU account most of new installed wind turbine. In Fig. 2.2, Japan is classified as others country, and accounts for 0.2 % of 45 GW in 2012. Japanese cumulative wind turbine capacity was reached to 2,614 MW in 2012. This represent around 0.5 % of the total power supply in Japan [1]. This is because of element of Japanese topography and restriction of installed areas. And some residents who are neighborhood of large scale wind turbines suffer from low frequency noise of wind turbines. That is why new large scale wind

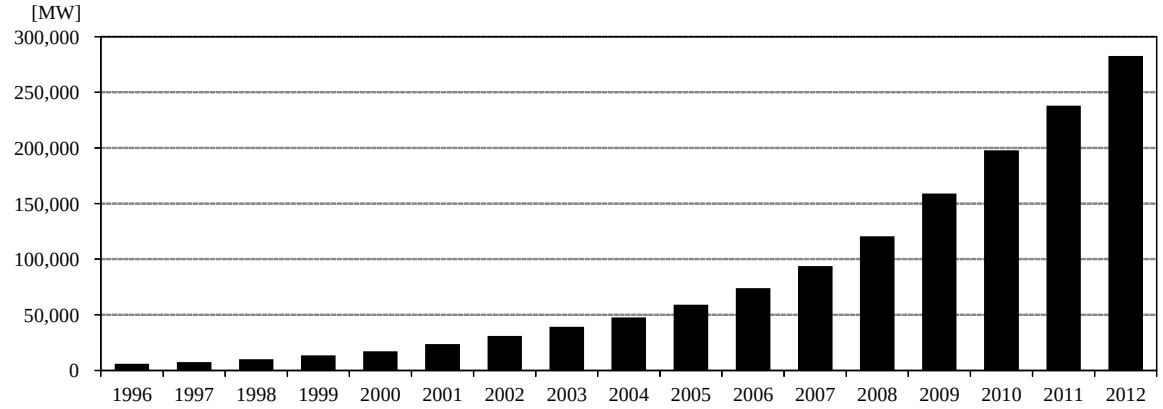

Figure 2.1: Global cumulative installed wind capacity 1996-2012 (GWEC)

turbines are difficult to install any more on land in Japan. Nowadays Japan is steadily moving towards installing wind turbine after the Fukushima accident in March 2011. Then off-shore wind turbine will increase in Japan because Japan has wide area of the sea and wind is stable on the sea comparing with on land. Experimental study of off-shore wind turbine started in Fukushima(2.0 MW), Chiba(2.4 MW), and Fukuoka(2.0 MW) prefecture, Japan in 2013. Installation structure of off-shore wind turbine in Chiba and Fukushima plant is bottom-mounted type, and that of Fukushima plant is floating type which is the first plant in Japan. Through the experimental study, Japan accumulates practical know-how in off-shore wind turbines. In addition, small wind turbine as shown in Fig. 2.3 will also increase as distribution power plant in urban area. Therefore small wind turbine can be emergency power supply when disaster occur such as earthquake, typhoon, and so on.

As mentioned above, the installation of wind turbine will grow in the future is expected. However, the output of wind turbines fluctuates widely depending on the cube of the wind speed. Therefore, if a lot of large scale wind turbines are connected to the power grid, some problems such as frequency change occur and affect stable power supply. Because the amount of electrical power supply and demand can not balance and then the generator of power plant absorb and release its rotational energy for trying to balance the electrical energy. Also, the output of small wind turbines located at urban area including houses, apartments, and office buildings is apt to fluctuate because of turbulence [2], [3] as well as remote areas [5]. In such area, it is desired that wind turbines efficiently convert wind energy to electrical energy [3]. Here, the

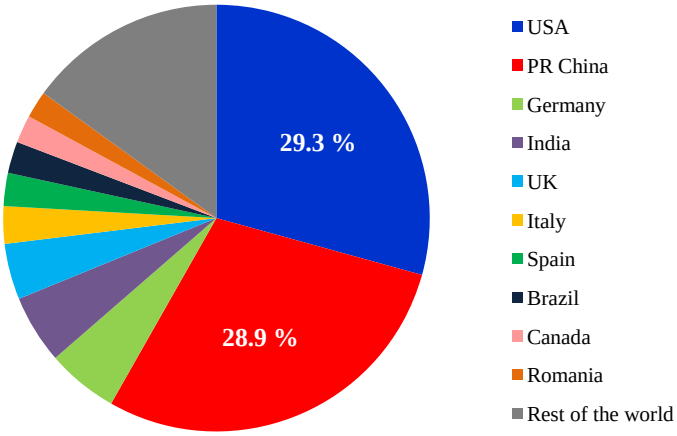

Figure 2.2: The share of new installed wind turbine capacity represented by individual countries (GWEC)

definitions of small wind turbine are that diameter of blades is up to 7 m and the output of wind turbine is not exceeding 20 kW. In a variety of types of wind turbines, a propeller typed three blades of horizontal axis wind turbine is popular in terms of its performances comparing with vertical axis type. Variable speed wind turbines are generally characterized as having higher efficiency than fixed speed wind turbines. Moreover fixed pitch with variable speed wind turbines are becoming more popular for lower installation cost [10]. To resolve those tasks for large scale and small wind turbines, wind speed prediction techniques is used.

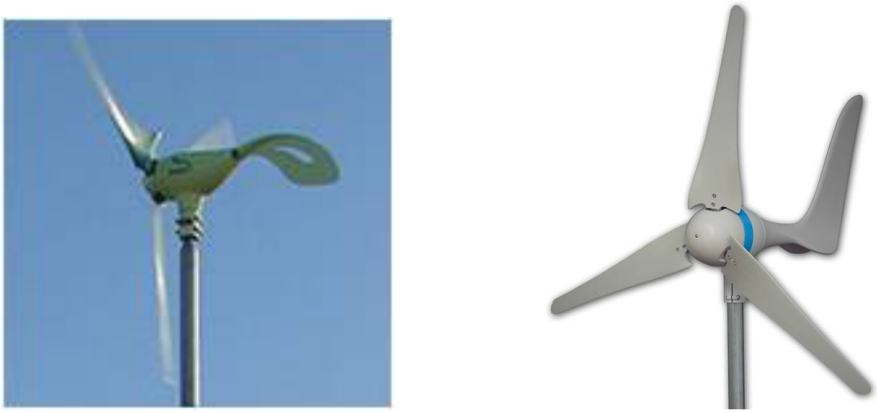

(a) Airdolphin
(Zephyr corporation)
https://www.zephyreco.co.jp

(b) Air doragon
(Sunforce products Inc.)
http://www.sunforceproducts.com

Figure 2.3: Examples of small wind turbines

2.2 Mathematical model of wind turbine

Figure 2.4 shows a generation system of wind turbine which consists of three main parts. The rotor of the wind turbine converts wind energy to rotational energy of the rotor, and the rotational energy is transmitted to the DC generator (called here, DCG). Then the DCG supplies a battery (E_b =24 V) including an internal resistance (R_b =1 Ω) with electrical power. Recent years, small wind turbines generally employ a synchronous generator. Then the AC generator can be driven by vector control system which operate a AC motor as like a DC motor. Therefore it is the reason why a DC generator in this research for easier simulation program is chose. Supply power for the battery is regulated by a power convert controller which consists of a typical boost chopper.

Figure 2.5 indicates configuration of ideal wind flow model proposed by Betz [26]. Then Betz assumed uniform wind flow v_1 and it decelerates to v_3 by a wind turbine rotor at infinite backward. Since the kinetic energy obtained from the wind turbine rotor is the difference of energy between upper stream v_1 and down stream v_3, the obtained energy P_{wind} is written in the next equation.

$$P_{wind} = \frac{1}{2}m(v_1^2 - v_3^2) = \frac{1}{2}\rho A v_2(v_1^2 - v_3^2) \tag{2.1}$$

where ρ is the air density. From the definition of $m = \rho A v$, all energy from wind power can not be obtained. If all wind energy is absorbed by wind turbine rotor, wind flow will be stopped. And also, if no wind energy is absorbed, wind turbine do not obtain wind energy [26]. It means that obtaining energy from wind needs wind flow at certain

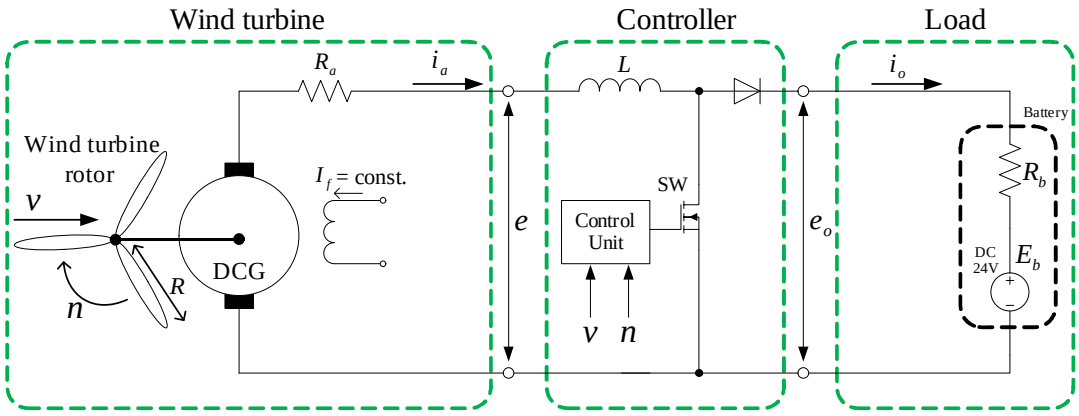

Figure 2.4: Generation system of wind turbine

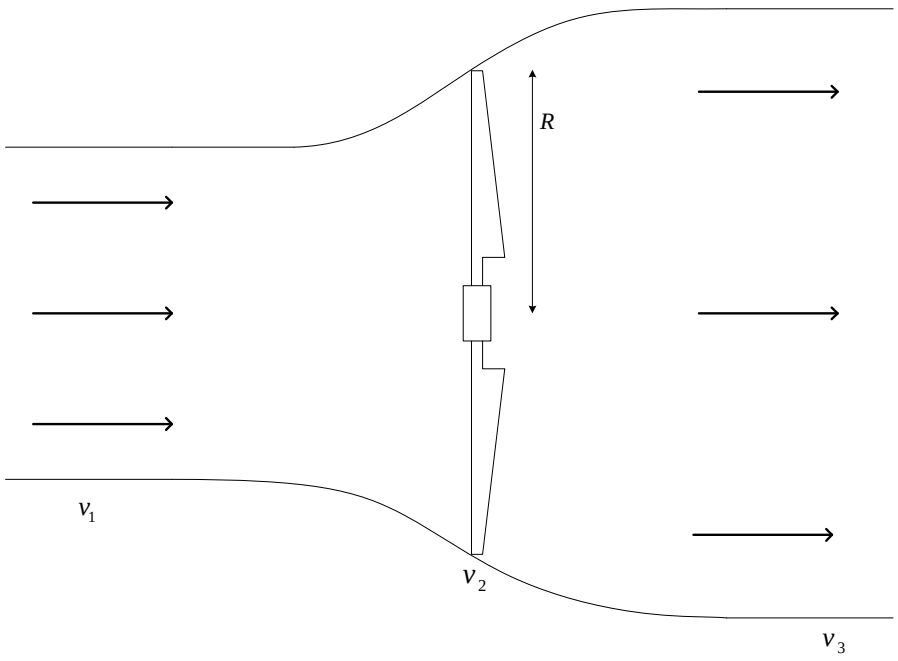

Figure 2.5: Configuration of ideal wind flow model proposed by Betz

rate. Here, v_2 is derived and proved it by Rankine-Froude theory as follow:

$$v_2 = \frac{1}{2}(v_1 + v_3). \tag{2.2}$$

From (2.1) and (2.2), P_{wind} is obtained as:

$$\begin{aligned} P_{wind} &= \frac{1}{2}\rho A v_2 (v_1^2 - v_3^2) && (2.3)\\ &= \frac{1}{2}\rho A \left\{\frac{1}{2}(v_1 + v_3)\right\}(v_1^2 - v_3^2) && (2.4)\\ &= \frac{1}{2}\rho A v_1^3 \frac{1}{2}\left\{1 - \frac{v_3^2}{v_1^2} + \frac{v_3}{v_1} - \frac{v_3^3}{v_1^3}\right\} && (2.5)\\ &= \frac{1}{2}\rho A v_1^3 \left\{\frac{1}{2}\left(1 + \frac{v_3}{v_1}\right)\left[1 - \left(\frac{v_3}{v_1}\right)^2\right]\right\}. && (2.6) \end{aligned}$$

Here, power coefficient of wind turbine C_p is defined as follows:

$$C_p = \frac{1}{2}\left(1 + \frac{v_3}{v_1}\right)\left[1 - \left(\frac{v_3}{v_1}\right)^2\right]. \tag{2.7}$$

From (2.7), C_p is a function of v_3/v_1. The power coefficient C_p is a maximum point when v_3/v_1 equals 1/3 [26]. Then $C_{p\ max}$ is obtained below in theoretically and called Betz limit.

$$C_{p\ max} = \frac{16}{27} = 0.59 \tag{2.8}$$

However $C_{p\ max}$ is usually under 0.45 in practically [25]. From (2.6) and (2.7), wind energy P_{wind} is as follows:

$$P_{wind} = \frac{1}{2} C_p \rho A v_1^3 \tag{2.9}$$

where P_{wind} is generated electric power under a constant wind speed v_1 and means the static characteristics of the wind turbine [27].

The thrust force T_h of wind turbine blade is obtained as follows:

$$T_h = m(v_1 - v_3) = \rho A v_2 (v_1 - v_3) = \rho A \frac{1}{2}(v_1 + v_3)(v_1 - v_3) \tag{2.10}$$

From (2.10) and $v_3 = \alpha v_1$, T_h becomes as follows:

$$T_h = \frac{1}{2} \rho A v_1^2 (1 - \alpha^2) = \frac{1}{2} C_{Th} \rho A v_1^2 \tag{2.11}$$

where $\alpha = v_3/v_1$ and C_{Th} is the thrust coefficient. Therefore wind turbine torque t_w is as follows:

$$t_w = T_h R = \frac{1}{2} C_T \rho A v_1^2 R \tag{2.12}$$

where R is the blade radius of wind turbine and C_T is the torque coefficient of wind turbine. Thus given torque t_w from the wind turbine rotor to the DCG is as indicated below:

$$t_w = \frac{1}{2} C_T \rho \pi R^3 v^2. \tag{2.13}$$

From (2.13), given torque t_w is proportional to the square of wind speed v. And the torque coefficient C_T in (2.13) is approximated by quadratic function of tip speed ratio λ [28] as follow:

$$C_T(\lambda) = \alpha \lambda^2 + \beta \lambda + \gamma \tag{2.14}$$

$$\lambda = \frac{Rn}{v} \tag{2.15}$$

where α, β, and γ are coefficients with constant value respectively, and n is the rotational speed of the wind turbine. Thus λ is ratio of tip speed of wind turbine rotor Rn to wind speed v. Figure 2.6 shows the $C_T(\lambda)$ and the power coefficient of the wind turbine rotor $C_P(\lambda)$. Here, the relationship between power p and torque t, rotational

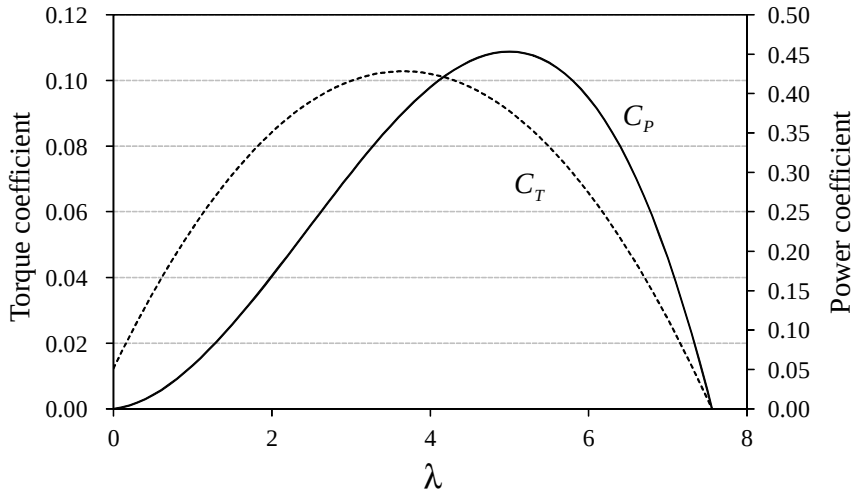

Figure 2.6: Characteristics of torque coefficient $C_T(\lambda)$, and power coefficient $C_P(\lambda)$

speed n is shown as (2.16).

$$p_w = t_w \, n \tag{2.16}$$

From (2.9), (2.13), (2.15), and (2.16), (2.17) is derived.

$$t_w \;\; = \;\; p_w \frac{C_T}{C_P} \frac{R}{v} = t_w n \frac{C_T}{C_P} \frac{R}{v} \tag{2.17}$$

Then the relationship between $C_T(\lambda)$ and $C_P(\lambda)$ by (2.18) [29] is obtained.

$$C_P(\lambda) = C_T \frac{Rn}{v} = \lambda C_T(\lambda) \tag{2.18}$$

Load torque t_{load} is calculated by

$$t_{load} = J \frac{dn}{dt} + F_v n + T_c + K_t i_a \tag{2.19}$$

where J is the inertia moment, F_v is the viscous friction coefficient, T_c is the coulomb friction torque, K_t is the generator torque coefficient, and i_a is the armature current. Voltage equation of the wind turbine generation system can be written as follows;

In the case of SW = Off

$$K_v n = (R_a + R_b) i_o + L \frac{di_o}{dt} + E_b \tag{2.20}$$

Table 2.1: Parameters of wind turbine model

Air density	ρ	1.225	kg/m^3
Blade radius	R	0.95	m
Windmill torque coefficient	α	-0.00676	
	β	0.04945	
	γ	0.01240	
Inertia moment	J	0.312	kgm^2
Viscous friction coefficient	F_v	0.00401	Nm/rad/s
Generator Torque coefficient	K_t	0.432	Nm/A
Coulomb friction torque	T_c	0.10	Nm
Electro motive force	K_v	0.432	V/rad/s
Armature resistance	R_a	0.34	Ω
Inductance	L	3.0	mH
Internal resistance of battery	R_b	1.0	Ω
Battery voltage	E_b	24.0	V

Table 2.2: Mechanical time constant of wind turbine in simulation of Fig. 2.7

Step size	0-3 m/s	0-5 m/s	0-8 m/s	0-10 m/s
Time constant [s]	6.0	3.2	1.9	1.5

In the case of SW = On

$$K_v n = R_a i_a + L\frac{di_a}{dt} \tag{2.21}$$

where K_v is the induced electro motive force, R_a is the armature resistance, L is the inductance, and i_o is the output current. Then brush voltage drop effect is ignored. The details of each parameters are shown in Table 2.1.

Figure 2.7 indicates step response (wind speed v = 3, 5, 8, and 10 m/s) of the wind turbine model. At time = 0 s, the wind changes from 0 m/s to specific wind speed mentioned above. Table 2.2 shows mechanical time constant of the wind turbine calculated from simulation result in Fig. 2.7. From these results, the wind turbine has nonlinear characteristics can be confirmed.

Figures 2.8 $\sim$ 2.11 show the response of wind turbine and load current when sinusoidal wind speed is applied. Then the amplitude of wind speed is 2.5 m/s, the offset of wind speed is 2.5 m/s, the frequency of wind speed changes from 0.02 Hz to

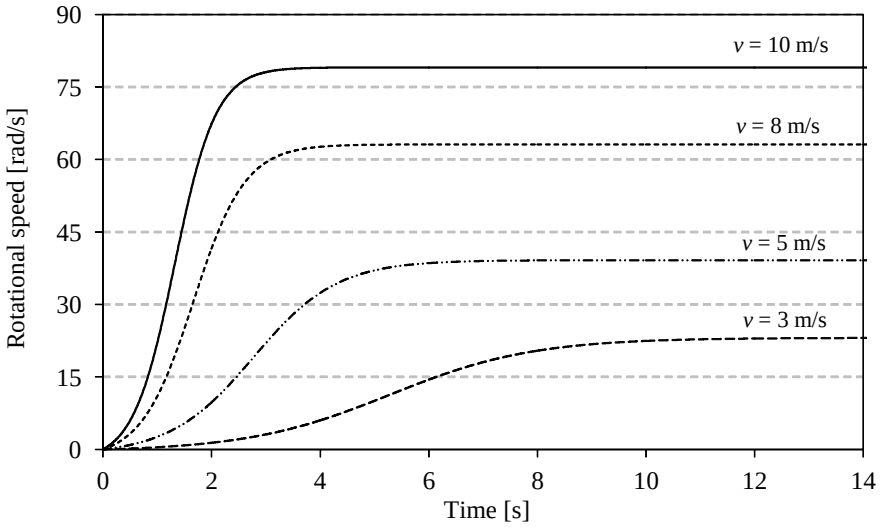

Figure 2.7: Step responses of the wind turbine model

1.00 Hz, the load resistance is 1 Ω. Figures 2.12 ∼ 2.13 show the response of wind turbine at no load condition when sinusoidal wind speed is applied. Then the amplitude of wind speed is 2.5 m/s, the offset of wind speed is 2.5 m/s, the frequency of wind speed changes from 0.02 Hz to 1.00 Hz. Figures 2.14 ∼ 2.17 show the response of wind turbine and load current when sinusoidal wind speed is applied. Then the amplitude of wind speed is 2.5 m/s, the offset of wind speed is 5.0 m/s, the frequency of wind speed changes from 0.02 Hz to 1.00 Hz, the load resistance is 1 Ω. Figures 2.18 ∼ 2.19 show the response of wind turbine at no load condition when sinusoidal wind speed is applied. Then the amplitude of wind speed is 2.5 m/s, the offset of wind speed is 5.0 m/s, the frequency of wind speed changes from 0.02 Hz to 1.00 Hz.

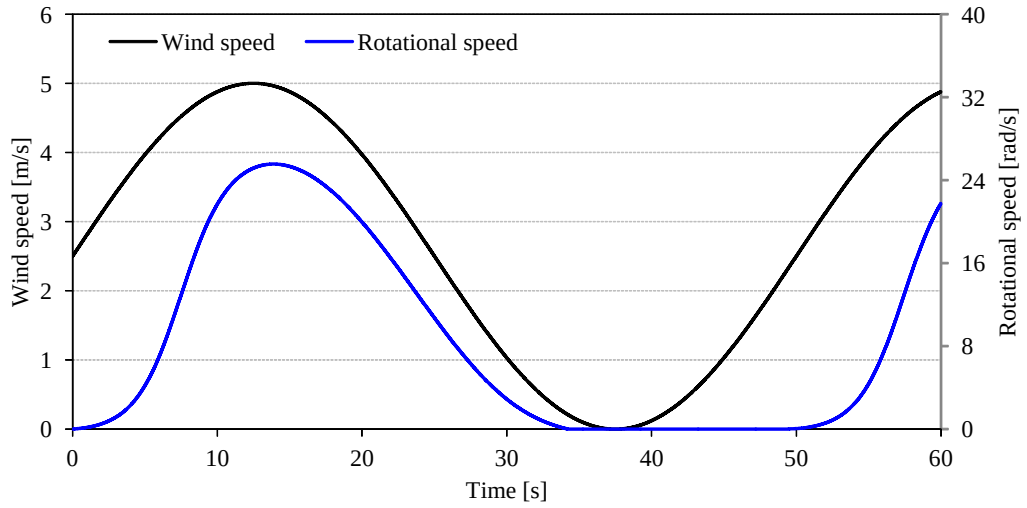

(a) Wind seed and rotational speed

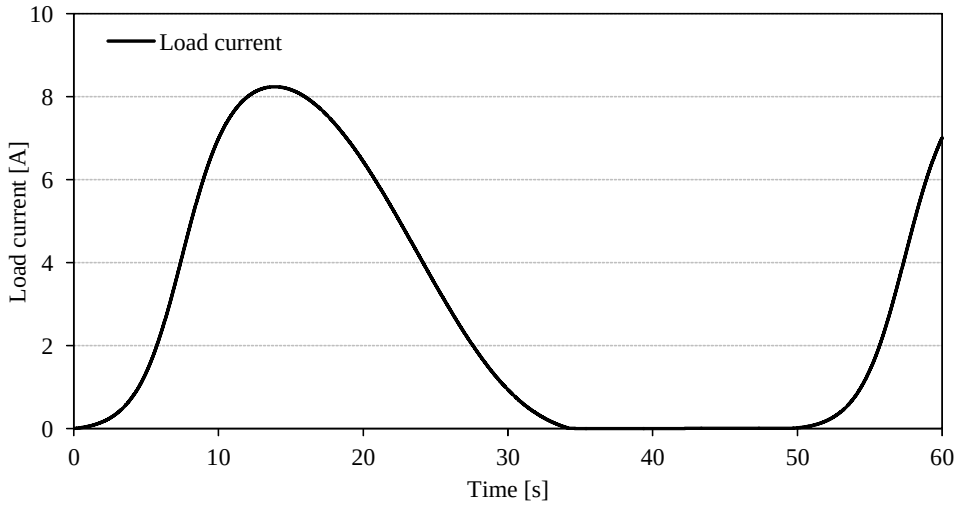

(b) Load current

Figure 2.8: Response of wind turbine for sinusoidal wind data with frequency 0.02 Hz, amplitude 2.5 m/s, and offset 2.5 m/s (Load:R =1 Ω)

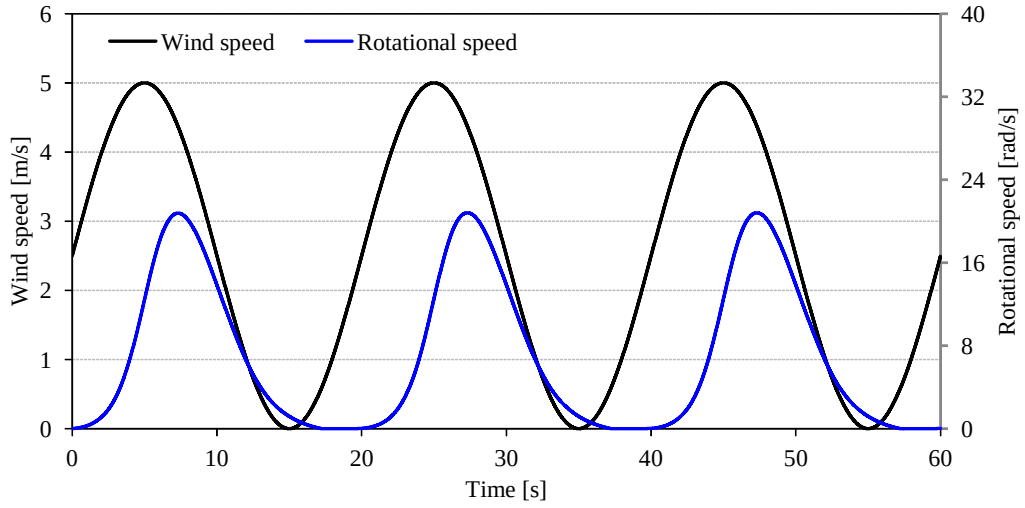

(a) Wind seed and rotational speed

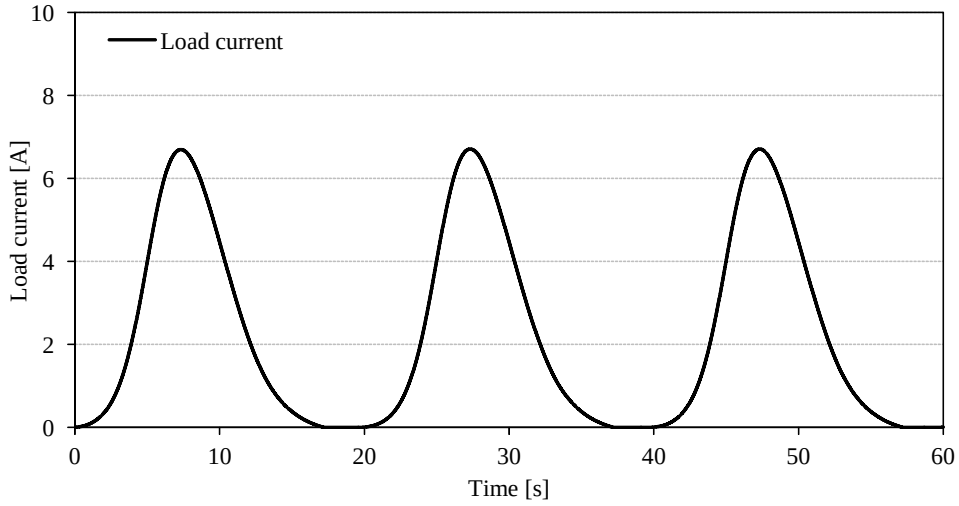

(b) Load current

Figure 2.9: Response of wind turbine for sinusoidal wind data with frequency 0.05 Hz, amplitude 2.5 m/s, and offset 2.5 m/s (Load:R =1 Ω)

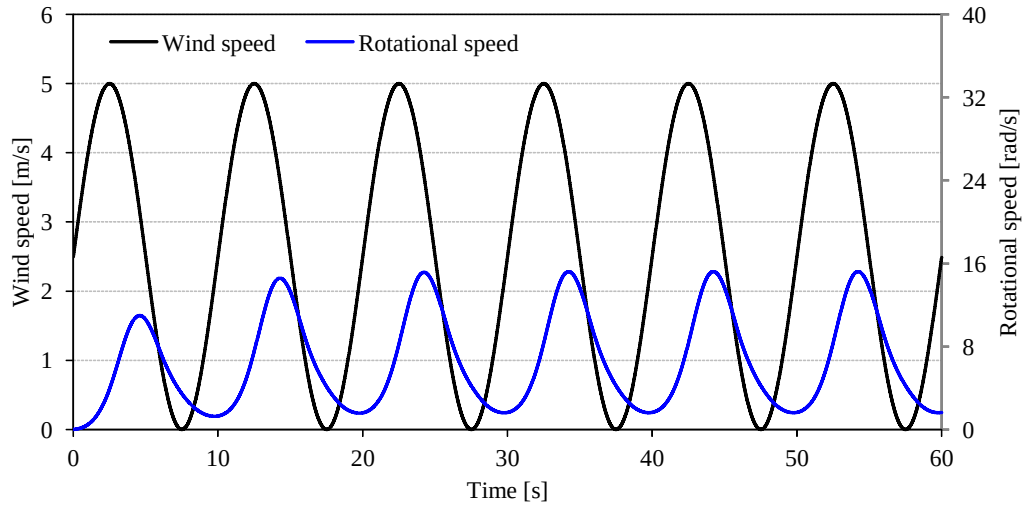

(a) Wind seed and rotational speed

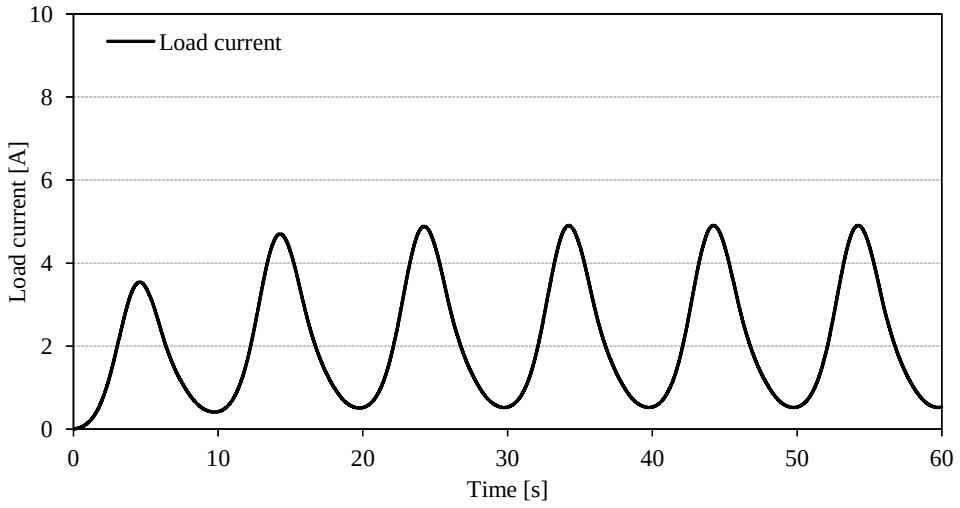

(b) Load current

Figure 2.10: Response of wind turbine for sinusoidal wind data with frequency 0.10 Hz, amplitude 2.5 m/s, and offset 2.5 m/s (Load:R =1 Ω)

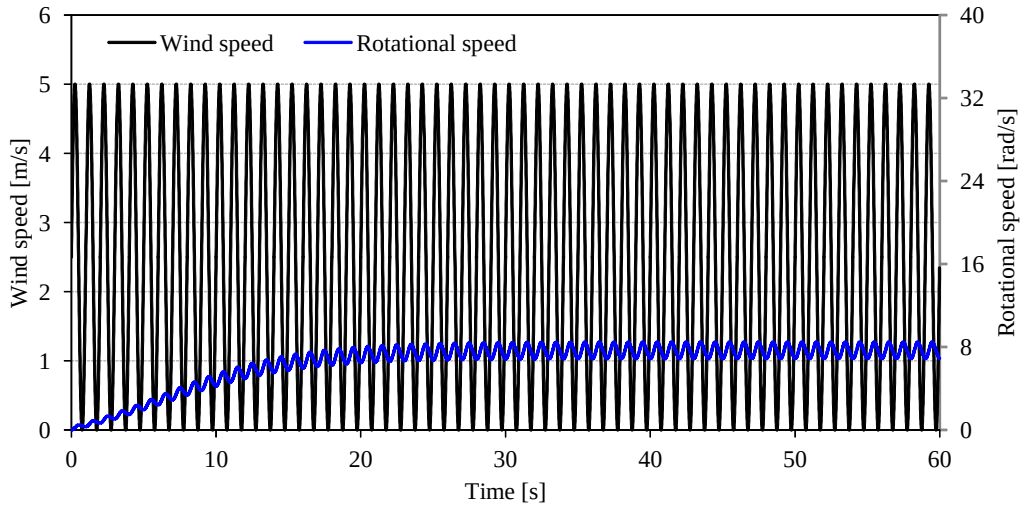

(a) Wind seed and rotational speed

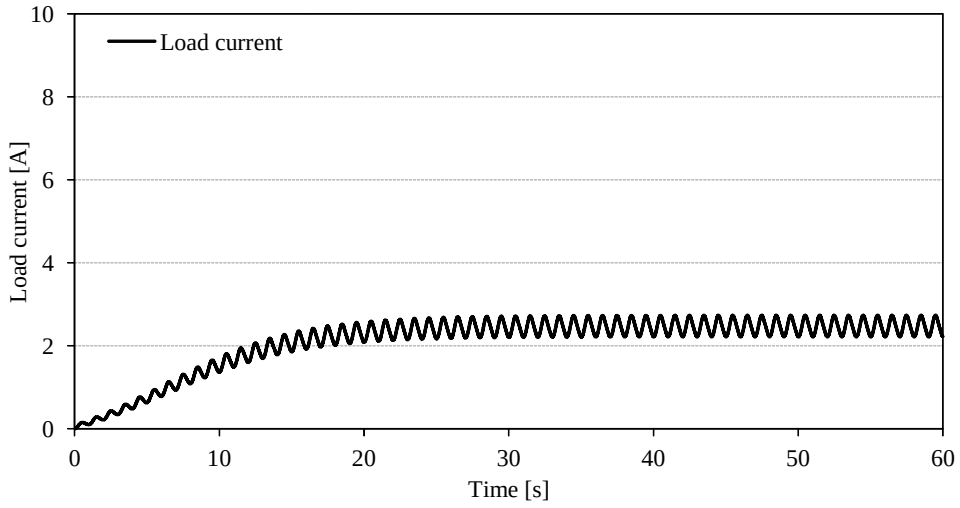

(b) Load current

Figure 2.11: Response of wind turbine for sinusoidal wind data with frequency 1.00 Hz, amplitude 2.5 m/s, and offset 2.5 m/s (Load:R =1 Ω)

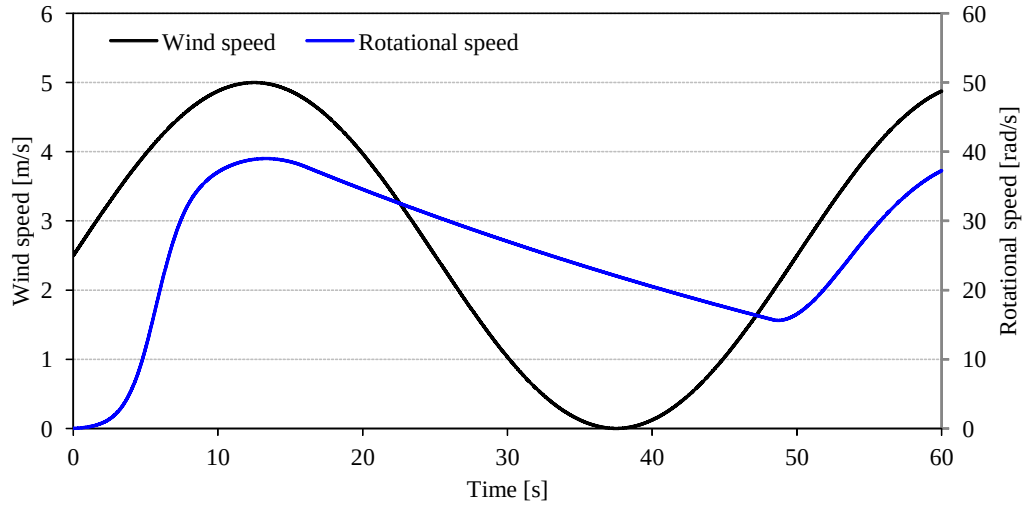

(a) Frequency 0.02 Hz

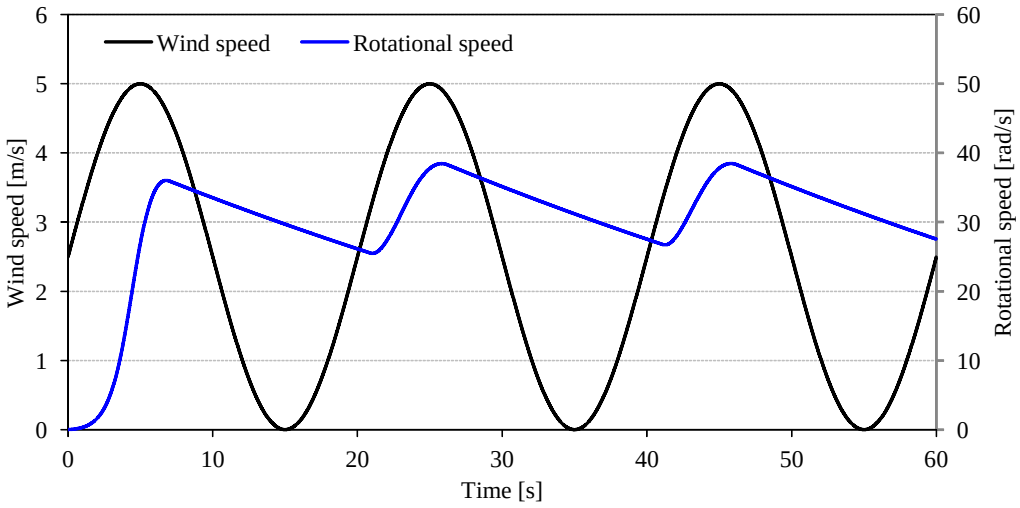

(b) Frequency 0.05 Hz

Figure 2.12: Response of wind turbine for sinusoidal wind data with frequency 0.02 Hz and 0.05 Hz, amplitude 2.5 m/s, and offset 2.5 m/s (No load)

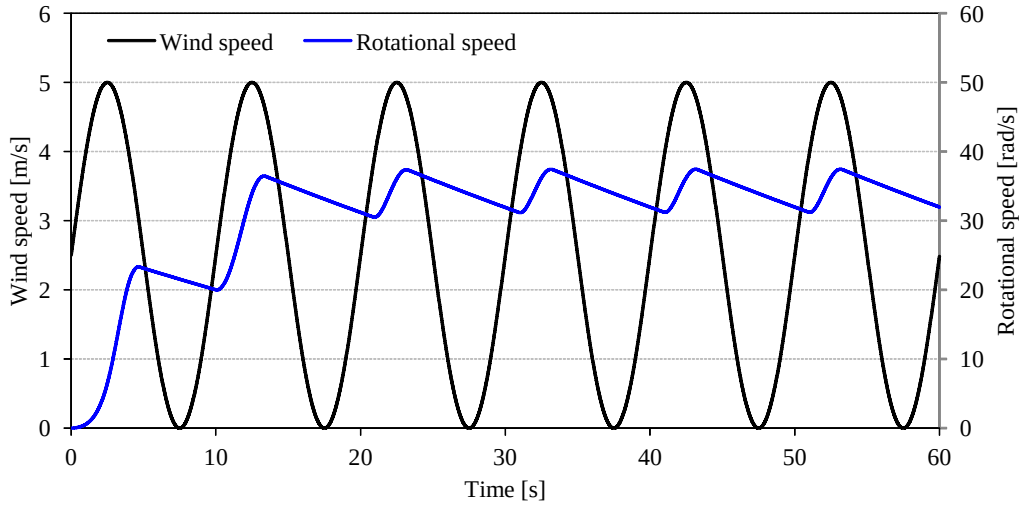

(a) Frequency 0.10 Hz

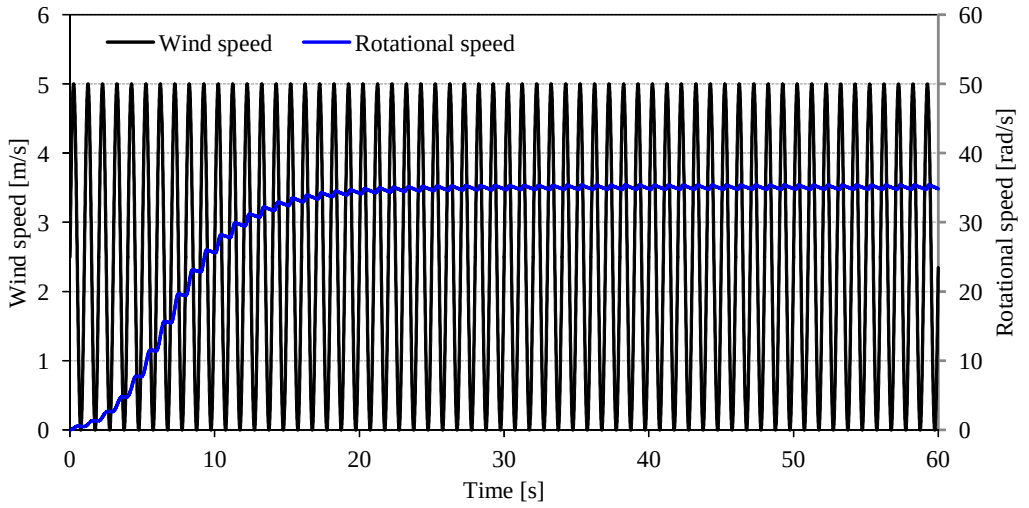

(b) Frequency 1.00 Hz

Figure 2.13: Response of wind turbine for sinusoidal wind data with frequency 0.10 Hz and 1.00 Hz, amplitude 2.5 m/s, and offset 2.5 m/s (No load)

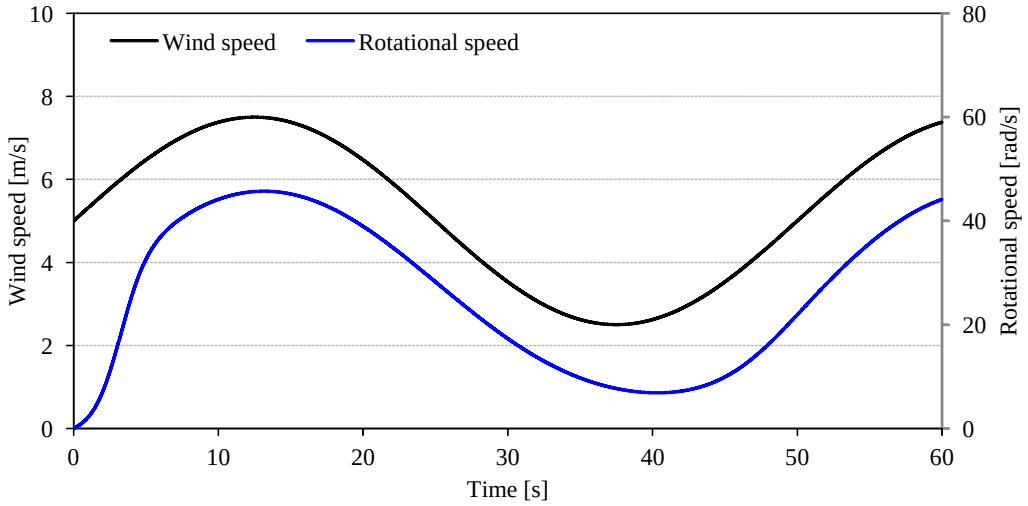

(a) Wind seed and rotational speed

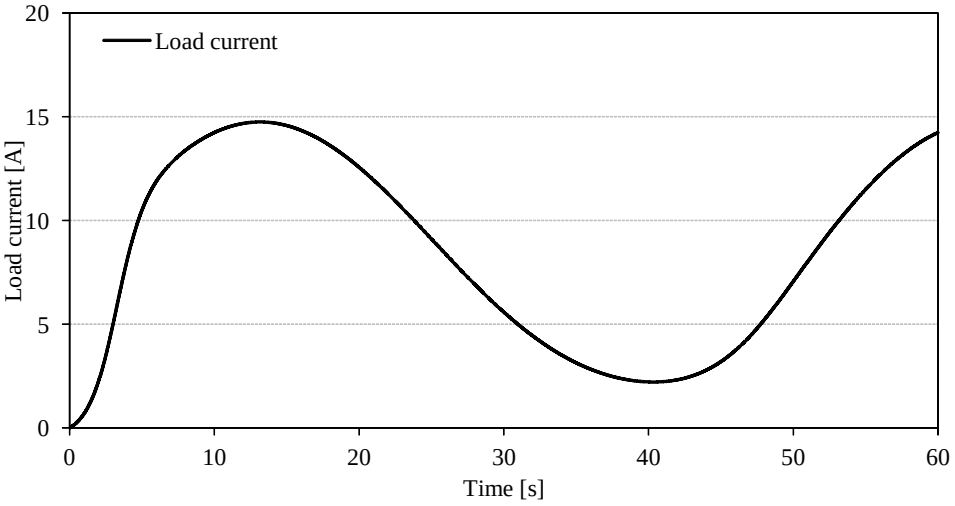

(b) Load current

Figure 2.14: Response of wind turbine for sinusoidal wind data with frequency 0.02 Hz, amplitude 2.5 m/s, and offset 5.0 m/s (Load:R =1 Ω)

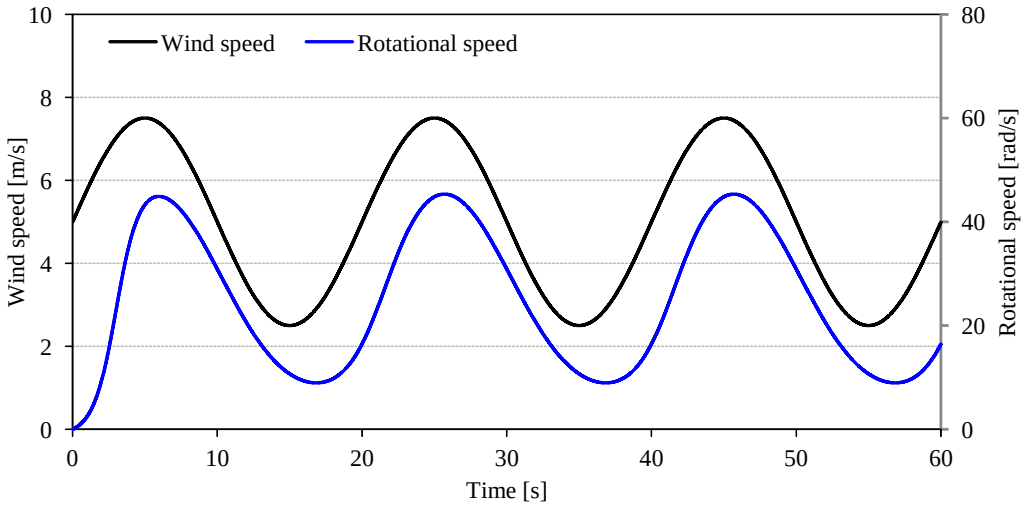

(a) Wind seed and rotational speed

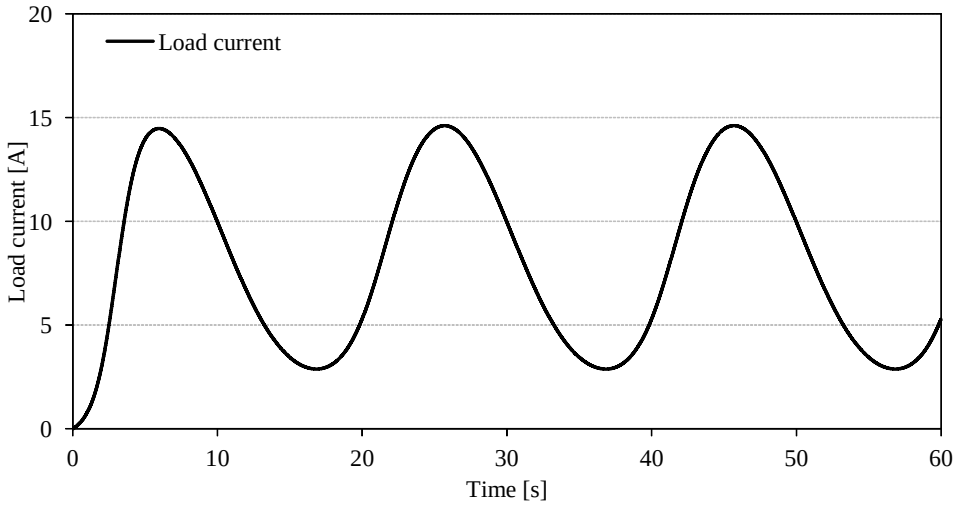

(b) Load current

Figure 2.15: Response of wind turbine for sinusoidal wind data with frequency 0.05 Hz, amplitude 2.5 m/s, and offset 5.0 m/s (Load:R =1 Ω)

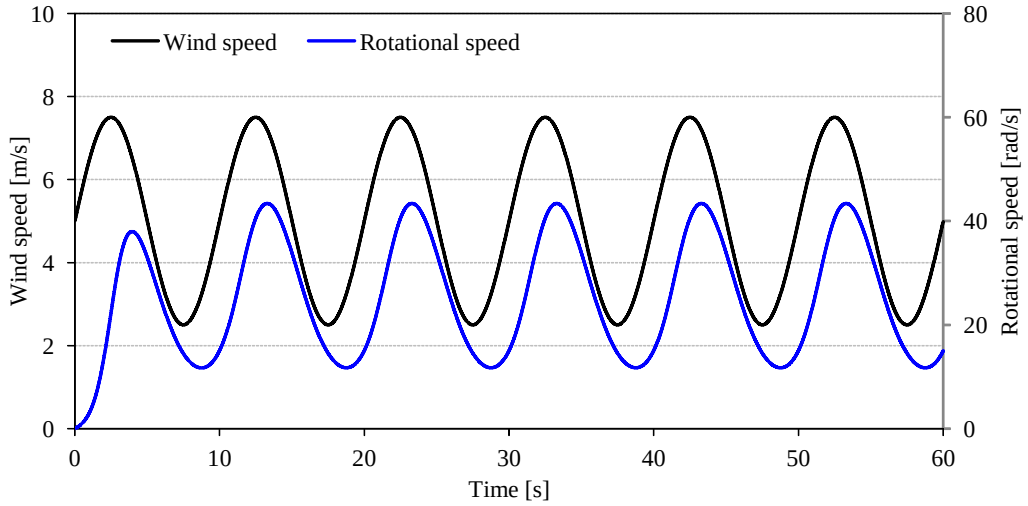

(a) Wind seed and rotational speed

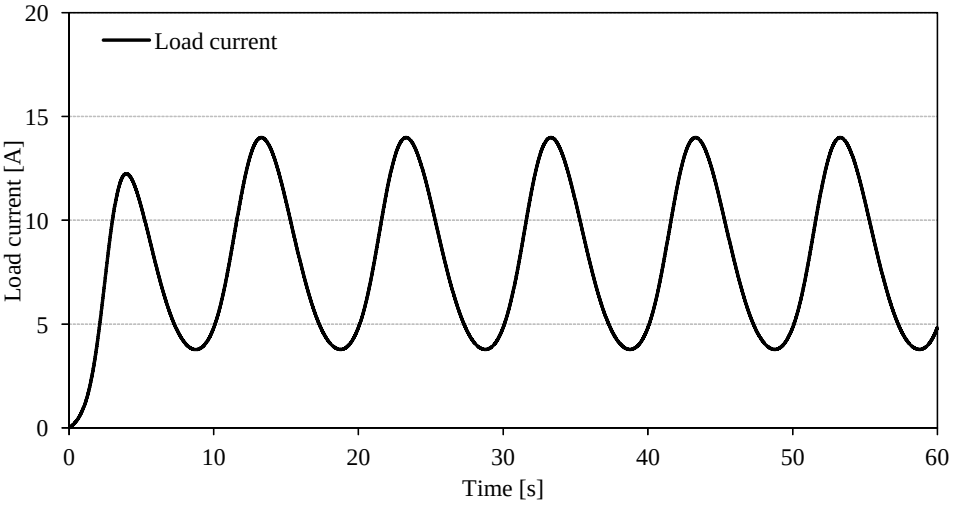

(b) Load current

Figure 2.16: Response of wind turbine for sinusoidal wind data with frequency 0.10 Hz, amplitude 2.5 m/s, and offset 5.0 m/s (Load:R =1 Ω)

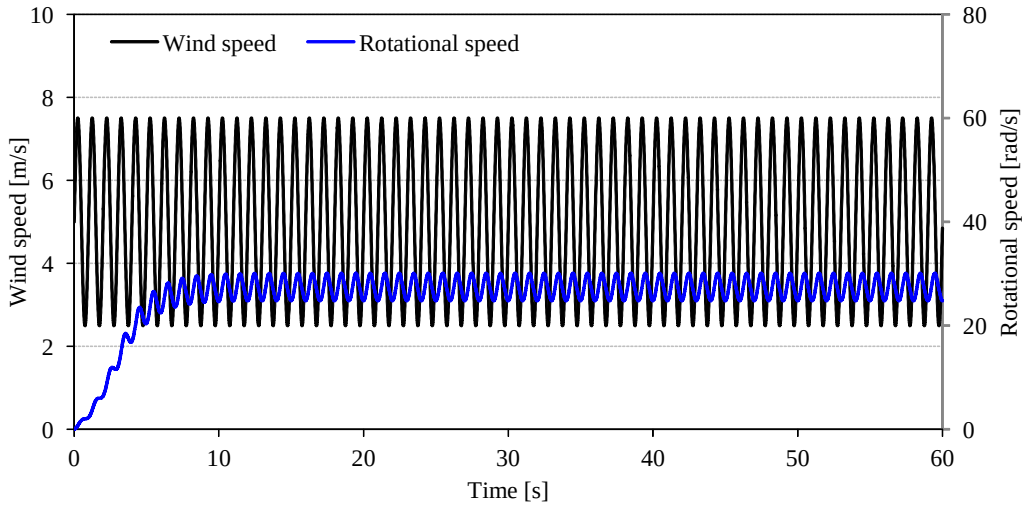

(a) Wind seed and rotational speed

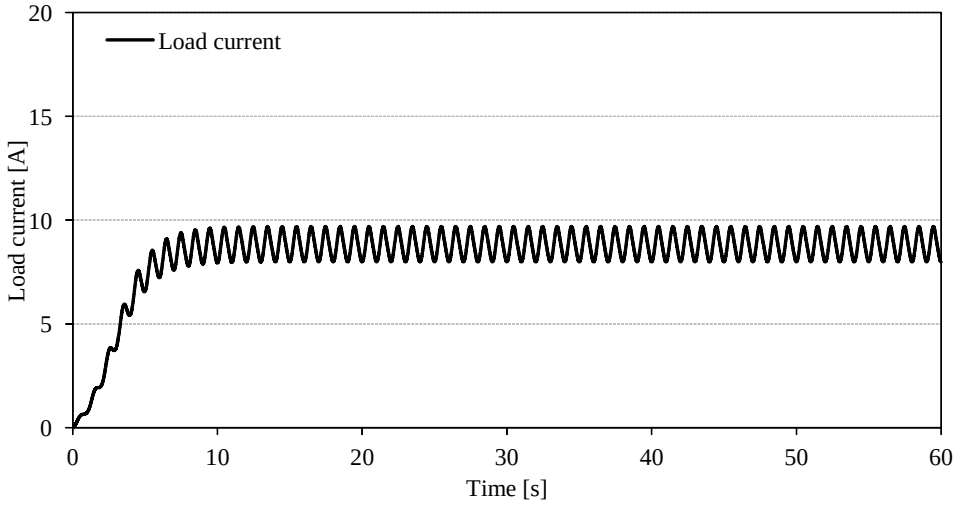

(b) Load current

Figure 2.17: Response of wind turbine for sinusoidal wind data with frequency 1.00 Hz, amplitude 2.5 m/s, and offset 5.0 m/s (Load:R =1 Ω)

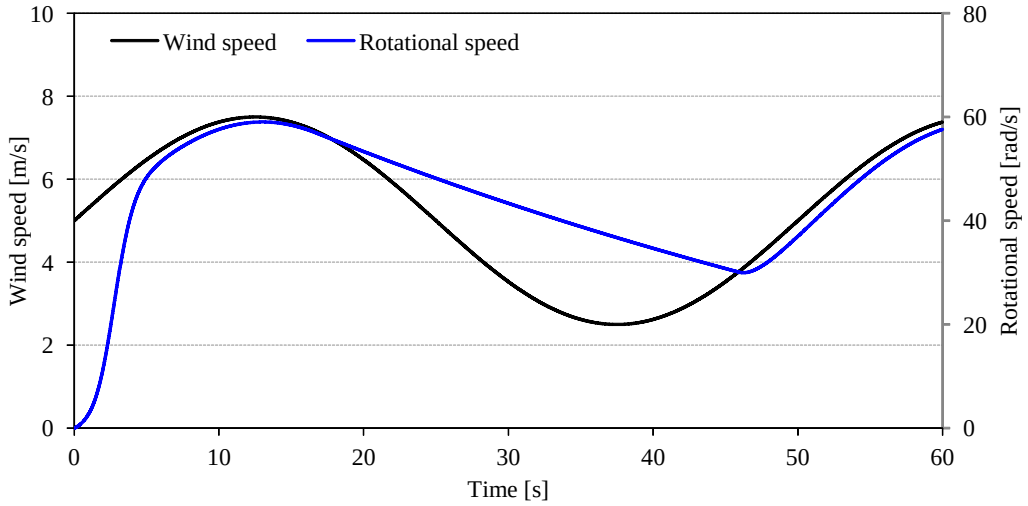

(a) Frequency 0.02 Hz

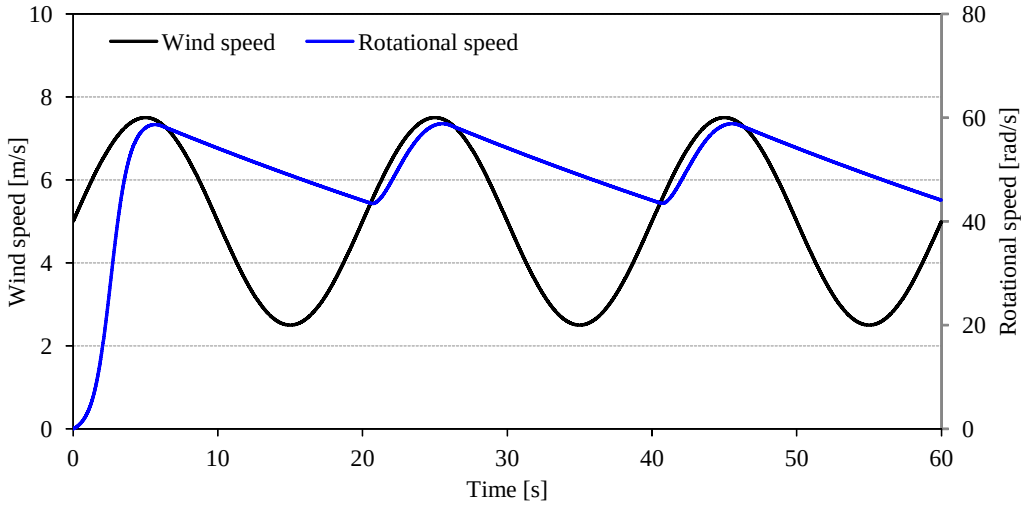

(b) Frequency 0.05 Hz

Figure 2.18: Response of wind turbine for sinusoidal wind data with frequency 0.02 Hz and 0.05 Hz, amplitude 2.5 m/s, and offset 5.0 m/s (No load)

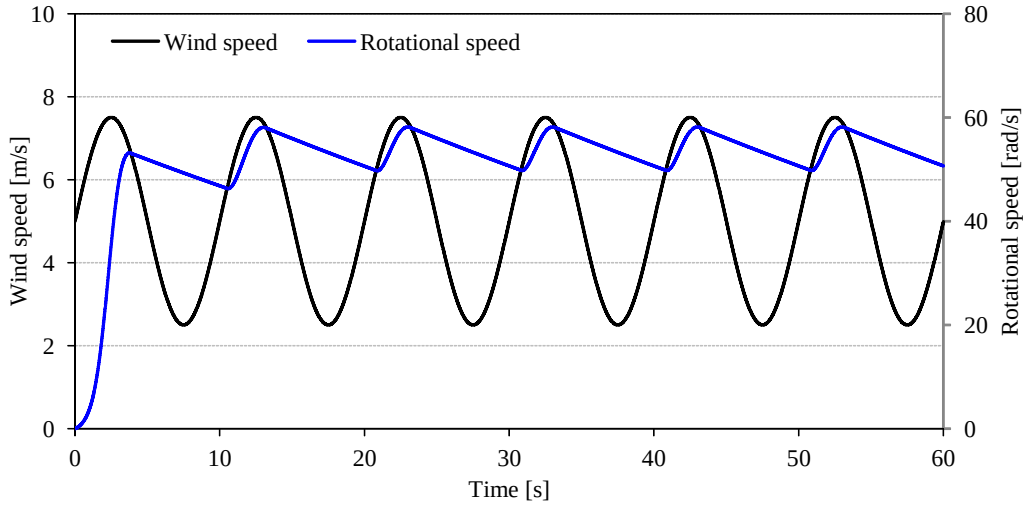

(a) Frequency 0.10 Hz

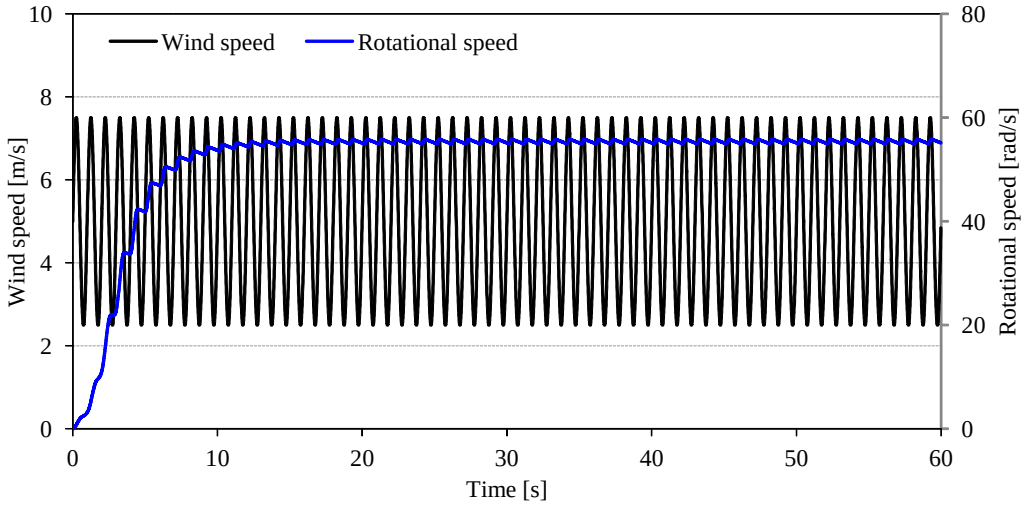

(b) Frequency 1.00 Hz

Figure 2.19: Response of wind turbine for sinusoidal wind data with frequency 0.10 Hz and 1.00 Hz, amplitude 2.5 m/s, and offset 5.0 m/s (No load)

2.3 Maximum power control system

To extract maximum power from the wind turbine, it is required that the wind turbine runs at the top of the $C_P(\lambda)$ curve [30], [31]. The extracted output power of wind turbine p_w is defined as follow:

$$p_w = t_w n. \tag{2.22}$$

Then optimal rotor speed of wind turbine n_{opt} which can extract maximum power is derived by $dp/dn = 0$ using (2.13), (2.14), (2.15), and (2.22) as follows:

$$\begin{aligned}
p &= t_w n = \frac{1}{2} C_T \rho \pi R^3 v^2 n && (2.23)\\
&= \frac{1}{2} \rho \pi R^3 v^2 (\alpha\lambda^2 + \beta\lambda + \gamma) n && (2.24)\\
&= \frac{1}{2} \rho \pi R^3 v^2 \left\{ \alpha \left(\frac{Rn}{v} \right)^2 + \beta \frac{Rn}{v} + \gamma \right\} n && (2.25)\\
&= \frac{1}{2} \rho \pi R^3 \left\{ \alpha R^2 n^3 + \beta R v n^2 + \gamma v^2 n \right\} && (2.26)\\
\frac{dp}{dn} &= \frac{1}{2} \rho \pi R^3 \left\{ 3\alpha R^2 n^2 + \beta R v n + \gamma v^2 \right\} = 0 && (2.27)\\
& && (2.28)\\
n_{opt} &= \frac{-\beta - \sqrt{\beta^2 - 3\alpha\gamma}}{3\alpha R} v && (2.29)
\end{aligned}$$

Also, n_{opt} is expressed by using (2.15) as follow [32]:

$$n_{opt} = \frac{\lambda_{opt}}{R} v \tag{2.30}$$

where λ_{opt} is the tip speed ratio at maximum value of $C_P(\lambda)$ curve derived by $dC_P/d\lambda = 0$.

$$\lambda_{opt} = \frac{-\beta - \sqrt{\beta^2 - 3\alpha\gamma}}{3\alpha} \tag{2.31}$$

From (2.29) and (2.30), these equations indicate that the optimal rotor speed can be decided by the wind speed v.

2.4 Proposed maximum power control algorithm

In the case that a wind turbine is controlled by only using observed wind speed at the present to extract maximum power. Because of the large inertia of the wind turbine,

time lag of control occurs. Therefore, a novel approach is proposed and then predict the wind speed a few seconds ahead and calculate the rotational speed reference of the wind turbine which can generate maximum power under the predicted wind speed. Then the wind turbine can be controlled catching up with the reference for efficiently power generation.

2.4.1 Configuration of control system

Figure 2.20 shows the configuration of the control block diagram of the wind turbine system, where v is the wind speed, $\hat{v}$ is the mean wind speed predicted ahead of a few seconds, n is the rotational speed of the wind turbine, and n_{tra} is the reference trajectory of the rotational speed of the wind turbine. The wind turbine starts rotation at n [rad/s] by inputting wind speed v. Then, the air flow of wind is always perpendicular to the rotational plane of the wind turbine is assumed. At the same time, the wind speed prediction system predicts the mean wind speed $\hat{v}$ from the present to a few seconds ahead based on the observed wind speed. After getting the predicted wind speed, in the wind turbine model, the mechanical time constant of the wind turbine is computed under the assumption that the predicted wind speed is steady blowing. Finally the wind turbine model decides the reference trajectory n_{tra} based on the mechanical time constant and the reference of the rotational speed n_{ref} that the wind power generator can generate a maximum power under the predicted wind speed $\hat{v}$ by using (2.30). The reference trajectory n_{tra} considered the response of the wind turbine is set to catch up with fluctuation of the wind speed so that the obtained power becomes maximum under the predicted wind speed $\hat{v}$. The load regulator compares the present rotational speed of the wind turbine n with reference trajectory

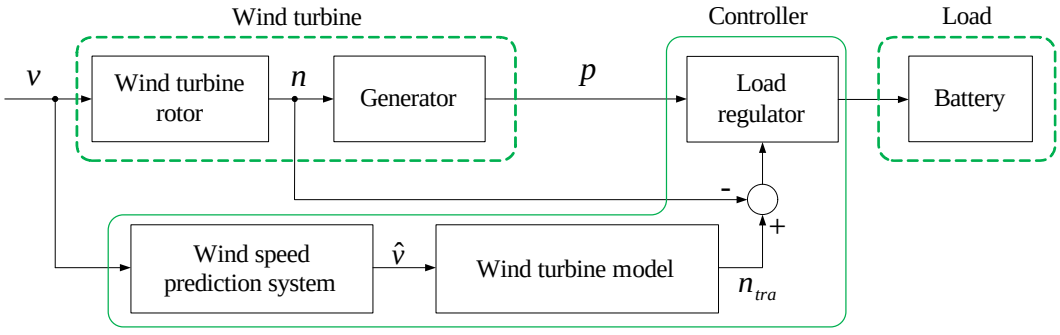

Figure 2.20: Block diagram of the proposed control system

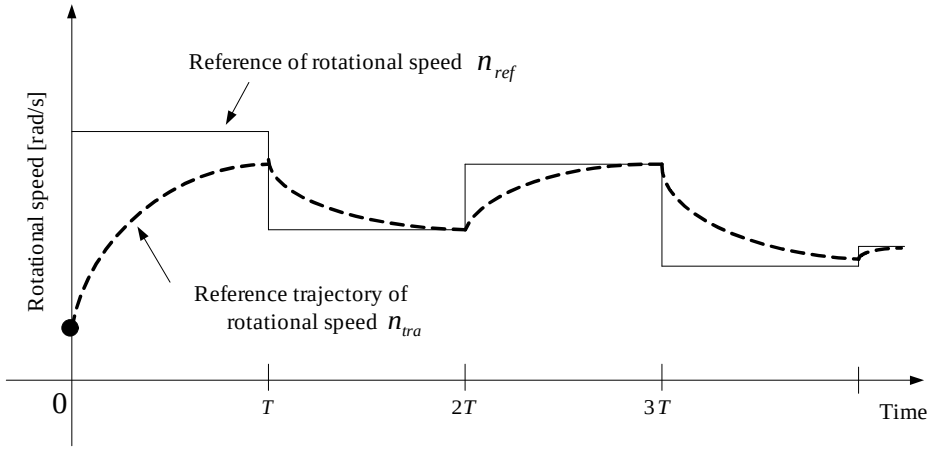

Figure 2.21: Setting image of reference trajectory of rotational speed

of the rotational speed n_{tra} and controls the speed. In the system, a battery is used as the load of wind turbine. The wind turbine generation system usually employs a battery as a energy storage device for providing stable and reliable electricity because wind energy has variability and intermittent characters [33], [27]. This control system generates electricity efficiently because the system uses forward information $\hat{v}$.

2.4.2 Control algorithm

Figure 2.21 shows the setting image of reference trajectory n_{tra} of wind turbine rotational speed. The feature of the proposed control method is to set a reference trajectory n_{tra} of a wind turbine rotational speed based on the predicted wind speed ahead of a few seconds and the mechanical time constant of the wind turbine. The effect of using the predicted data is the controller can efficiently operate the wind turbine based on the trajectory so that rotational speed of the wind turbine catches up with reference speed at maximum power point. The line shaped like a step in Fig. 2.21 indicates the rotational speed reference of the wind turbine n_{ref} which can be obtained by using (2.30) based on the predicted mean wind speed $\hat{v}$. Since it is difficult to predict instantaneous wind speed accurately, the mean wind speed $\hat{v}$ ahead of a few seconds is predicted. The reference trajectory n_{tra} is set from the present rotational speed n to the rotational speed reference n_{ref} by

$$n_{tra}(t) = n_{ref} - \{n_{ref} - n(kT)\}\, e^{-\frac{t}{\tau_m}} \tag{2.32}$$

where τ_m is the mechanical time constant of the wind turbine and $kT \leq t < (k + 1)T, (k = 0, 1, 2, ...)$. It is important to set the reference trajectory considering the response of the wind turbine since large variation of the speed reference cause of speed control vibration [15]. The reference trajectory n_{tra} is updated at specified time interval T, which is the same as execution of the wind speed prediction T in the proposed control algorithm.

CHAPTER 3

Simulation Results of Proposed Control System

3.1 Wind speed data used in simulation

In this chapter, several kinds of computer simulations were conducted in order to confirm the usefulness of the proposed control system (called here, Type A) mentioned in previous chapter. In those simulations, wind speed data which have been observed at Department of Electrical and Electronic Engineering, The University of Tokushima, Japan are used. The observed data which are one second average and obtained every at one second interval are measured by ultrasonic wind sensor Vaisala WMT-702. The specification of the wind sensor is indicated in Table 3.1. WMT-702 has no mechanical drive parts like a propeller, generator, and so on, since it is a ultrasonic typed wind sensor. Therefore the response of the wind sensor is very quickly compared with propeller type. Figure 3.1 shows wind speed data of 120 seconds observed by the wind sensor.

3.2 Comparison objects for proposed control system

For a comparison object of the proposed control system Type A , three types of control systems are prepared. The first one is a control system without the mechanical time constant of the wind power generator (called here, Type B). In Type B, the reference trajectory n_{tra} is set linearly so that the present rotational speed n follows to

Table 3.1: Specifications of wind sensor WMT-702 Vaisala (WMO and ICAO compliant)

Wind speed	
Measurement range	0-65 m/s
Accuracy	± 0.1 m/s or 2 % of reading, whichever is greater
Starting threshold	0.01 m/s
Resolution	0.01 m/s
Wind direction	
Measurement	0-360 °
Accuracy	± 2 °
Starting threshold	0.1 m/s
Resolution	1 °
Output	
Readout update interval	0.25 second
Available average time	3,600 second

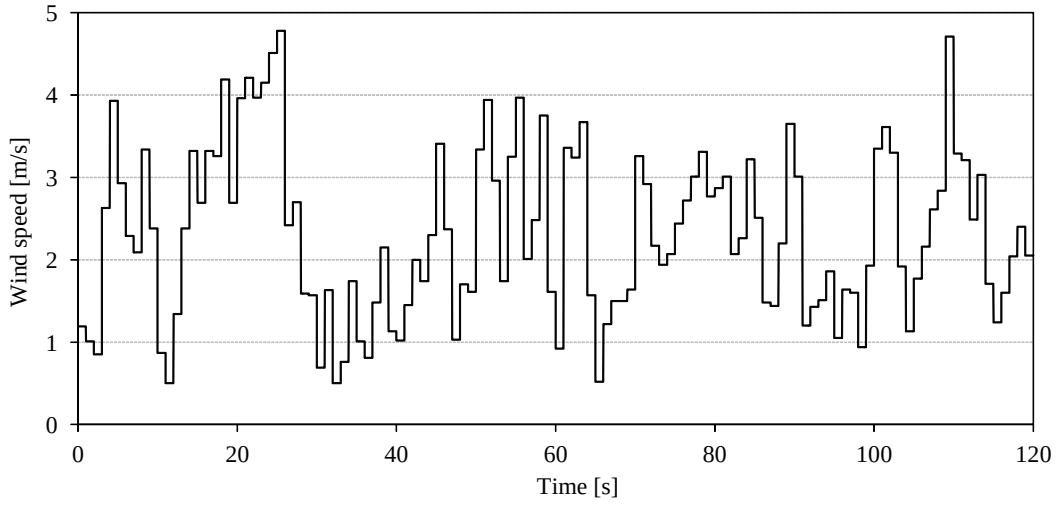

Figure 3.1: Observed wind speed data by WMT-702 and used in simulations

the reference speed n_{ref} as shown below:

$$n_{tra}^{TypeB}(t) = \frac{n_{ref} - n(kT)}{T} t + n(kT) \qquad \{kT \leq t < (k+1)T, k = 0, 1, 2, ...\} \quad (3.1)$$

where T is the renewal interval of the reference trajectory. The second one is a control system that the reference rotational speed of wind turbine n_{ref} is introduced as a

reference trajectory (called here, Type C) as shown in (3.2).

$$n_{tra}^{TypeC}(t) = n_{ref} \qquad \{kT \leq t < (k+1)T, k = 0, 1, 2, ...\} \tag{3.2}$$

where n_{ref} is the reference value of the rotational speed of wind turbine, and its value is obtained by using (2.30). Then predicted wind speed $\hat{v}$ is used as the wind speed v in (2.30). Moreover, a conventional control system is used which does not use forward information (called here, Type D) as a third comparison object. The conventional control system Type D controls the wind turbine based on only the present wind speed and the reference value of rotational speed is decided by (2.30).

In this section, there are mainly three types of simulation results with discussion focused on wind speed prediction, one is a result that the wind speed prediction is precisely predicted without error is assumed. The second is a simulation result in case that predicted wind speed includes prediction error with normal distribution which is generated by Box Muller's method. The other is a result that the wind speed is predicted by a persistent model.

3.3 Control results with precise prediction of wind speed

In this section, the control result in case which is assumed the predicted wind speed is obtained accurately without error is discussed. Table 3.2 shows an integral power consumption of the simulation result with accurate wind speed prediction. The integral power consumption means amount of generated power during simulation time. The prediction time T was changed from 1.0 second to 10.0 seconds at 1.0 second interval as shown in Table 3.2. Here when the prediction time is T [s], the predicted wind speed indicates the average wind speed from the present to prediction time T. Comparing the result of the proposed control system with the other comparison control system which are Type B, and Type C, the proposed control system with 1.0 second wind speed prediction is the best result in the simulation. Figure 3.2 shows the integral power consumption of simulation results expressed as bar chart. From this figure, the integral power consumption of Type A and Type B decreases by setting longer prediction time and almost converges. In terms of control system Type C, the integral power consumption increases while prediction time is up to 4.0 s. It means that shorter prediction time is not useful for Type C because the rotational speed reference

Table 3.2: Simulation results with precise prediction: integral power consumption [Ws]

Prediction time T[s]	Type A	Type B	Type C
1.0	980.9	951.4	876.3
2.0	970.8	966.5	904.9
3.0	942.5	937.0	922.6
4.0	944.0	925.9	919.6
5.0	944.9	923.7	922.1
6.0	934.6	917.0	927.0
7.0	927.6	908.0	914.0
8.0	933.7	910.1	923.2
9.0	921.9	904.6	912.9
10.0	922.7	914.9	913.6

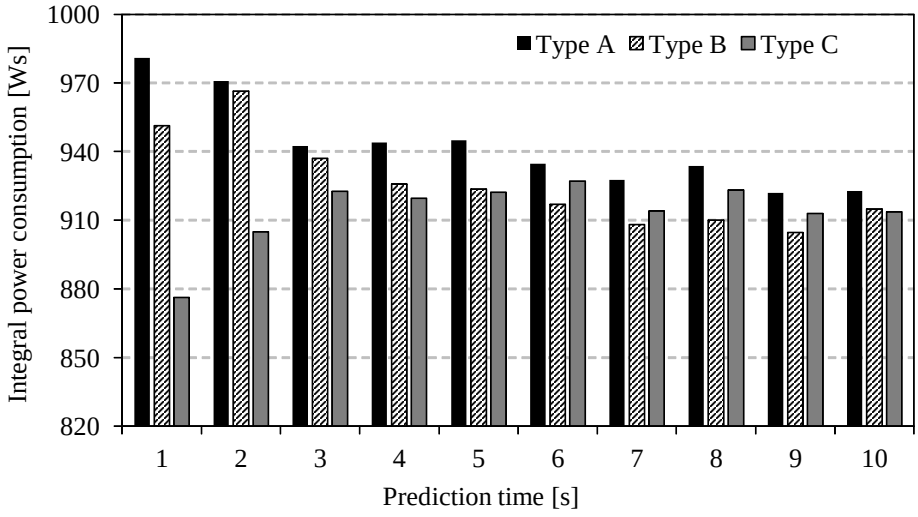

Figure 3.2: Integral power consumption that prediction time is set from 1.0 s to 10.0 s for control system Type A, Type B, and Type C

changes widely without considering the response of wind turbine based on wind speed fluctuation.

Figure 3.3 indicates the wind speed data of 60 seconds used in the simulation. Here, the wind speed fluctuates every second as shown in Fig. 3.3. Therefore, the result with wind speed prediction ahead of 1.0 second becomes the best since the proposed control system updates the reference trajectory every second considering the response of the wind turbine. In the case of the conventional control system Type D

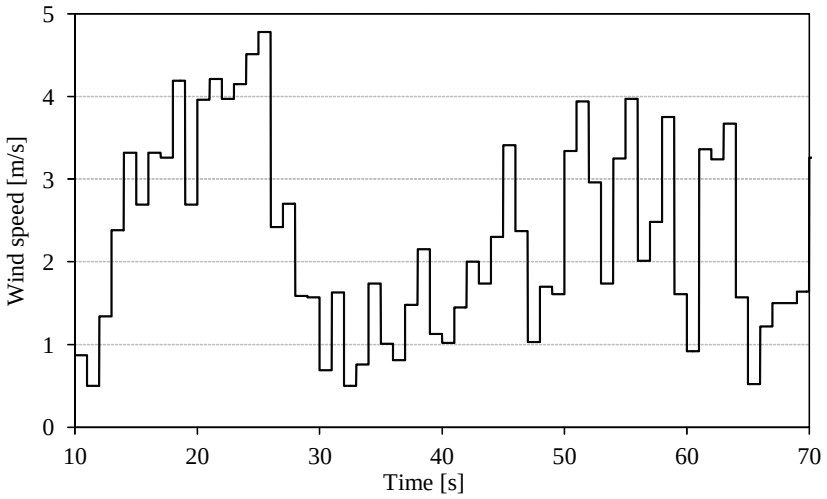

Figure 3.3: A part of wind speed data (60 seconds) used in simulations

which does not use forward information, the integral power consumption is 871.3 Ws. Thus, the power generation efficiency of the proposed control system is improved about 12.6 % compared with the conventional system.

Figures 3.4 (a) $\sim$ (d) indicate the rotational speed of the simulation results in each control system, Type A, Type B, Type C, and Type D, respectively. Each figure shows the reference trajectory and the actual rotational speed of wind turbine. The actual rotational speed means simulated rotational speed by input the wind speed data and controlling. From these figures, the actual rotational speed of the proposed control system Type A is in good agreement with the reference trajectory comparing with others can be confirmed. In simulation results of Type B, Type C, and Type D, there are differences between the actual rotational speed and the reference trajectory due to without the dynamics of the wind turbine for creating the reference trajectory. Figure 3.5 shows the time transition of integral power consumption during in 120 seconds simulation for Type A, Type B, Type C, and Type D. The proposed control system Type A has better characteristics compared with the other control systems.

Figure 3.6 shows the simulation results of control system Type A that the prediction time is from 2.0 second to 5.0 second. Figure 3.7 shows the simulation results of control system Type B that the prediction time is from 2.0 second to 5.0 second. Figure 3.8 shows the simulation results of control system Type C that the prediction time is from 2.0 second to 5.0 second. In case of longer prediction time, since the predicted wind speed is average value of T, the error between actual wind speed and predicted

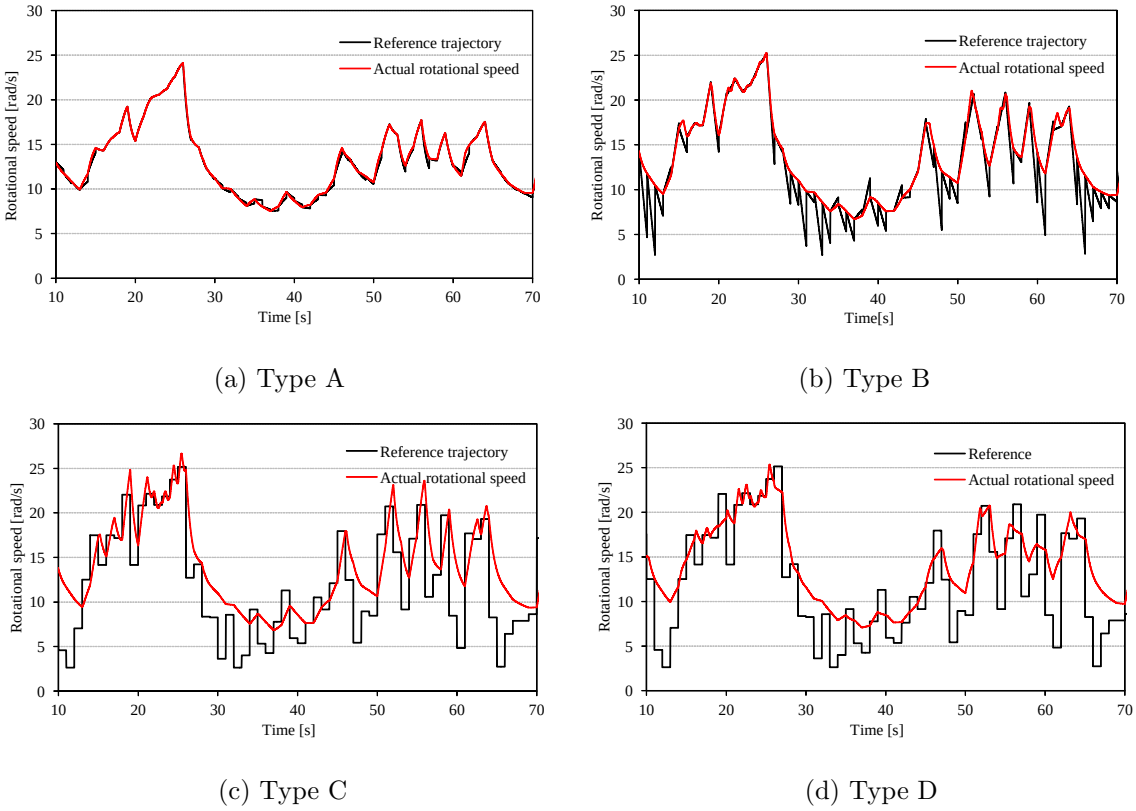

Figure 3.4: Simulation results: actual rotational speed and reference trajectory for each control system

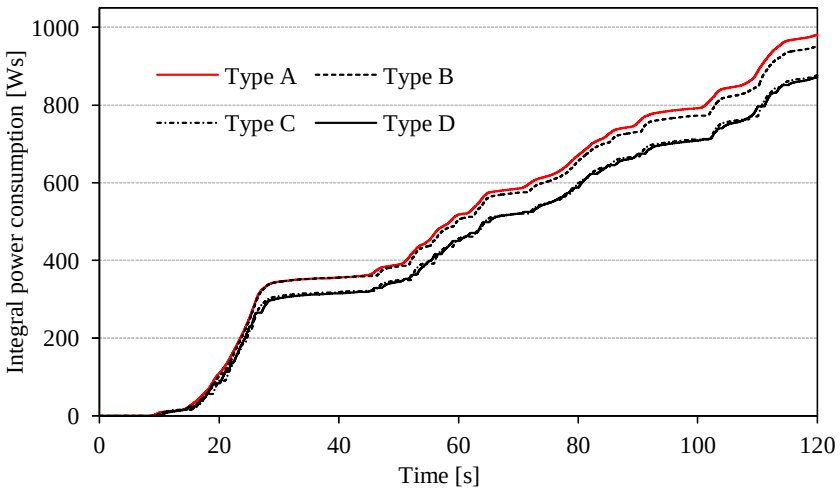

Figure 3.5: Time transition of integral power consumption comparing proposed control system Type A with the others Type B, Type C, and Type D

wind speed is occurred. Then, the reference trajectory is not optimal for maximum power control because the reference trajectory is required to catch up with wind speed varying from every second.

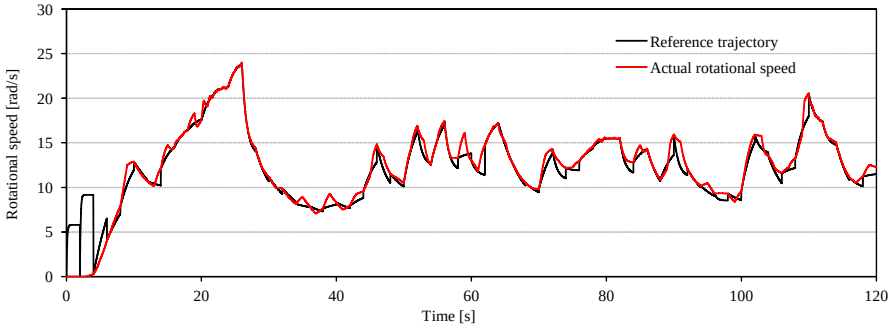

(a) 2.0 second

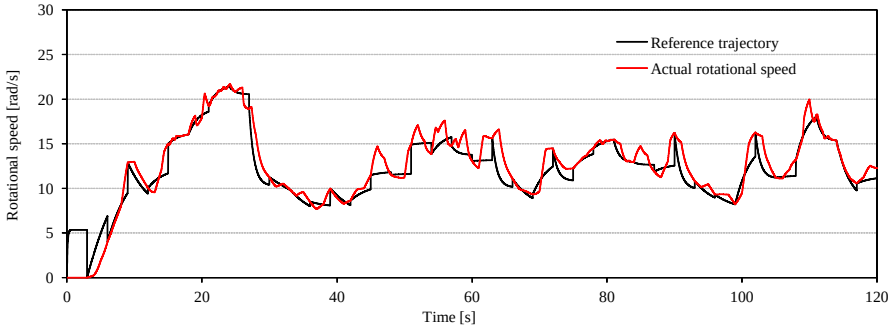

(b) 3.0 second

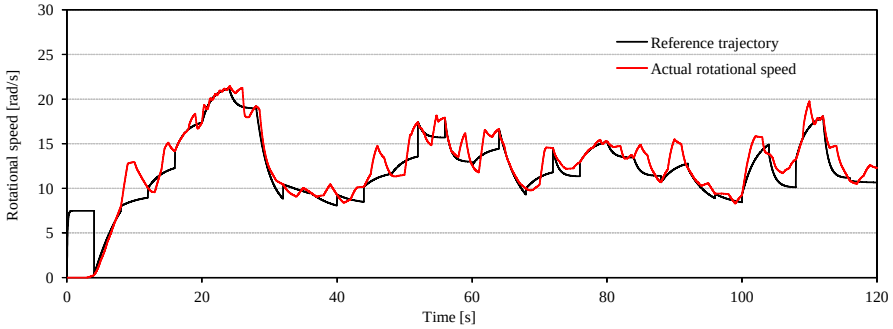

(c) 4.0 second

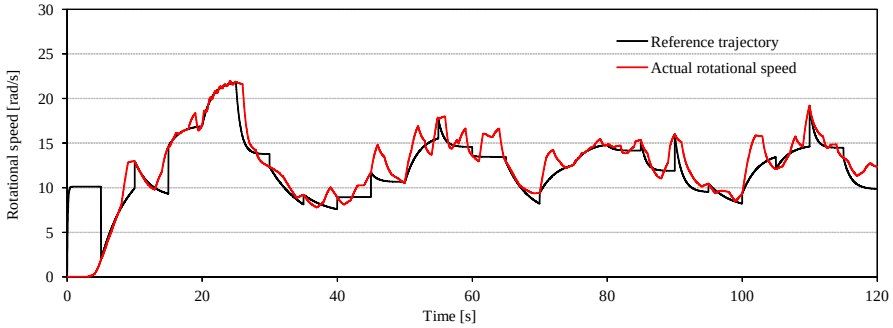

(d) 5.0 second

Figure 3.6: Simulation result of control system Type A: prediction time is from 2.0 second to 5.0 second

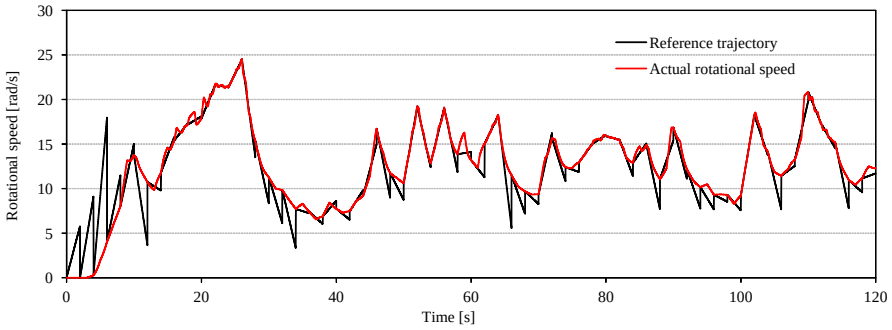

(a) 2.0 second

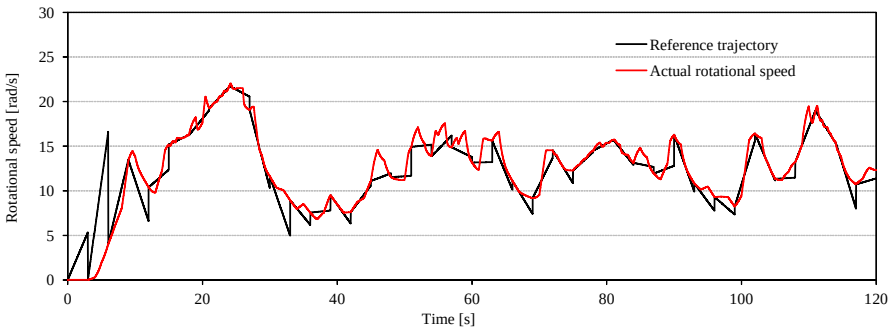

(b) 3.0 second

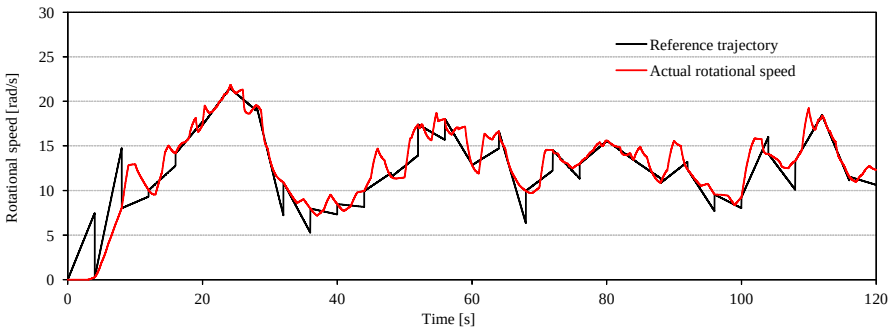

(c) 4.0 second

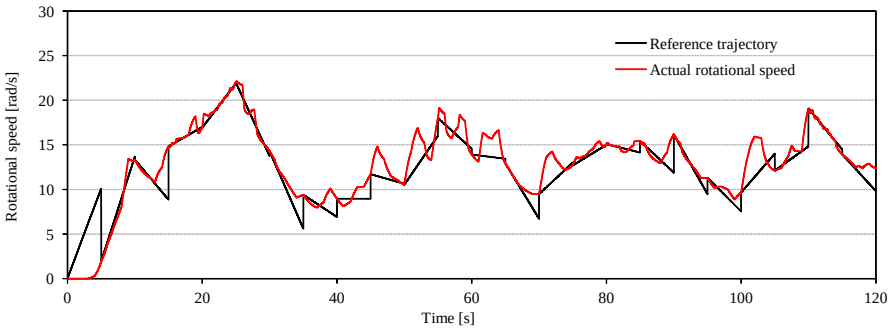

(d) 5.0 second

Figure 3.7: Simulation result of control system Type B: prediction time is from 2.0 second to 5.0 second

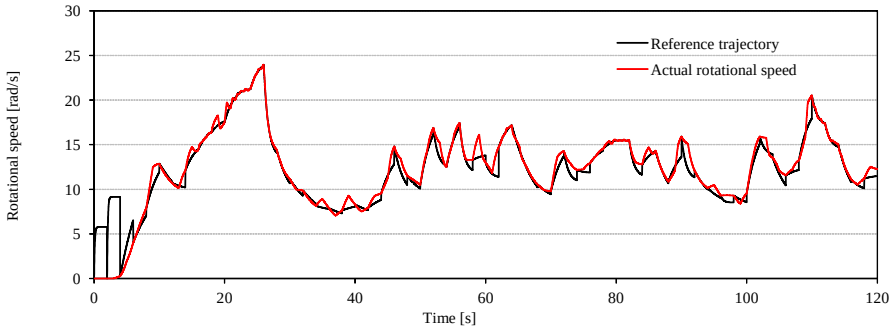

(a) 2.0 second

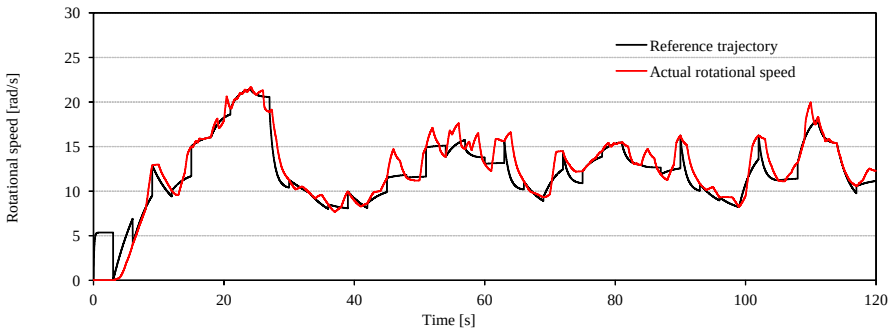

(b) 3.0 second

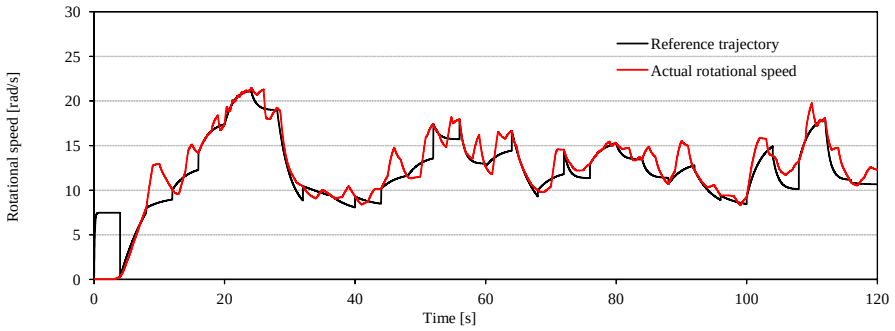

(c) 4.0 second

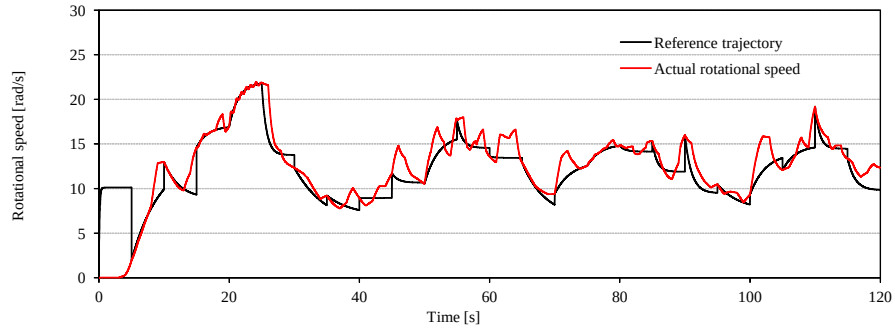

(d) 5.0 second

Figure 3.8: Simulation result of control system Type C: prediction time is from 2.0 second to 5.0 second

3.4 Discussion for the influence of wind speed prediction error

In general, predicted wind speed data has prediction error. Therefore, simulations in the case of including prediction error of wind speed to discuss the influence of the error for control performances are carried out. Then prediction error which is normal distribution is generated by the Box Muller's method [34]. The Box Muller's method is often used to convert uniform random number U to normal random number X. The calculation formula is as follow:

$$X = \sqrt{-2 \ln U_1} \cos(2\pi U_2) \tag{3.3}$$

where U_1, and U_2 are uniform random numbers, which have different value on the interval (0, 1). In the simulation, X divided by coefficient with constant value c is added to the accurate predicted wind speed, and use it for creating the reference trajectory. Since it is difficult to obtain prediction error for specific rate definitely, the value c is adjusted by trial and error so that prediction error is close to target prediction error. The predicted wind speed with 5 %, 10 %, 20 %, 50 % prediction error and actual wind speed are shown in Figs. 3.9 (a) $\sim$ (d).

Figure 3.10 and Table 3.3 indicate transition of integral power consumption when prediction error of wind speed changes in simulation Type A. The prediction error is changed from 0 % to 50 %. From this result, small prediction error is better to improve generation efficiency can be confirmed. In case of 10 % improvement from the conventional control, prediction error must be less than 20 %. Figures 3.11 (a) and (b) show the predicted wind speed with 20 % error and the reference trajectory and the actual rotational speed of the wind turbine in simulation result Type A with 20 %, respectively. Figures 3.11 (c) and (d) show the predicted wind speed with 50 % error and the reference trajectory and the actual rotational speed of the wind turbine in simulation result Type A with 50 %, respectively. Comparing Fig. 3.4 (a) with Fig. 3.11 (b), it can be seen the deviation between the reference trajectory and the actual rotational speed, the actual rotational speed is in agreement with the reference. In the case of wind speed prediction error at 50 % shown in Fig. 3.11 (d), the integral power consumption is 882.9 Ws which is still better than the conventional system.

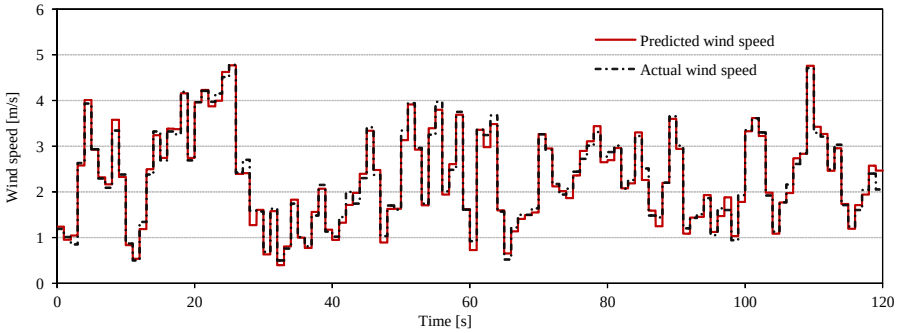

(a) Prediction error: 5 %

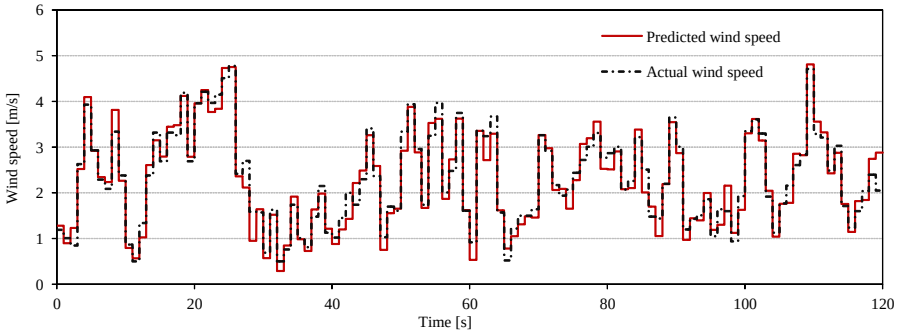

(b) Prediction error: 10 %

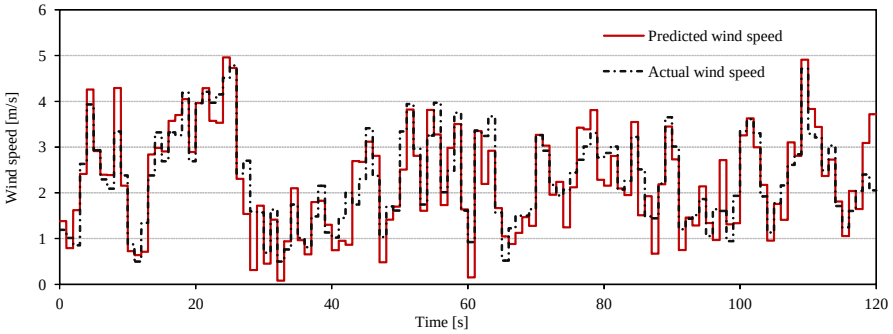

(c) Prediction error: 20 %

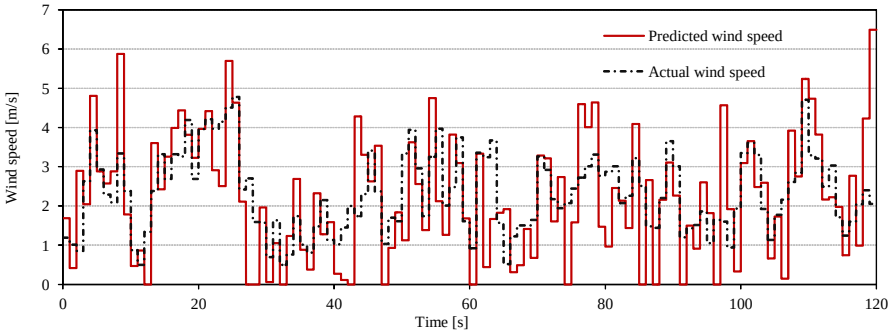

(d) Prediction error: 50 %

Figure 3.9: Predicted wind speed including error generated by Box Muller's method

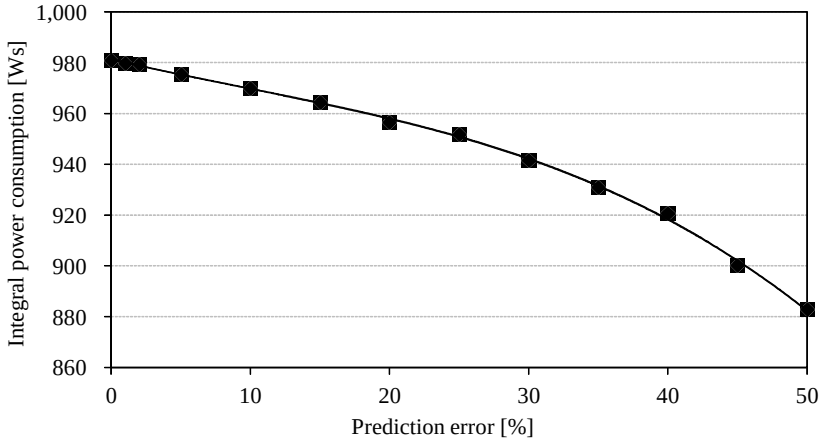

Figure 3.10: Simulation results: Transition of integral power consumption when increasing prediction error: Type A

Table 3.3: Simulation results: Transition of integral power consumption when increasing prediction error Type A

Target error	Prediction error	Integral power consumption
0.0	0.0	980.9
1.0	1.0	979.9
2.0	2.1	979.5
5.0	5.1	975.5
10.0	10.3	970.0
15.0	14.9	964.5
20.0	20.6	956.8
25.0	24.9	951.8
30.0	29.9	941.7
35.0	34.7	930.9
40.0	39.2	920.8
45.0	45.2	900.1
50.0	50.1	882.9

3.5 Control results with persistent model prediction

In this section, simulations of wind turbine control using persistent model prediction are carried out. The persistent model is often used for wind speed prediction

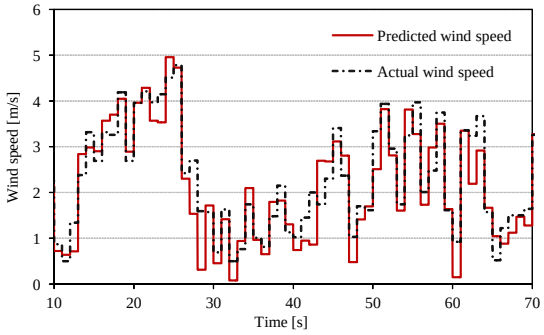

(a) Actual wind speed and predicted wind speed with 20 % error

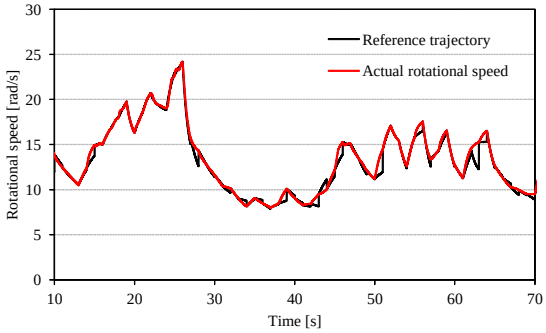

(b) Control result with 20 % prediction error

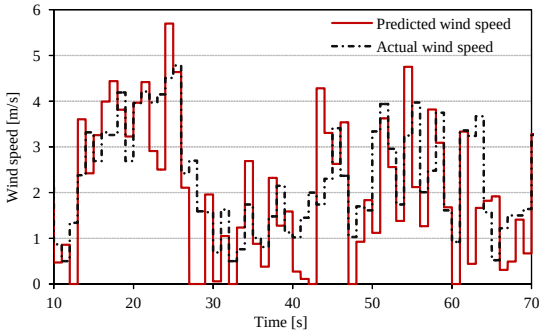

(c) Actual wind speed and predicted wind speed with 50 % error

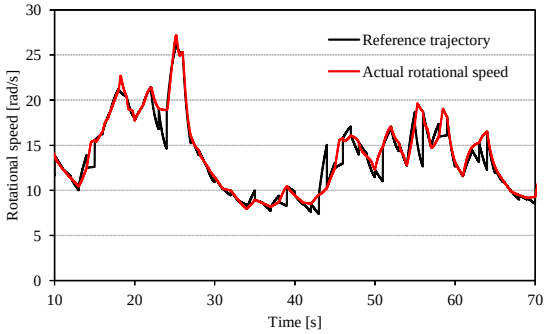

(d) Control result with 50 % prediction error

Figure 3.11: Simulation results including prediction error

in short term. In this model, the measured wind speed becomes the predicted wind speed ahead of prediction time. Table 3.4 shows an integral power consumption of the simulation result using the persistent model. The prediction time T was changed from 1.0 second to 8.0 second at 1.0 second interval. In one second ahead prediction, the prediction error is about 40 % for the observed wind. Figure 3.12 indicates the histogram of wind speed prediction error at one second ahead for the persistent model. This figure means the prediction error has normal distribution characteristics which are average (-0.001) and standard deviation (0.934). Comparing the result of the proposed control system with the result of the other control system, the proposed control system is slightly better. In the case of the conventional control method Type D, the integral power consumption of the method is 871.3 Ws. Thus the power generation efficiency of the proposed control system Type A at one second ahead prediction is improved about 3.6 % compared with the conventional system.

Table 3.4: Simulation results with persistent prediction model: integral power consumption [Ws]

Prediction time T[s]	Type A	Type B	Type C
1.0	903.0	899.7	871.3
2.0	877.5	878.8	852.8
3.0	904.6	903.1	893.4
4.0	878.0	880.0	870.1
5.0	861.0	867.4	841.4
6.0	862.7	864.2	846.9
7.0	865.6	853.1	862.1
8.0	839.6	826.1	831.8

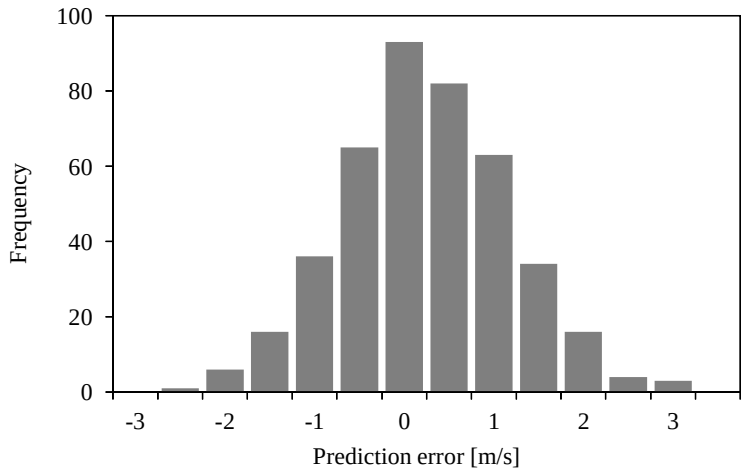

Figure 3.12: Histogram of wind speed prediction error for persistent model: one second ahead prediction

CHAPTER 4

Long Term Prediction System of Wind Speed

In recent years, renewable and clean natural energy has attracted much attention as a solution to depletion of fossil fuels and global warming due to the emission of carbon dioxide. Therefore, wind turbines are being rapidly introduced as alternative electric power generation systems using renewable energy worldwide. However the new installation of wind turbines is increasing at a slow pace in Japan. Mainly because of two problems, which is the limitations of installation sites, the other is unstable output of wind turbines. The limitations mean wind turbines can not install since the installation sites are in national park, are close to residents suffering from low frequency noise of wind turbines, or has poor power system network. The unstable means the output of wind turbines fluctuates widely because the output is proportional to the cube of the wind speed. And it will be cause of frequency change and voltage change in power systems [35, 36]. The problems for site limitation will be resolved by enhancement of power systems and building off-shore wind farms at Japanese boundless sea. Building off-shore wind farms are great idea since there are no residents, and the wind is strong and stable comparing with on the land [37, 38]. However as regarding the output fluctuation problem still exist in the future even if wind turbines are on both the land and the sea. Thus, wind speed prediction system is required for prediction of the output of wind turbines, and using its information to run power systems stably which are combination of conventional power plant such as thermal power and renewable power plant such as wind turbine.

As regards wind speed prediction, there are mainly two types of approaches, which

are generally both based on meteorological data such as wind speed. One is the method by solving dynamic equation [39, 40]. However it requires solving complex differential equation with large meteorological and topographic data. In order to obtain accurate prediction data, more detailed and accurate topographic data is necessary. Although the performances of computers are recently getting better and better, required prediction accuracy and detail are also increasing in accordance with the changes in the times. Thus, the method needs high performance computers and long processing time in any age. The other is the statistical method as represented by neural network, which is powerful application tools for nonlinear data and not required complicated calculation with mathematical model. It also convinced that some papers have reported about wind speed prediction by using feed-forward neural network (FNN) [22, 41–44] or recurrent neural network (RNN) [45–47]. FNN can predicts time series data by converting time series pattern to spatial pattern, and RNN is suitable for treating it due to internal feed-back structure of RNN. In those papers, input data of NN is only observed meteorological data, such as wind speed, temperature, and atmospheric pressure, etc. Then it is confirmed that NN has good ability for wind speed prediction from 10 minutes ahead to several hours ahead. Moreover, S.L. Goh et al. proposed that wind information express in vector quantity or complex number [48] and use it as input information of complex-valued neural network (called here, CVNN) to improve prediction accuracy. Then, the paper reported the proposed method give a reasonable prediction result up to six step ahead by using historical observed data of wind information. However, S. Salcedo-Sanz et al. mentioned that accurate prediction in long time ahead must include meteorological (numerical weather prediction) model in long time prediction (mean hourly or mean daily forecasts) [49].

In this dissertation, the features of CVNN is focused and in order to improve the prediction accuracy of conventional prediction systems, a novel prediction systems for long-term and extremely short-term prediction are proposed. For long-term prediction, the prediction system integrates a hierarchical typed CVNN with multipoint meteorological data surrounding a wind prediction point. The prediction data in long-term is useful for not only management of a battery installed with wind turbines, and also stabilization of power systems. In addition, a simple prediction system consisting of a recurrent typed CVNN required only observed wind speed data for wind turbine control is proposed for extremely short-term prediction in chapter 5. The new feature

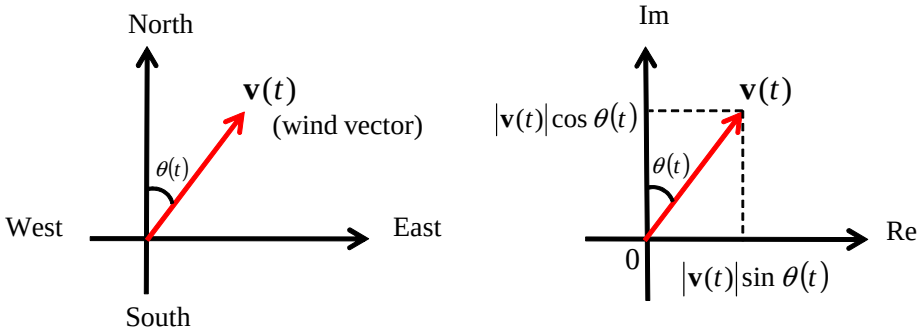

(a) Vector diagram (b) Complex plane

Figure 4.1: Definition of the wind speed and direction on each coordinate system

of the proposed system has ability to predict wind speed and direction at the same time by a NN. Simulation results of proposed and conventional prediction systems are compared to show usefulness and advantage of the proposed prediction system clearly. Then, t-test is conducted which is a method to ensure the validity of difference between proposed prediction system and conventional prediction system. In the simulations, conventional prediction systems are real-valued neural network (RVNN).

4.1 Definition of wind speed and direction

In general, the wind is represented by the wind speed and direction as shown in Fig.4.1(a). In other words, the wind can be also expressed as a complex number $v(t)$ on a complex coordinates as shown in Fig.4.1(b). This point is focused, and the wind vector is defined as follows:

$$v(t) = \Re v(t) + j\Im v(t) = |v(t)|\{\sin\theta(t) + j\cos\theta(t)\} \tag{4.1}$$

where $\Re v(t)$ and $\Im v(t)$ are the real and imaginary part of the complex number $v(t)$. $\Re v(t)$ and $\Im v(t)$ indicate an east-west and south-north components of the wind speed, respectively. The following is treated the wind speed and direction as a complex number.

4.2 Complex-valued neural network

Neural network is popular tool for processing nonlinear data and time series data such as voice recognition, image recognition, and time series forecasting after learning method which is back propagation algorithm was proposed. Neural network is consisted a lot of artificial neurons which is model of human's neuron of brain. It means that neural network can learn a lot of things through a learning process like a human beings. Then neural network is powerful ability for learning data which can not model with formulation such as nonlinear phenomena.

The CVNN is very useful neural network for an operation of complex number and nonlinear data [50–53]. Many people has the same question that what the difference between CVNN and RVNN which is double size for the CVNN. The freedom of CVNN is limited for calculation and learning compared with RVNN by multiplication of complex number. As for RVNN, the real part and imaginary part of complex number are input to RVNN separately, and calculated as independent real number.

In this research, the wind information (wind speed and direction) can be treated as a complex number on the complex coordinates is assumed, and use it as input information of the CVNN. Advantage of treating wind as complex number is to maintain relationship between wind speed and direction inside the CVNN.

4.2.1 Complex-valued neuron of complex-valued neural network

Figure 4.2 shows a model of a complex-valued neuron. The CVNN consists of a number of the neurons. The input data (wind speed data), weights , thresholds and output data (predicted wind speed) of the neuron are all complex numbers. The net input u_l to the complex-valued neuron l is defined as:

$$u_l = \sum_k W_{lk} I_k + \Phi_l \tag{4.2}$$

where W_{lk} is the complex-valued weight connecting complex-valued neurons l and k, I_k is the complex-valued input data from the complex-valued neuron k, and Φ_l is the complex-valued threshold value of neuron l. To obtain the complex-valued output data H_l, convert the net input u_l into its real and imaginary parts as follows: $u_l = x+jy = z$, where j denotes $\sqrt{-1}$. The complex-valued output data is defined to be

$$H_l = f_C(z) = f_R(x) + j f_R(y), \tag{4.3}$$

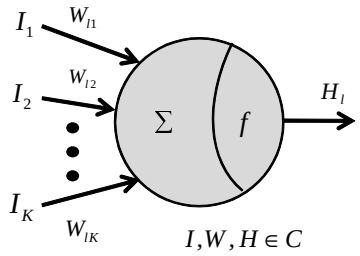

Figure 4.2: Complex-valued neuron

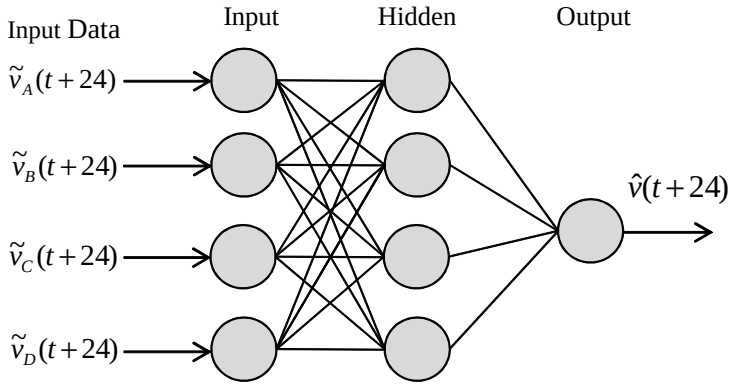

Figure 4.3: Wind information and prediction system using CVNN

where $f_R(u) = 1/(1 + \exp(-u))$, $u \in \boldsymbol{R}$ ($\boldsymbol{R}$ denotes the set of real numbers), that is, the real and imaginary parts of an output of a neuron mean the sigmoid functions of the real part x and imaginary part y of the net input z to the neuron, respectively. The CVNN consists of such complex-valued neurons described above [52] and finally NN outputs O_m as a predicted wind vector $\hat{v}(t + 24)$ in proposed prediction system explained in the next section.

4.3 Long-term prediction system of wind speed

Figure 4.3 shows the configuration of the wind speed prediction system using the hierarchical typed CVNN, which consists of three layers: input layer, hidden layer and output layer. The numbers of neurons of each layers are as follows: input layer, 4; hidden layer, 4; and output layer, 1.

As input information of the CVNN, wind data of numerical weather prediction

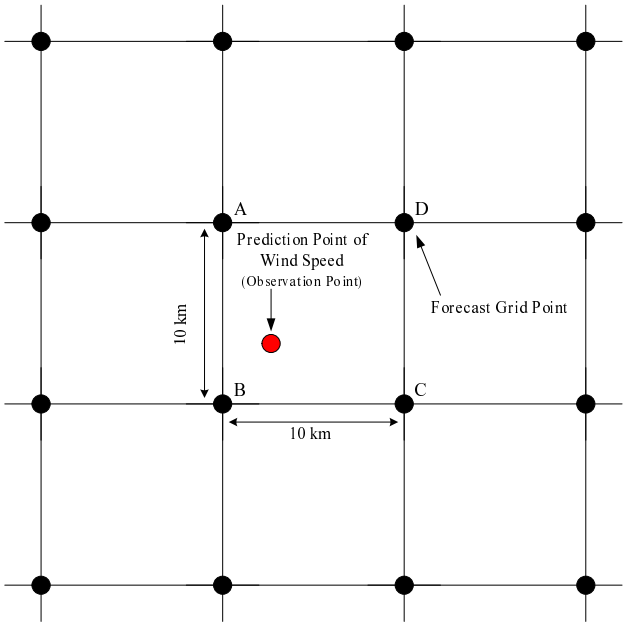

Figure 4.4: The schematic of relation between forecast grid points and the prediction (Observation) point of wind speed

(Meso-scale Spectral Model Grid Point Value: MSM-GPV) is used, which are provided by Japan Meteorological Agency (JMA) every 6 hours at 24 hours ahead forecasting, to realize long time prediction. Therefore, the prediction process is conducted at 6 hour-intervals in this research. The MSM-GPV data of the numerical weather prediction is obtained on grid points which are calculated position and set at 10 km interval covering Japanese area in barometric surface data. To obtain forecast data of MSM-GPV, it takes over two hours by using a forecasting model including geophysical phenomena, topographical information, etc. Then, multipoint data of the MSM-GPV is used, which are surrounding the wind prediction point (assume that the point is set a wind turbine). In Fig. 4.4, black dots indicate forecast grid point of the MSM-GPV surrounding prediction point, and the schematic of relation between the multipoint data and the prediction (observation) point of wind speed is also shown: where $\tilde{v}_A$, $\tilde{v}_B$, $\tilde{v}_C$, and $\tilde{v}_D$ in Fig. 4.3 are forecast wind data of the MSM-GPV at barometric surface of 975 hPa on the grid points (A, B, C, and D) which are surrounding the wind prediction point. Here, the barometric surface of 975 hPa is decided so that forecast data do not include the factor of the land surface. In this dissertation, prediction area is Ikata in Ehime, Japan, and exact location of multipoint point of MSM-GPV and prediction point are

Table 4.1: Coordinates of longitude and latitude of MSM-GPV and prediction point (Ikata)

	Longitude	Latitude
Point A	E132°15′00”	N33°30′00”
Point B	E132°15′00”	N33°24′00”
Point C	E132°22′30”	N33°24′00”
Point D	E132°22′30”	N33°30′00”
Prediction Point	E132°15′24”	N33°26′48”

shown in Table 4.1. By inputting these data to the CVNN, the CVNN is expected can take into account wind dynamics on two-dimensional space during the prediction process and predict wind speed more accurately in case of away from forecast grid point. Then, all input data are expressed into the complex number with an east-west component (real part) and a north-south component (imaginary part) of the forecast wind speed data ahead of 24 hours. Finally, the CVNN outputs the predicted wind speed $\hat{v}(t+24)$ of 24 hours ahead from the present time t. Here, the structure of the proposed CVNN is a hierarchical type because the input data (MSM-GPV) are already forecasted data and those data includes time series dynamics. Then, the CVNN has two important roles by itself. The tasks of the CVNN are to correct both forecast error of the MSM-GPV in itself and the difference of topographical factor. The latter correction means correcting topographical factor between forecast point of the MSM-GPV and wind prediction point. Since the predicted value of the CVNN is complex number, the wind speed and direction can be obtained by calculating amplitude and phase.

The forecasting configuration of MSM-GPV at barometric surface is indicated below.

- Initial time of forecasting:
  - 39 hours ahead forecasting: 03, 09, 15, 21 (UTC)
    (Delivery time: Initial time + 150 minute)
- Grid interval:
  - On barometric surface: latitude 0.1 deg. × longitude 0.125 deg.

(The number of grids: 241 × 253)

- Forecasting area: North-West point 47.6N, 120E, South-East point 22.4N, 150E
- Data format: GRIB2
- Contents: Wind speed (East-West, North-South component), Temperature, Relative humidity, etc.
- Barometric surface level for forecasting [hPa]: 1000, 975, 950, 925, 900, 850, 800, 700, 600, 500, 400, 300, 250, 200, 150, 100

4.3.1 Complex-BP algorithm

Connection weights of the CVNN are learned by using the complex-BP algorithm [50] which is a complex-valued version of the real-BP. This learning algorithm enables the network to learn complex-valued numbers naturally [52].

It can be assumed that $v(t+24)$ is a supervised data (actually observed wind vector) and $\hat{v}(t+24)$ is the output data (predicted wind vector) of the output layer's neuron, then square error E is defined as:

$$
\begin{aligned}
E &= \frac{1}{2}(T^{each} - O)^2 = \frac{1}{2}\left|v(t+24) - \hat{v}(t+24)\right|^2 && (4.4)\\
&= \frac{1}{2}\left|\{\Re v(t+24) - \Re\hat{v}(t+24)\} + j\{\Im v(t+24) - \Im\hat{v}(t+24)\}\right|^2 && (4.5)\\
&= \frac{1}{2}\left\{\sqrt{[\Re v(t+24) - \Re\hat{v}(t+24)]^2 + [\Im v(t+24) - \Im\hat{v}(t+24)]^2}\right\}^2 && (4.6)\\
&= \frac{1}{2}\left\{[\Re v(t+24) - \Re\hat{v}(t+24)]^2 + [\Im v(t+24) - \Im\hat{v}(t+24)]^2\right\} && (4.7)
\end{aligned}
$$

where T^{each} is the supervised data, and O is the output of CVNN. Amount of correction $\triangle w_{ml}$, and $\triangle w_{lk}$ are as follows:

$$
\begin{aligned}
\triangle w_{ml} &= -\eta\left\{\frac{\partial E}{\partial \Re w_{ml}} + j\frac{\partial E}{\partial \Im w_{ml}}\right\} && (4.8)\\
\triangle w_{lk} &= -\eta\left\{\frac{\partial E}{\partial \Re w_{lk}} + j\frac{\partial E}{\partial \Im w_{lk}}\right\} && (4.9)
\end{aligned}
$$

where w_{ml} is the complex-valued connection weight between the output neuron m and the hidden neuron l, w_{lk} is the connection weight between the hidden neuron l and the input neuron k, and η is the learning coefficient.

At first, the amount of correction $\triangle w_{ml}$ for w_{ml} is derived as follows. The first term of (4.8) is the amount of correction for the real part of $\triangle w_{ml}$, and the second

term of (4.8) is the amount of correction for the imaginary part of $\triangle w_{ml}$. The each term is derived as follows:

$$\begin{aligned}\frac{\partial E}{\partial \Re w_{ml}} &= \frac{\partial E}{\partial \Re O_m}\frac{\partial \Re O_m}{\partial \Re net_m}\frac{\partial \Re net_m}{\partial \Re w_{ml}} + \frac{\partial E}{\partial \Re O_m}\frac{\partial \Re O_m}{\partial \Im net_m}\frac{\partial \Im net_m}{\partial \Re w_{ml}} \\ &+ \frac{\partial E}{\partial \Im O_m}\frac{\partial \Im O_m}{\partial \Re net_m}\frac{\partial \Re net_m}{\partial \Re w_{ml}} + \frac{\partial E}{\partial \Im O_m}\frac{\partial \Im O_m}{\partial \Im net_m}\frac{\partial \Im net_m}{\partial \Re w_{ml}} \end{aligned} \tag{4.10}$$

where the second term and the third term become zero because of $O_m = f_C(net_m) = f_R(\Re net_m) + j f_R(\Im net_m)$. And also net_m is as follows.

$$net_m = \sum_l^L \{(\Re w_{ml}\Re H_l - \Im w_{ml}\Im H_L) + j(\Im w_{ml}\Re H_l + \Re w_{ml}\Im H_l)\} \tag{4.11}$$

From (4.11) and (4.10), (4.12) is derived.

$$\begin{aligned}\frac{\partial E}{\partial \Re w_{ml}} &= \frac{\partial E}{\partial \Re O_m}\frac{\partial \Re O_m}{\partial \Re net_m}\frac{\partial \Re net_m}{\partial \Re w_{ml}} + \frac{\partial E}{\partial \Im O_m}\frac{\partial \Im O_m}{\partial \Im net_m}\frac{\partial \Im net_m}{\partial \Re w_{ml}} \\ &= -(\Re T_m^{each} - \Re O_m)(1 - \Re O_m)^2 \Re H_l \\ &- (\Im T_m^{each} - \Im O_m)(1 - \Im O_m)^2 \Im H_l \end{aligned} \tag{4.12}$$

In the same way, the amount of correction for the imaginary part is derived as follows.

$$\begin{aligned}\frac{\partial E}{\partial \Im w_{ml}} &= \frac{\partial E}{\partial \Re O_m}\frac{\partial \Re O_m}{\partial \Re net_m}\frac{\partial \Re net_m}{\partial \Im w_{ml}} + \frac{\partial E}{\partial \Re O_m}\frac{\partial \Re O_m}{\partial \Im net_m}\frac{\partial \Im net_m}{\partial \Im w_{ml}} \\ &+ \frac{\partial E}{\partial \Im O_m}\frac{\partial \Im O_m}{\partial \Re net_m}\frac{\partial \Re net_m}{\partial \Im w_{ml}} + \frac{\partial E}{\partial \Im O_m}\frac{\partial \Im O_m}{\partial \Im net_m}\frac{\partial \Im net_m}{\partial \Im w_{ml}} \\ &= \frac{\partial E}{\partial \Re O_m}\frac{\partial \Re O_m}{\partial \Re net_m}\frac{\partial \Re net_m}{\partial \Im w_{ml}} + \frac{\partial E}{\partial \Im O_m}\frac{\partial \Im O_m}{\partial \Im net_m}\frac{\partial \Im net_m}{\partial \Im w_{ml}} \\ &= -(\Re T_m^{each} - \Re O_m)(1 - \Re O_m)^2(-\Im H_l) \\ &- (\Im T_m^{each} - \Im O_m)(1 - \Im O_m)^2 \Re H_l \end{aligned} \tag{4.13}$$

From (4.8), (4.12), and (4.13), (4.14) is derived.

$$\begin{aligned}\triangle w_{ml} &= \eta\{(\Re T_m^{each} - \Re O_m)(1 - \Re O_m)^2 \\ &\quad + j(\Im T_m^{each} - \Im O_m)(1 - \Im O_m)^2\}\overline{(\Re H_l + j\Im H_l)} \end{aligned} \tag{4.14}$$

In the same way as the derivation of the amount of correction of connection weight between output layer and hidden layer, the amount of correction of connection weight $\triangle w_{ji}$ between hidden layer and input layer is derived as follows. The first term of (4.9) is the amount of correction for the real part of $\triangle w_{lk}$, and the second term of (4.9) is

the amount of correction for the imaginary part of $\triangle w_{lk}$. The each terms are derived as follows.

$$
\begin{aligned}
\frac{\partial E}{\partial \Re w_{lk}} &= \sum_m \left\{ \frac{\partial E}{\partial \Re O_m} \frac{\partial \Re O_m}{\partial \Re net_m} \frac{\partial \Re net_m}{\partial \Re H_l} \right\} \frac{\partial \Re H_l}{\partial \Re net_l} \frac{\partial \Re net_l}{\partial \Re w_{lk}} \\
&+ \sum_m \left\{ \frac{\partial E}{\partial \Re O_m} \frac{\partial \Re O_m}{\partial \Re net_m} \frac{\partial \Re net_m}{\partial \Im H_l} \right\} \frac{\partial \Im H_l}{\partial \Im net_l} \frac{\partial \Im net_l}{\partial \Re w_{lk}} \\
&+ \sum_m \left\{ \frac{\partial E}{\partial \Im O_m} \frac{\partial \Im O_m}{\partial \Im net_m} \frac{\partial \Im net_m}{\partial \Re H_l} \right\} \frac{\partial \Re H_l}{\partial \Re net_l} \frac{\partial \Re net_l}{\partial \Re w_{lk}} \\
&+ \sum_m \left\{ \frac{\partial E}{\partial \Im O_m} \frac{\partial \Im O_m}{\partial \Im net_m} \frac{\partial \Im net_m}{\partial \Im H_l} \right\} \frac{\partial \Im H_l}{\partial \Im net_l} \frac{\partial \Im net_l}{\partial \Re w_{lk}} \\
&= \sum_m \left\{ -(\Re T_m^{each} - \Re O_m)(1 - \Re O_m)^2 \Re w_{ml} \right\} \Re H_l (1 - \Re H_l) \Re I_k \\
&+ \sum_m \left\{ -(\Re T_m^{each} - \Re O_m)(1 - \Re O_m)^2 (-\Im w_{ml}) \right\} \Im H_l (1 - \Im H_l) \Im I_k \\
&+ \sum_m \left\{ -(\Im T_m^{each} - \Im O_m)(1 - \Im O_m)^2 \Im w_{ml} \right\} \Re H_l (1 - \Re H_l) \Re I_k \\
&+ \sum_m \left\{ -(\Im T_k^{each} - \Im O_m)(1 - \Im O_m)^2 \Re w_{ml} \right\} \Im H_l (1 - \Im H_l) \Im I_k \qquad (4.15)
\end{aligned}
$$

$$
\begin{aligned}
\frac{\partial E}{\partial \Im w_{lk}} &= \sum_m \left\{ \frac{\partial E}{\partial \Re O_m} \frac{\partial \Re O_m}{\partial \Re net_m} \frac{\partial \Re net_m}{\partial \Re H_l} \right\} \frac{\partial \Re H_l}{\partial \Re net_l} \frac{\partial \Re net_l}{\partial \Im w_{lk}} \\
&+ \sum_m \left\{ \frac{\partial E}{\partial \Re O_m} \frac{\partial \Re O_m}{\partial \Re net_m} \frac{\partial \Re net_m}{\partial \Im H_l} \right\} \frac{\partial \Im H_l}{\partial \Im net_l} \frac{\partial \Im net_l}{\partial \Im w_{lk}} \\
&+ \sum_m \left\{ \frac{\partial E}{\partial \Im O_m} \frac{\partial \Im O_m}{\partial \Im net_m} \frac{\partial \Im net_m}{\partial \Re H_l} \right\} \frac{\partial \Re H_l}{\partial \Re net_l} \frac{\partial \Re net_l}{\partial \Im w_{lk}} \\
&+ \sum_m \left\{ \frac{\partial E}{\partial \Im O_m} \frac{\partial \Im O_m}{\partial \Im net_m} \frac{\partial \Im net_m}{\partial \Im H_l} \right\} \frac{\partial \Im H_l}{\partial \Im net_l} \frac{\partial \Im net_l}{\partial \Im w_{lk}} \\
&= \sum_m \left\{ -(\Re T_m^{each} - \Re O_m)(1 - \Re O_m)^2 \Re w_{ml} \right\} \Re H_l (1 - \Re H_l)(-\Im I_k) \\
&+ \sum_m \left\{ -(\Re T_m^{each} - \Re O_m)(1 - \Re O_m)^2 (-\Im w_{ml}) \right\} \Im H_l (1 - \Im H_l) \Re I_k \\
&+ \sum_m \left\{ -(\Im T_m^{each} - \Im O_m)(1 - \Im O_m)^2 \Im w_{ml} \right\} \Re H_l (1 - \Re H_l)(-\Im I_k) \\
&+ \sum_m \left\{ -(\Im T_m^{each} - \Im O_m)(1 - \Im O_m)^2 \Re w_{ml} \right\} \Im H_l (1 - \Im H_l) \Re I_k \qquad (4.16)
\end{aligned}
$$

From (4.15), and (4.16), (4.9) becomes as follows.

$$
\triangle w_{lk} = \eta \{ \frac{\partial E}{\partial \Re w_{lk}} + j \frac{\partial E}{\partial \Im w_{lk}} \}
$$

$$
\begin{aligned}
&= \eta[\{(\Re T_m^{each} - \Re O_m)(1-\Re O_m)^2 \Re w_{ml} \\
&+ (\Im T_m^{each} - \Im O_m)(1-\Im O_m)^2 \Im w_{ml}\} \Re H_l (1-\Re H_l) \\
&- j\{(\Re T_m^{each} - \Re O_m)(1-\Re O_m)^2 \Im w_{ml} \\
&- (\Im T_m^{each} - \Im O_m)(1-\Im O_m)^2 \Re w_{ml}\} \Im H_l (1-\Im H_l)] \\
&\quad \overline{(\Re I_k + j\Im I_k)}
\end{aligned} \tag{4.17}
$$

By using the complex-valued BP, a NN is able to learn naturally complex number. The interesting ability of CVNN is seen such as graphics transformation and so on [50] that can not be processed by RVNN easily.

The CVNN is learned each month for a year (in 2008) because wind condition changes from season to season. Then the supervised data is the observation data of wind speed of 10 minutes average at 6 hour-intervals, which is observed by AMeDAS in Ikata, Japan (observation point is Seto , and the observation height is 6.6 m from the ground). AMeDAS stands for automated meteorological data acquisition system, which is set up and observe meteorological data such as wind speed and direction, amount of solar radiation, and precipitation, and so on, in Japan. In this case, the proposed system predicts wind speed at 6.6 m high from the ground, however large scale wind power generation system is at least 60 m high. In order to get a arbitrary different height of wind speed, it can be calculated by using height conversion method proposed by T. Iizaka et al. [54].

Figure 4.5 shows the transition of root mean square error, $RMSE$ [m/s] when the CVNN was learning of each month. From this result, it is confirmed that leaning error is convergent and we used the CVNN, which has been learned, for wind speed prediction. Here, the learning coefficient η is set to 0.01. The parameters of the CVNN are decided by trial-and-error approach. $RMSE$ is defined as follow:

$$
RMSE = \sqrt{\frac{\sum_{i=1}^{N}(v_i - \hat{v_i})^2}{N}} \tag{4.18}
$$

where v_i is the i-th supervised data of wind speed, $\hat{v_i}$ is the i-th output value of the CVNN, N is the number of all pattern, which are relationship between the observed wind speed and the predicted wind speed.

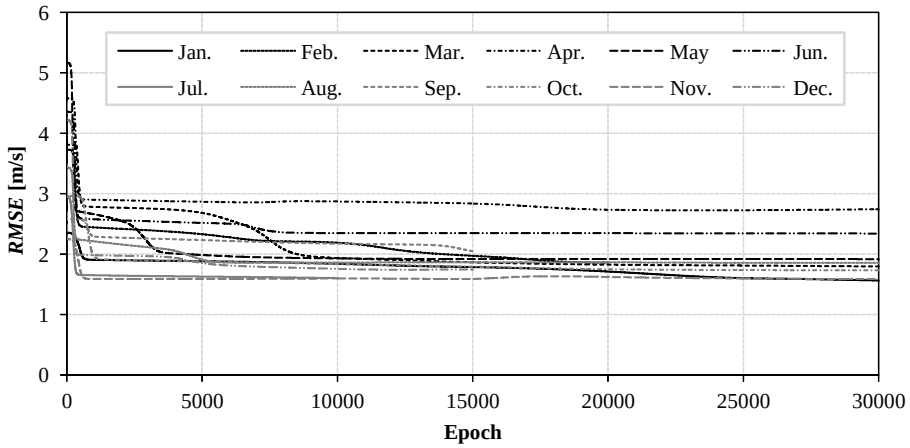

Figure 4.5: Transition of $RMSE$ during learning of the CVNN

4.3.2 Comparison object for proposed wind speed prediction system

Figure 4.6 indicates the configuration of the wind speed prediction system using the RVNN, which is a comparison object of the prediction system using the CVNN. To compare the validity of the proposed prediction system using the CVNN, the input information and parameters of the RVNN are the same to those of the CVNN. However, the numbers of neurons of RVNN are as follows: input layer, 8; hidden layer, 4; and output layer, 2. It can be seen that the number of neuron both input layer and output layer are doubled. Because it is needed for input/output data of wind velocity, which has real and imaginary part of the wind and input/output them to the RVNN separately. The number of hidden layer's neuron are decided so that it becomes the same as the number of connection weight of the CVNN.

Here, back propagation algorithm for real value is introduced. Square error E is defined as:

$$E = \frac{1}{2}\sum_{m=1}^{M=2}(T_m^{each} - O_m)^2 \tag{4.19}$$

where T_m^{each} and O_m are real value, respectively. The amount of correction for connection weight between output layer and hidden layer is as follows.

$$\triangle w_{ml} = -\eta\frac{\partial E}{\partial w_{ml}} = -\eta\frac{\partial E}{\partial O_m}\frac{\partial O_m}{\partial net_m}\frac{\partial net_m}{\partial w_{ml}} \tag{4.20}$$

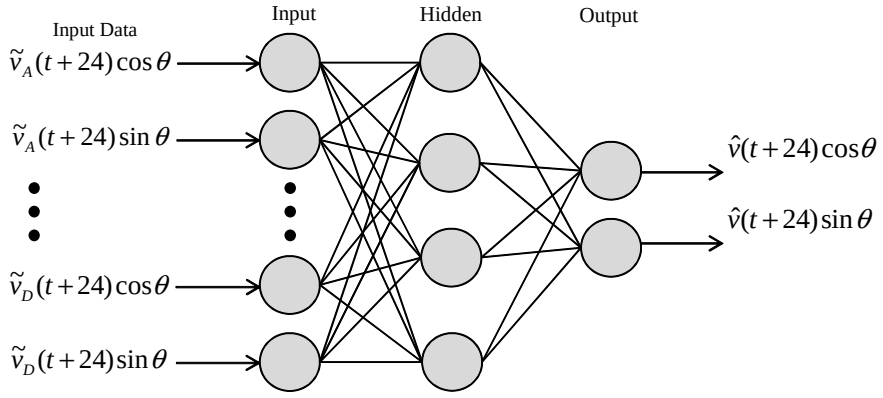

Figure 4.6: Wind information and prediction system using RVNN

Here, the each differential equation of (4.20) are as follows.

$$\frac{\partial E}{\partial O_m} = \frac{\partial}{\partial O_m}\frac{1}{2}\sum_{m=1}^{M}(T_m^{each}-O_m)^2 = -(T_m^{each}-O_m) \tag{4.21}$$

$$\frac{\partial O_m}{\partial net_m} = \frac{\partial}{\partial net_m}\{tanh(net_m)\} = (1-O_m)^2 \tag{4.22}$$

$$\frac{\partial net_m}{\partial w_{ml}} = \frac{\partial \sum_l^L w_{ml}H_l}{\partial w_{ml}} = H_l \tag{4.23}$$

In the same way, the amount of correction for connection weight between hidden layer and input layer is as follows.

$$\begin{aligned}
\triangle w_{lk} &= -\eta\frac{\partial E}{\partial w_{lk}} \\
&= -\eta\frac{\partial E}{\partial O_m}\frac{\partial O_m}{\partial net_m}\frac{\partial net_m}{\partial O_l}\frac{\partial O_l}{\partial net_l}\frac{\partial net_l}{\partial w_{lk}} \\
&= -\eta\frac{\partial}{\partial O_m}\left\{\frac{1}{2}\sum_m^M(T_m^{each}-O_m)^2\right\}f\prime(net_m)w_{ml}f\prime(net_l)I_k \\
&= \eta\sum_m^M(T_m^{each}-O_m)(1-O_m)^2w_{ml}H_l(1-H_l)I_k
\end{aligned} \tag{4.24}$$

4.4 Wind speed prediction results of long term

At first, in order to confirm the usefulness of the proposed prediction system, the wind speed and direction ahead of 24 hours for each month in 2009 by using the learned CVNN is predicted. Here, it is important to note that the wind speed data in 2009 is not used as the supervised data for learning the CVNN. And also, the simulations about single-input prediction system for the CVNN and the RVNN is

conducted, respectively to compare the multi-input prediction system of wind speed. Then, as input information of the single-input prediction, the wind information at point B is used, which is the nearest point from the wind prediction point in Fig. 4.4.

Figure 4.7 (a) and Fig. 4.8 (a) show the prediction results of the wind speed using the CVNN and RVNN with multi-input ahead of 24 hours on January in 2009. In these figures, the MSM-GPV data at point B and observed data are indicated. From these results, the CVNN is confirmed that can correct the wind speed of the MSM-GPV so that the output of the CVNN is closed to the actual observation wind speed. Figures 4.9 (a) $\sim$ 4.30 (a) indicate the simulation results of wind speed using the CVNN and RVNN from February to December, respectively.

Figures 4.7 (b) $\sim$ 4.30 (b) show the prediction results of the wind direction using the CVNN and RVNN ahead of 24 hours from January to December in 2009, respectively. In these figures, Y-axis shows wind direction from -180 degrees to +180 degrees. It indicates that maximum value and minimum value in Y-axis are the same direction. The mean absolute prediction errors (MAE) of wind direction are 39.2 degree in January by using the CVNN, and MSM-GPV at point B are 54.3 degree, respectively. The definition of MAE is defined as follow:

$$MAE = \frac{1}{N}\sum_{i=1}^{N} |v_i^{dir} - \hat{v_i}^{dir}| \tag{4.25}$$

where v_i^{dir} is the i-th observed data of wind direction, $\hat{v_i}^{dir}$ is the i-th predicted output value of the CVNN, N is the number of all data during the simulation and note that $|v_i^{dir} - \hat{v_i}^{dir}|$ is less than 180 degree. From these results, the CVNN can reduce prediction error about 25% than MSM-GPV.

In this dissertation, $RMSE$ defined in (4.18) is used for the evaluation of wind speed prediction accuracy. Table 4.2(a) shows $RMSE$, which is a result of the wind speed prediction with multi-input MSM-GPV using the CVNN, the MSM-GPV data at point B, or the RVNN each month in 2009. At the bottom of the table, annual average of $RMSE$ is indicated for each prediction system. From this table, the CVNN is capable to decrease the prediction error about 54% in comparison with the MSM-GPV in annual average. And compared to the RVNN, the CVNN can reduce the prediction error about 3.5%.

Next, the multi-input with the single-input for each prediction system using the CVNN or the RVNN are compared. Table 4.2(b) shows $RMSE$, which is a result of

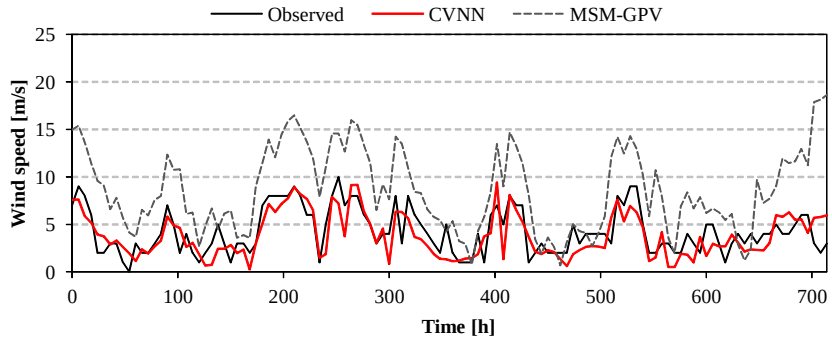

(a) Wind speed

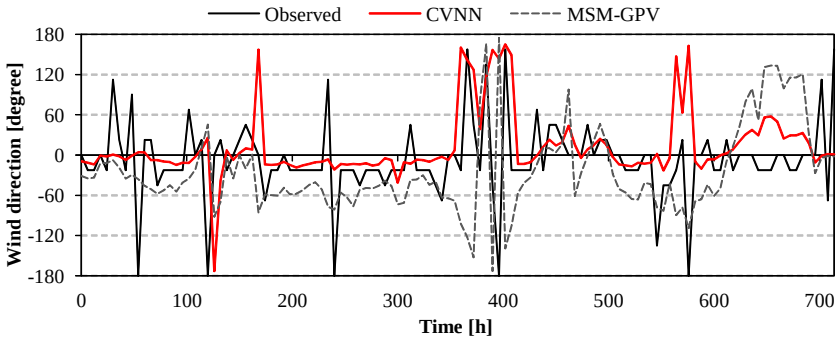

(b) Wind direction

Figure 4.7: Prediction results of wind speed and direction: CVNN (Jan. 2009)

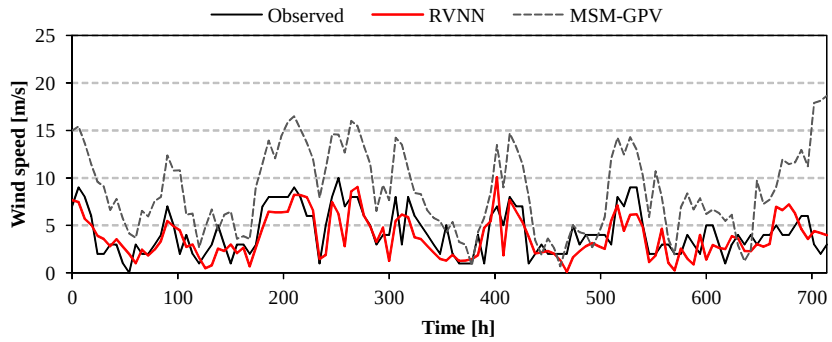

(a) Wind speed

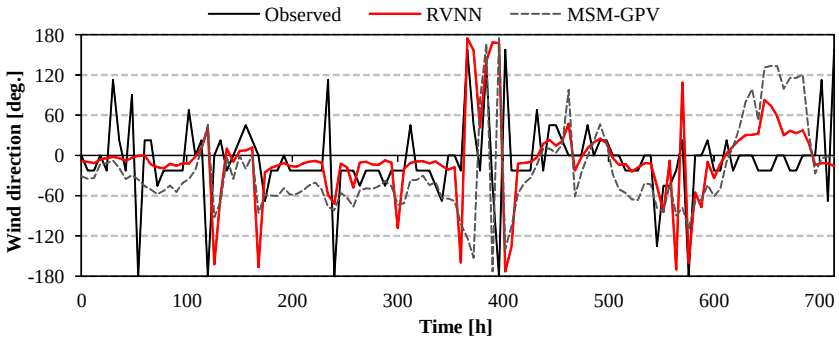

(b) Wind direction

Figure 4.8: Prediction results of wind speed and direction: RVNN (Jan. 2009)

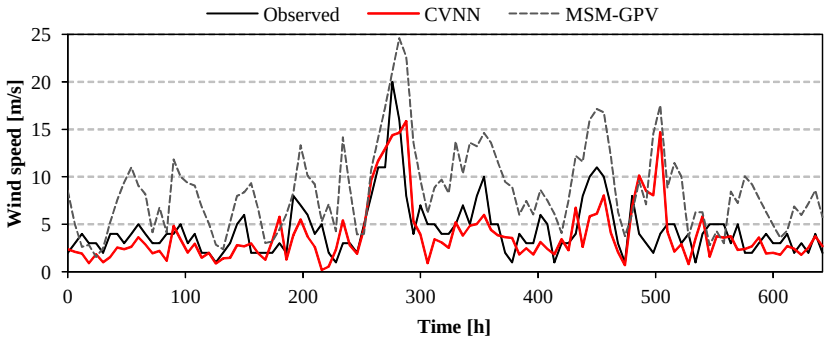

(a) Wind speed

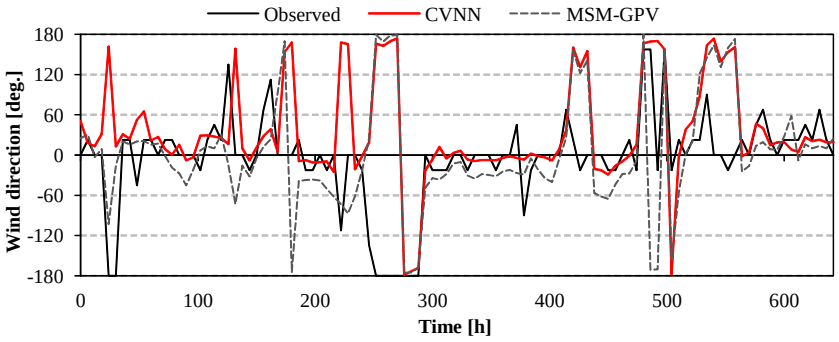

(b) Wind direction

Figure 4.9: Prediction results of wind speed and direction: CVNN (Feb. 2009)

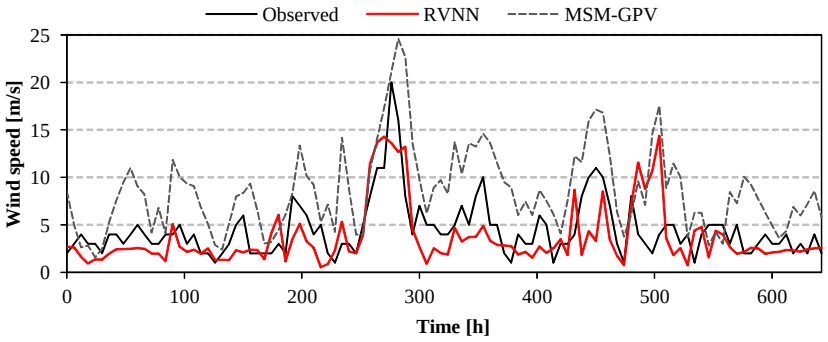

(a) Wind speed

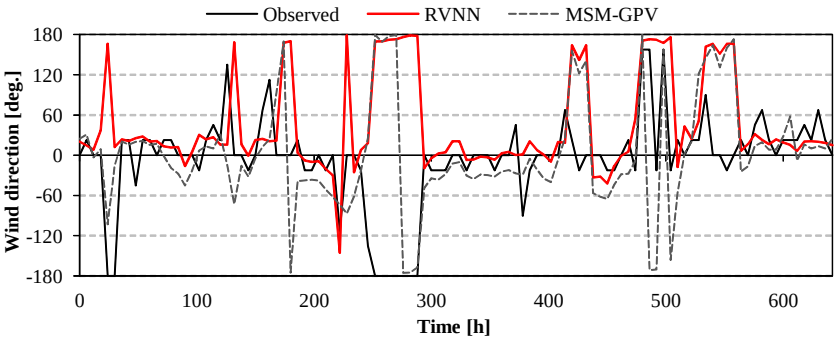

(b) Wind direction

Figure 4.10: Prediction results of wind speed and direction: RVNN (Feb. 2009)

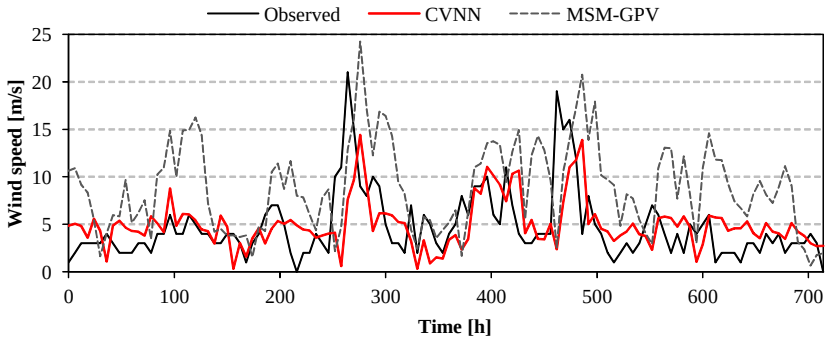

(a) Wind speed

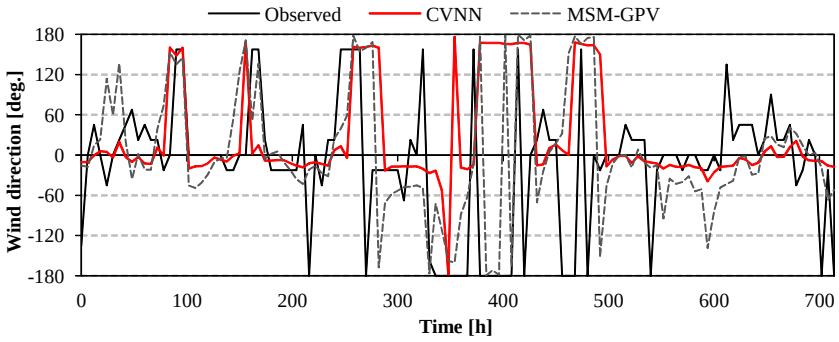

(b) Wind direction

Figure 4.11: Prediction results of wind speed and direction: CVNN (Mar. 2009)

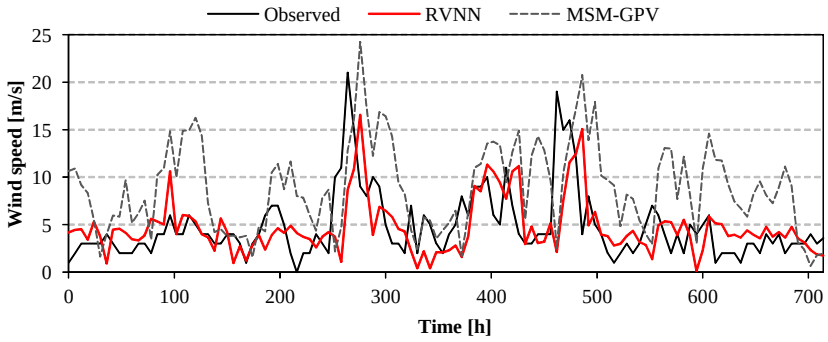

(a) Wind speed

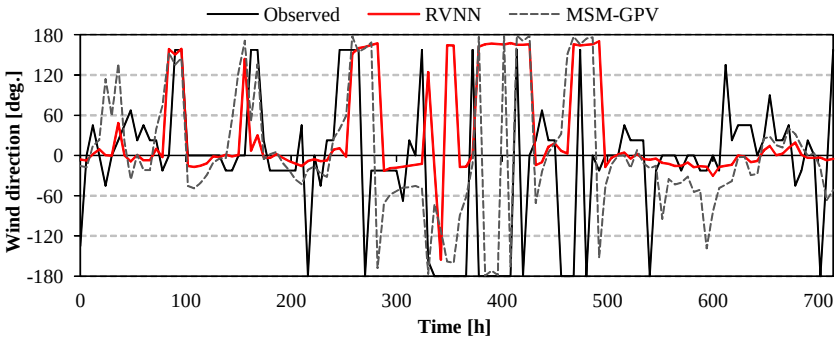

(b) Wind direction

Figure 4.12: Prediction results of wind speed and direction: RVNN (Mar. 2009)

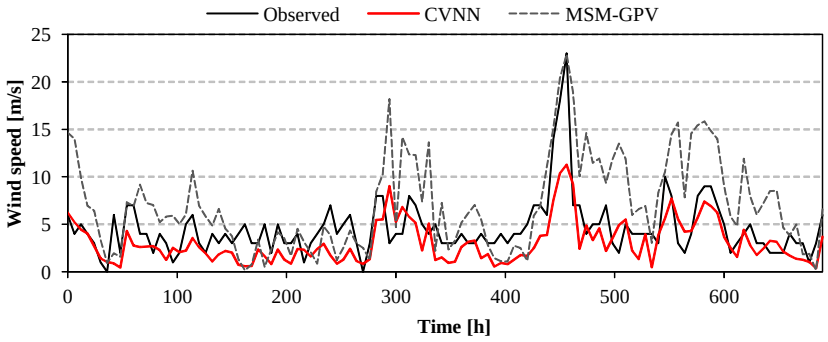

(a) Wind speed

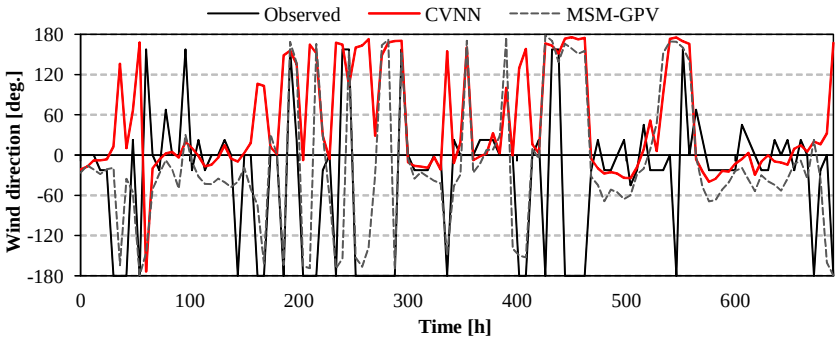

(b) Wind direction

Figure 4.13: Prediction results of wind speed and direction: CVNN (Apr. 2009)

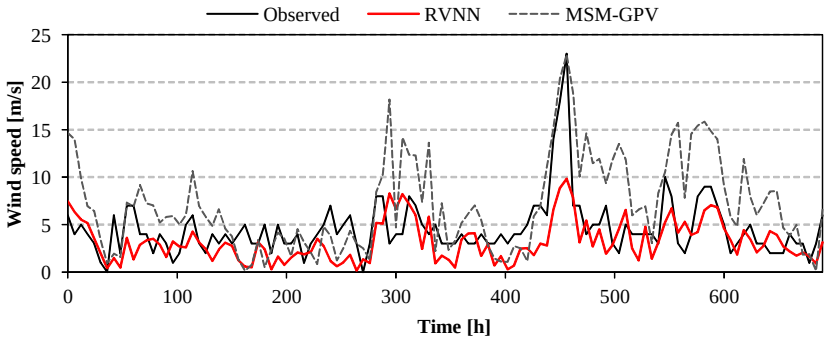

(a) Wind speed

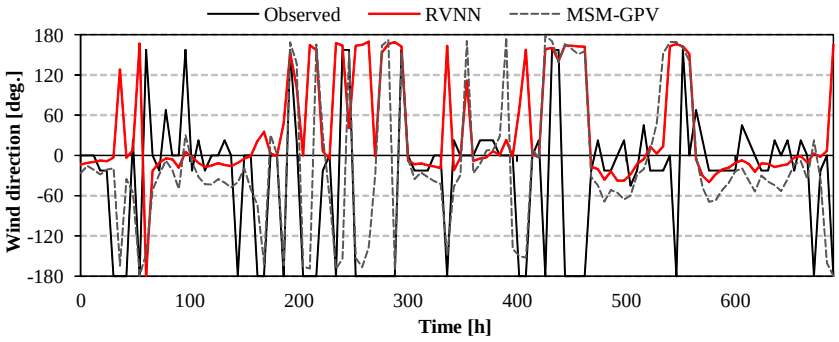

(b) Wind direction

Figure 4.14: Prediction results of wind speed and direction: RVNN (Apr. 2009)

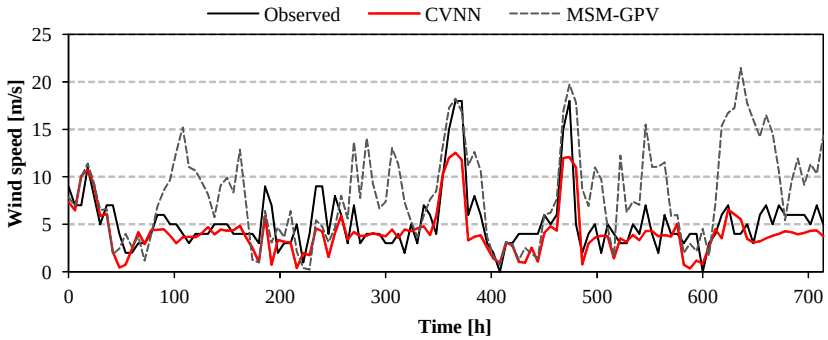

(a) Wind speed

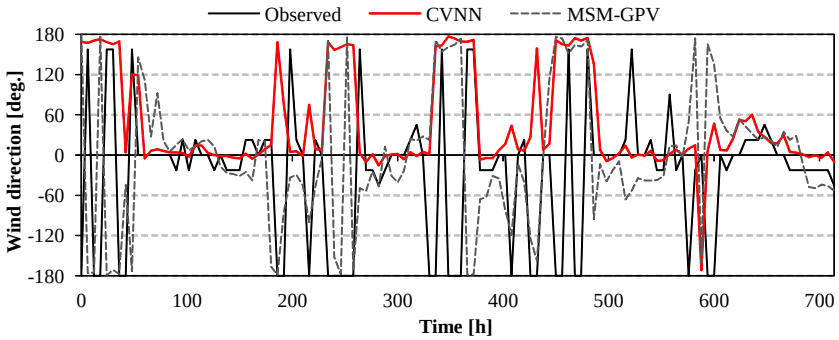

(b) Wind direction

Figure 4.15: Prediction results of wind speed and direction: CVNN (May 2009)

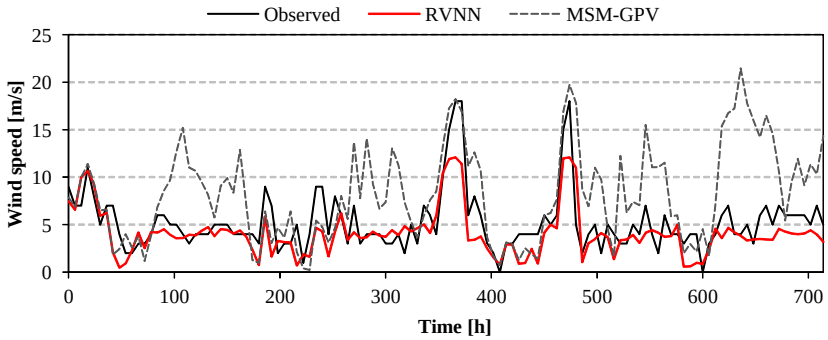

(a) Wind speed

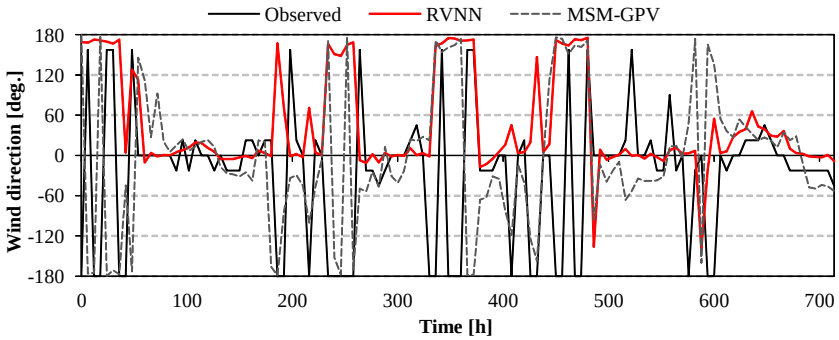

(b) Wind direction

Figure 4.16: Prediction results of wind speed and direction: RVNN (May 2009)

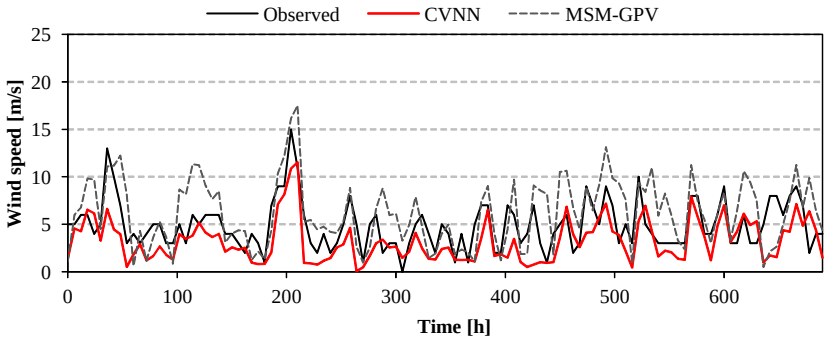

(a) Wind speed

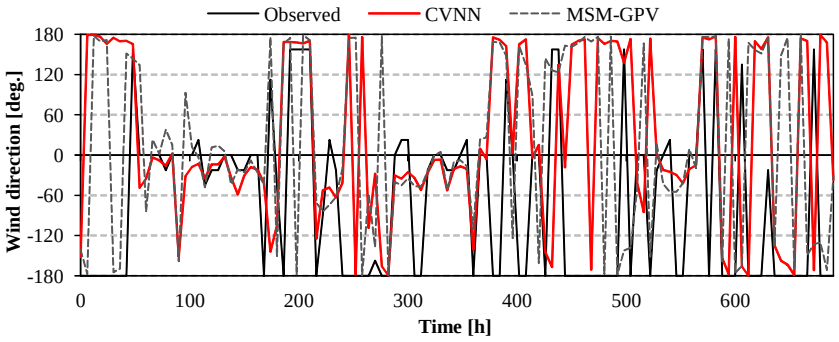

(b) Wind direction

Figure 4.17: Prediction results of wind speed and direction: CVNN (Jun. 2009)

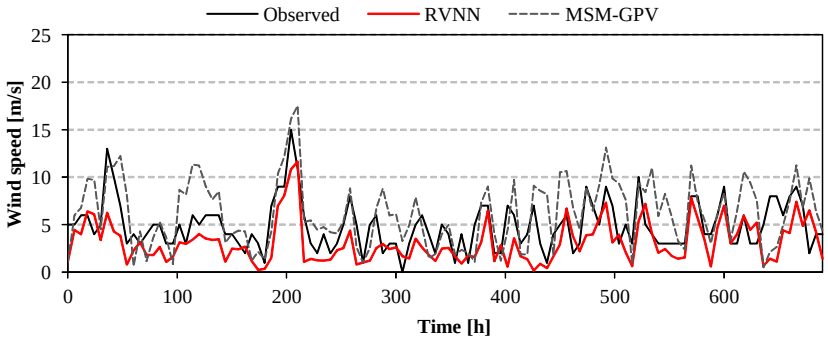

(a) Wind speed

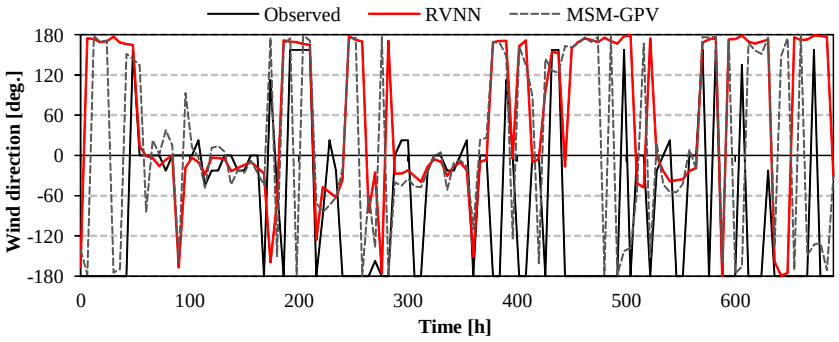

(b) Wind direction

Figure 4.18: Prediction results of wind speed and direction: RVNN (Jun. 2009)

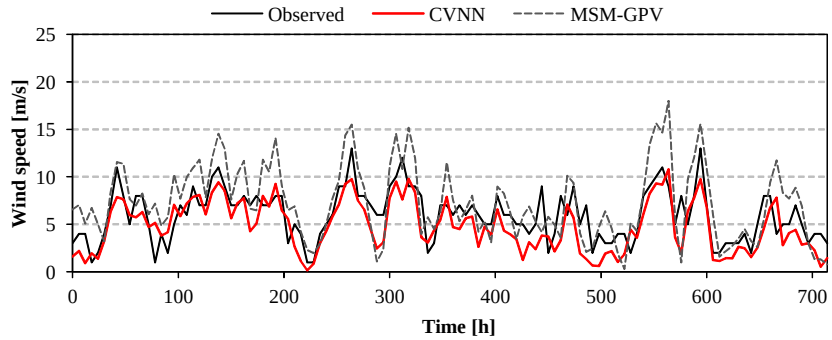

(a) Wind speed

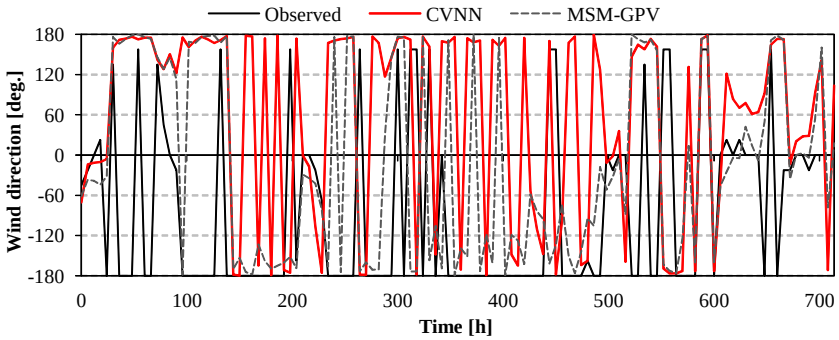

(b) Wind direction

Figure 4.19: Prediction results of wind speed and direction: CVNN (Jul. 2009)

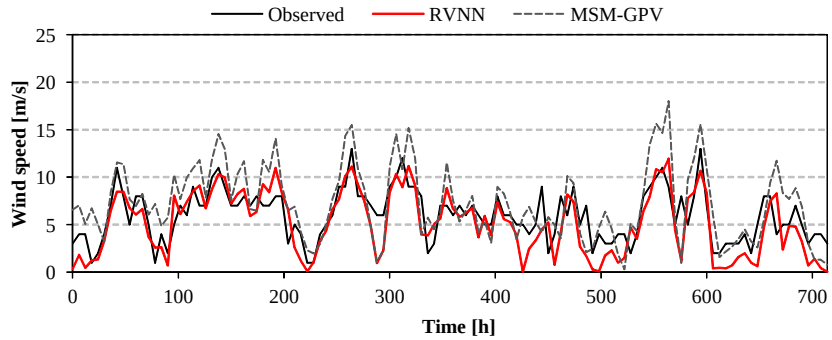

(a) Wind speed

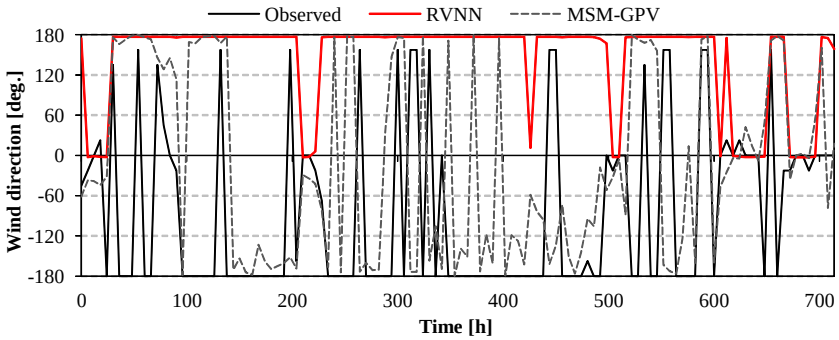

(b) Wind direction

Figure 4.20: Prediction results of wind speed and direction: RVNN (Jul. 2009)

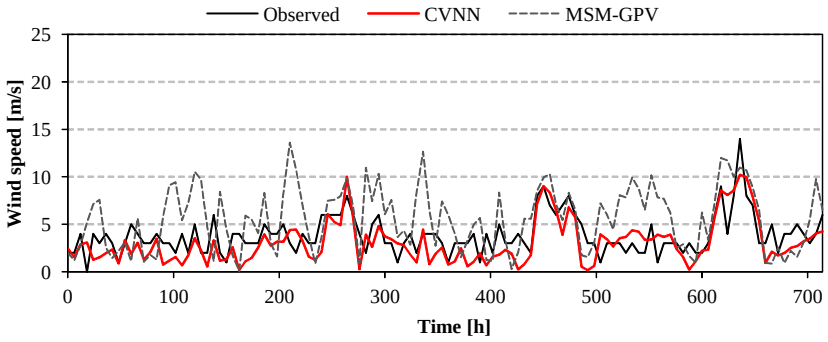

(a) Wind speed

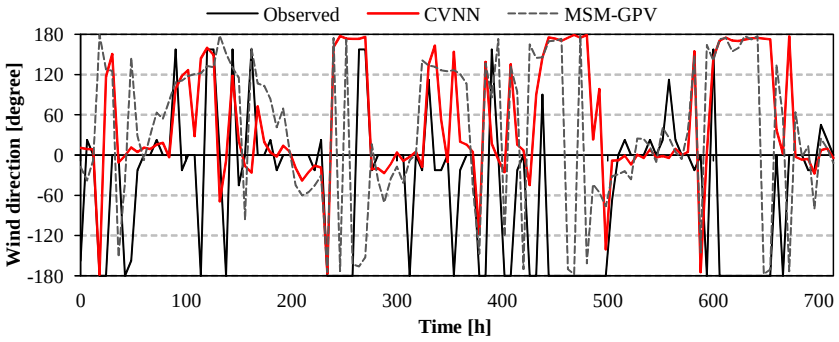

(b) Wind direction

Figure 4.21: Prediction results of wind speed and direction: CVNN (Aug. 2009)

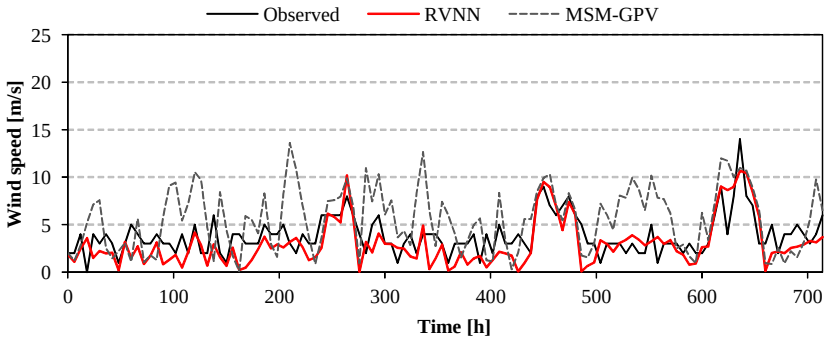

(a) Wind speed

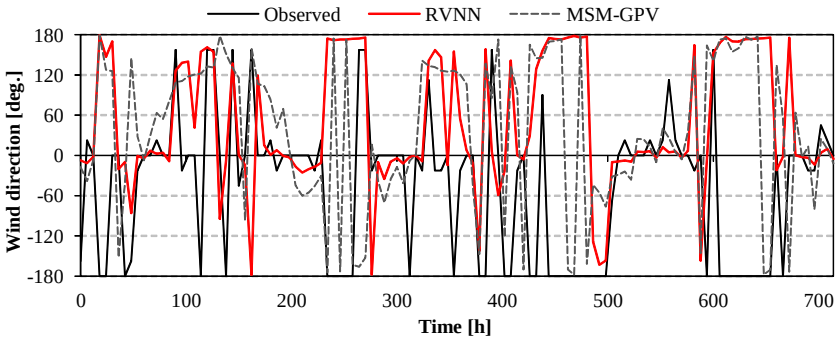

(b) Wind direction

Figure 4.22: Prediction results of wind speed and direction: RVNN (Aug. 2009)

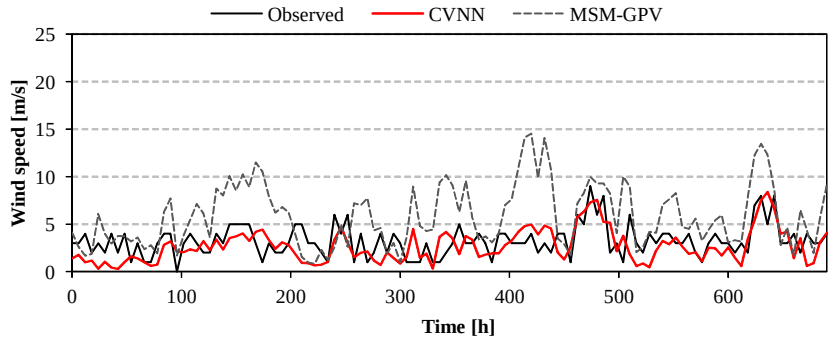

(a) Wind speed

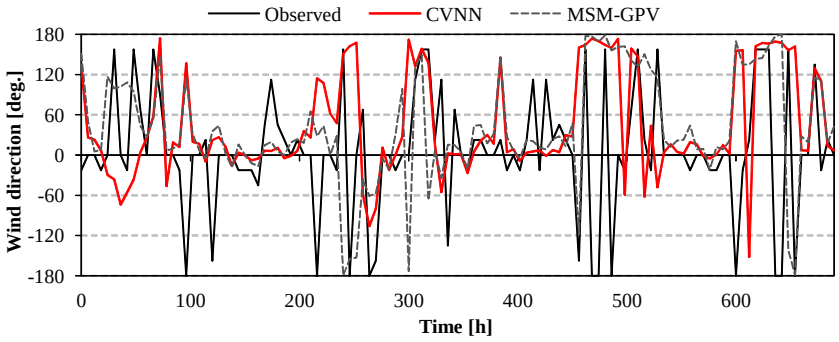

(b) Wind direction

Figure 4.23: Prediction results of wind speed and direction: CVNN (Sep. 2009)

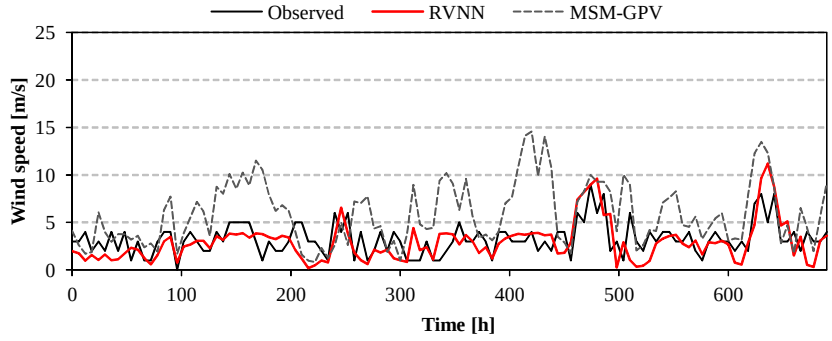

(a) Wind speed

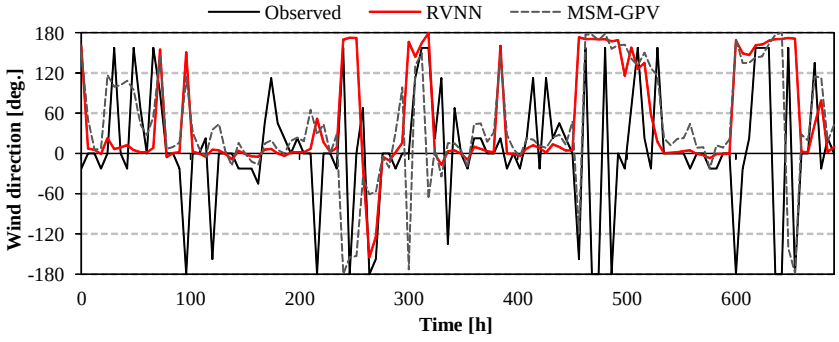

(b) Wind direction

Figure 4.24: Prediction results of wind speed and direction: RVNN (Sep. 2009)

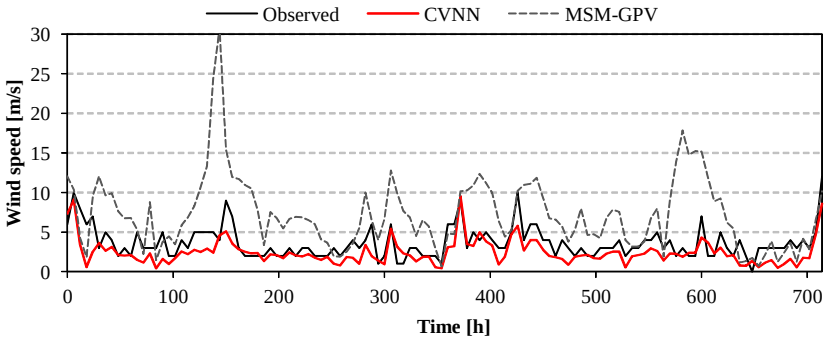

(a) Wind speed

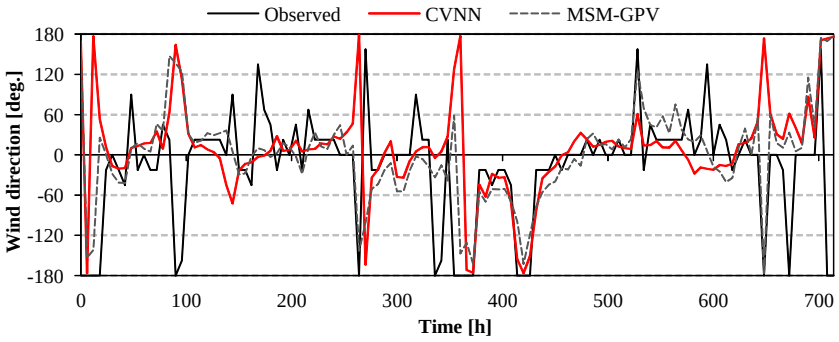

(b) Wind direction

Figure 4.25: Prediction results of wind speed and direction: CVNN (Oct. 2009)

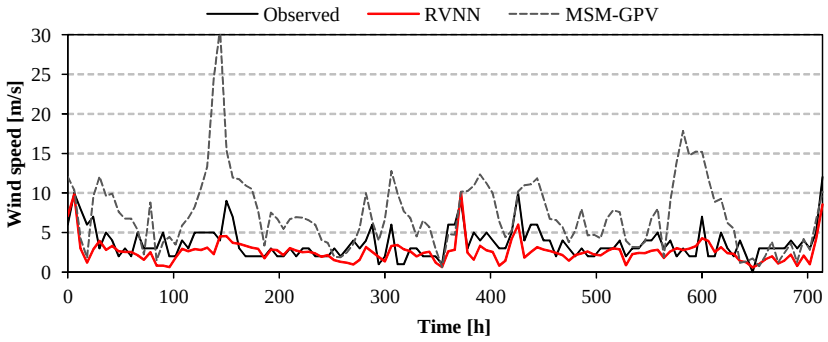

(a) Wind speed

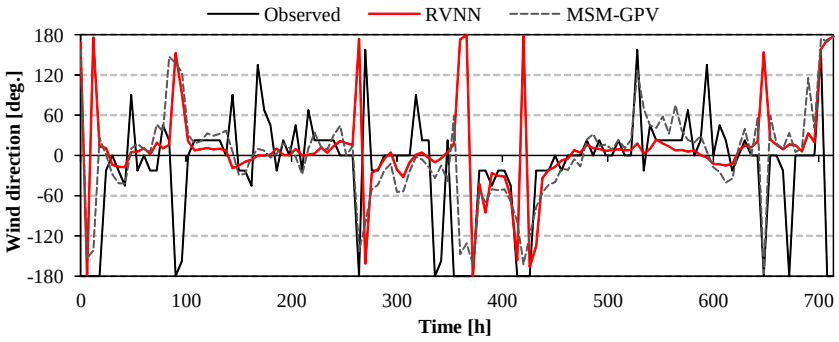

(b) Wind direction

Figure 4.26: Prediction results of wind speed and direction: RVNN (Oct. 2009)

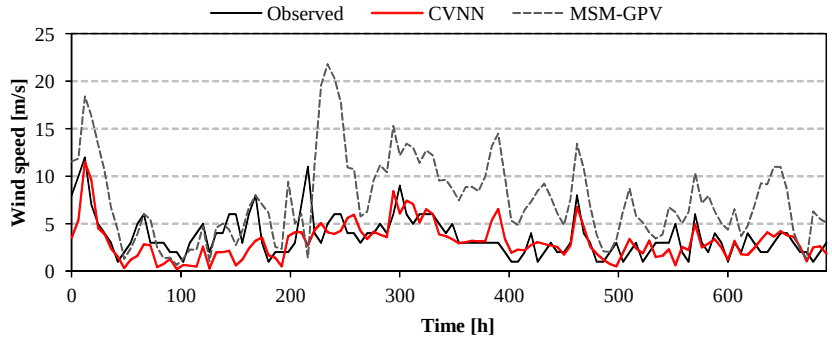

(a) Wind speed

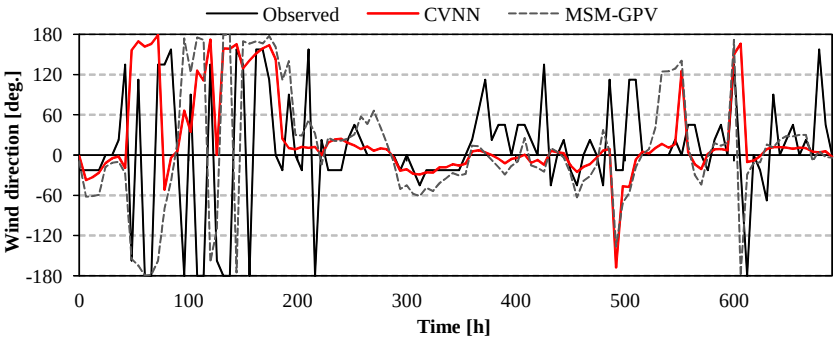

(b) Wind direction

Figure 4.27: Prediction results of wind speed and direction: CVNN (Nov. 2009)

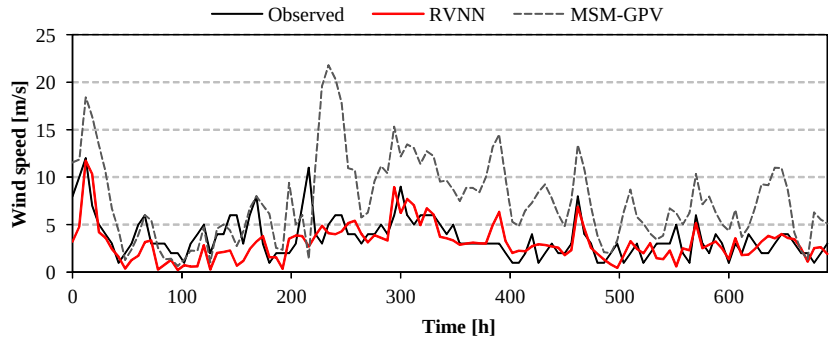

(a) Wind speed

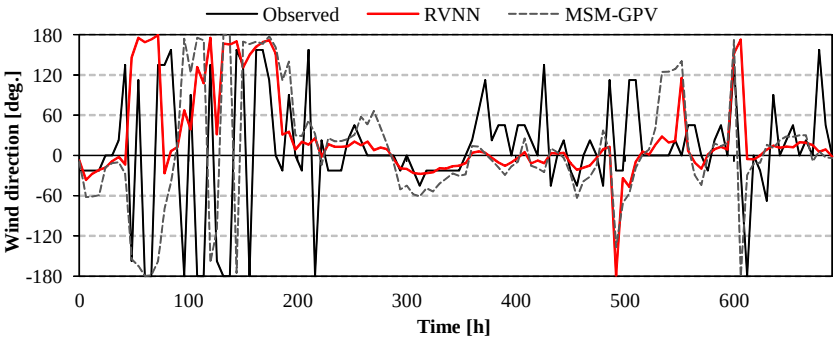

(b) Wind direction

Figure 4.28: Prediction results of wind speed and direction: RVNN (Nov. 2009)

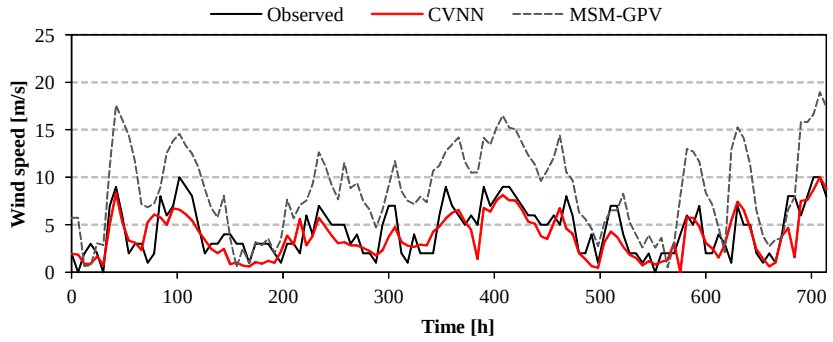

(a) Wind speed

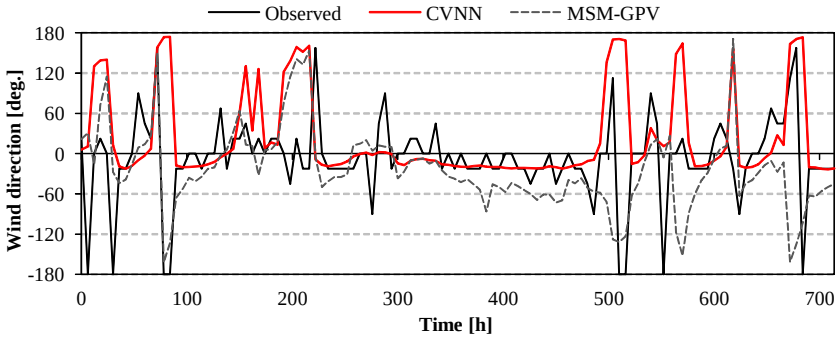

(b) Wind direction

Figure 4.29: Prediction results of wind speed and direction: CVNN (Dec. 2009)

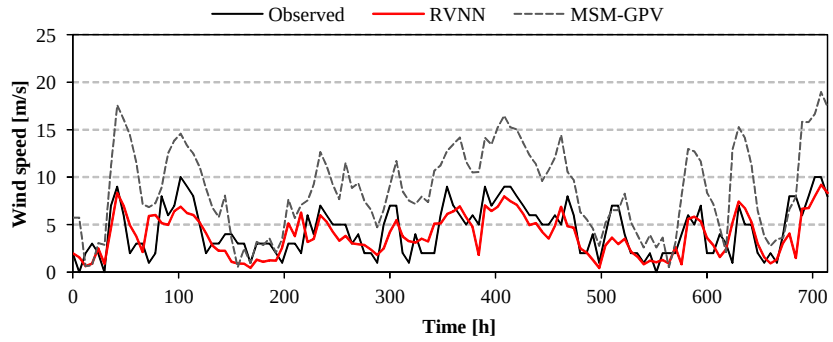

(a) Wind speed

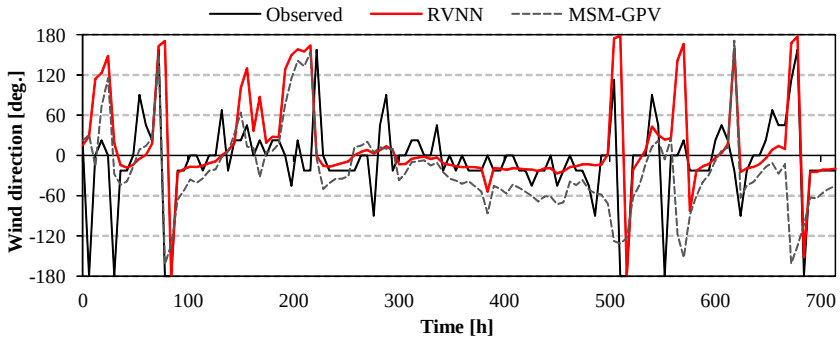

(b) Wind direction

Figure 4.30: Prediction results of wind speed and direction: RVNN (Dec. 2009)

the wind speed prediction with single-input using the CVNN, the MSM-GPV data, or the RVNN each month in 2009. At the bottom of the table, annual average of $RMSE$ is indicated for each prediction system. By comparing Table 4.2(a) with 4.2(b), it can be confirmed that the prediction result of wind speed using the CVNN with multi-input is the most accurate in all results. From Table 4.2, the prediction accuracy of the prediction system using the CVNN is better than that of using the RVNN is confirmed. And prediction accuracy of the prediction system using the CVNN with multi-input is better than with single-input.

Table 4.4 shows the average prediction error (MAE) of wind direction, and Table 4.5 shows the maximum error of wind direction prediction. As regards of MAE, the multi input is the better than single input for both the CVNN and the RVNN. Also as regard of maximum error of wind direction, all prediction systems are the almost same prediction accuracy.

Table 4.2: $RMSE$ [m/s] of wind speed prediction for each month

(a) Multi-input

Month	CVNN	MSM-GPV	RVNN
Jan.	1.68	5.42	1.75
Feb.	2.56	5.19	2.93
Mar.	3.53	6.49	3.53
Apr.	2.68	4.71	2.88
May	2.24	5.33	2.25
Jun.	2.59	3.18	2.70
Jul.	2.13	3.09	2.22
Aug.	1.84	3.72	1.88
Sep.	1.83	4.14	1.86
Oct.	1.82	5.69	1.83
Nov.	1.94	5.46	1.94
Dec.	1.83	5.26	1.87
Average	2.22	4.81	2.30

(b) Single-input

Month	CVNN	MSM-GPV	RVNN
Jan.	2.03	5.42	1.91
Feb.	2.74	5.19	2.86
Mar.	3.66	6.49	3.55
Apr.	2.69	4.71	2.72
May	2.44	5.33	2.40
Jun.	2.55	3.18	2.68
Jul.	2.17	3.09	2.24
Aug.	2.07	3.72	2.15
Sep.	2.01	4.14	1.96
Oct.	1.82	5.69	1.87
Nov.	2.01	5.46	2.02
Dec.	1.94	5.26	2.02
Average	2.34	4.81	2.37

Table 4.3: Maximum Error [m/s] of wind speed prediction for each month

(a) Multi-input

Month	CVNN	MSM-GPV	RVNN
Jan.	3.79	16.13	4.19
Feb.	10.70	14.64	10.34
Mar.	16.62	16.75	16.88
Apr.	11.74	15.16	13.16
May	6.24	17.46	6.59
Jun.	6.46	7.87	6.87
Jul.	5.99	9.00	6.75
Aug.	4.43	10.61	4.91
Sep.	4.17	11.13	6.19
Oct.	5.40	26.79	5.02
Nov.	8.28	16.80	8.28
Dec.	6.41	12.44	6.51
Average	7.52	14.57	7.97

(b) Single-input

Month	CVNN	MSM-GPV	RVNN
Jan.	6.18	16.13	4.98
Feb.	9.63	14.64	10.91
Mar.	17.99	16.75	18.07
Apr.	10.49	15.16	11.47
May	7.67	17.46	6.95
Jun.	7.26	7.87	7.70
Jul.	6.30	9.00	7.52
Aug.	5.30	10.61	5.83
Sep.	4.59	11.13	4.52
Oct.	5.04	26.79	5.42
Nov.	9.89	16.80	9.67
Dec.	6.49	12.44	6.66
Average	8.07	14.57	8.31

Table 4.4: MAE of prediction result of wind direction for each month [degree]

(a) Multi-input

Month	CVNN	MSM-GPV	RVNN
Jan.	39.16	54.34	40.60
Feb.	40.22	45.36	41.03
Mar.	51.68	55.61	49.47
Apr.	34.88	45.19	36.66
May	32.31	38.94	32.34
Jun.	31.93	40.80	30.03
Jul.	32.98	36.76	28.84
Aug.	43.56	57.24	41.55
Sep.	45.93	49.45	40.60
Oct.	32.21	36.61	30.13
Nov.	42.57	48.40	42.15
Dec.	38.75	47.28	36.98
Average	38.85	46.33	37.53

(b) Single-input

Month	CVNN	MSM-GPV	RVNN
Jan.	36.85	54.34	36.56
Feb.	47.95	45.36	46.13
Mar.	53.33	55.61	52.49
Apr.	39.48	45.19	37.63
May	33.43	38.94	34.78
Jun.	37.89	40.80	36.88
Jul.	37.33	36.76	29.80
Aug.	47.00	57.24	47.99
Sep.	45.82	49.45	43.53
Oct.	28.76	36.61	28.72
Nov.	39.60	48.40	40.28
Dec.	40.51	47.28	39.62
Average	40.66	46.33	39.53

Table 4.5: Maximum error of simulation result of wind direction [degree]

(a) Multi-input

Month	CVNN	MSM-GPV	RVNN
Jan.	177.21	170.67	179.61
Feb.	175.98	177.58	178.51
Mar.	179.58	178.51	177.06
Apr.	173.30	175.63	179.97
May	178.92	171.13	178.42
Jun.	162.24	166.27	166.68
Jul.	174.41	168.85	178.32
Aug.	178.84	178.12	179.62
Sep.	179.97	175.51	177.18
Oct.	175.54	154.04	169.90
Nov.	173.31	169.13	174.67
Dec.	178.85	175.80	178.41
Average	175.68	171.77	176.53

(b) Single-input

Month	CVNN	MSM-GPV	RVNN
Jan.	175.70	170.67	175.57
Feb.	179.34	177.58	176.44
Mar.	179.10	178.51	175.04
Apr.	176.20	175.63	179.75
May	177.77	171.13	179.96
Jun.	177.20	166.85	165.53
Jul.	179.26	168.85	179.58
Aug.	177.85	178.12	179.87
Sep.	176.64	175.51	178.89
Oct.	172.02	154.04	171.84
Nov.	171.44	169.13	175.19
Dec.	176.97	175.80	178.69
Average	176.62	171.77	176.36

In order to prove the validity of the proposed system that uses the CVNN with multi-input, the t-test is conducted by comparing with the other systems. The t-test is often used to evaluate whether the means of two groups has statistically different each other or not. The t-test needs t-value, which is ratio between difference of mean of two groups and standard deviation of two groups difference. To test the significance, a risk (significance) level needs to set that is usually set at 5% in most of research. The degree of freedom (dof) for the test also needs to determine that is 11 in this time because sample data is 12 (Jan.∼Dec.). The t-value is 2.597 when comparing prediction result using the CVNN with RVNN. Since the significance level, the dof, and the t-value are given, the t-value can be looked up whether is larger than significant or not. When the dof is 11 and the significance level is 5%, the significant t-value is 2.201 from standard table of significance. Thus, the t-value 2.597 is higher than 2.201, the prediction system using the CVNN is significant than using the RVNN can be concluded. On the other hand, the comparison of prediction system using the CVNN with multi-input with single-input is done. Since t-value is 3.739, accuracy of wind speed prediction system using the CVNN with multi-input is significant than with single-input. In addition, when the significant level is set to 1%, significant value is 3.106. Therefore, prediction system using the CVNN with multi-input is significant than with single-input in 1% significant level.

In Tables 4.3(a) and (b), the maximum error of wind speed prediction for each month are indicated. At the bottom of the table, annual average of maximum error is shown for the each prediction system. By compared Table 4.3(a) with (b), the maximum prediction error of wind speed using the CVNN with multi-inputs can be seen as the lowest in all results. Error reduction rate of the proposed prediction system is 5.6% compared with the RVNN in Table 4.3(a). Besides, error reduction rate is 9.5% compared with the RVNN with single-input in Table 4.3(b).

CHAPTER 5

Extremely Short Term Prediction System of Wind Speed

5.1 Extremely short-term prediction system of wind speed

Figure 5.1 shows the configuration of the wind speed prediction system using a recurrent typed CVNN, which consists of three layers: input layer with context layer, hidden layer, and output layer. The numbers of neurons of each layers are as follows: input layer, 10; hidden layer, 10; and output layer, 1. In this system, the CVNN has internal feedback structure called Elman type which is connected to context layer from hidden layer. Therefore, it is said that the recurrent typed neural network such as Elman type is suitable for processing time series data [55–58]. The input information of the CVNN is observed wind speed from 10 seconds ago to the present at one second interval T and average. By input them to the CVNN, the CVNN output predicted wind speed $\hat{v}(t+T)$ a second ahead (ex. $k=1$). The wind speed data are observed at Department of Electrical and Electronic Engineering, The University of Tokushima, Japan by ultra sonic wind sensor WT-700 (Vaisala). Table 5.1 and Fig. 5.2 show the auto-correlation of wind speed for learning data of the CVNN. Generally, it is said that correlation value under 0.2 means no correlation between the two data. Thus, it is sufficiently that the proposed prediction system is input observed wind speed data up to 10 second. Table 5.2 indicates parameters of the CVNN which are decided by

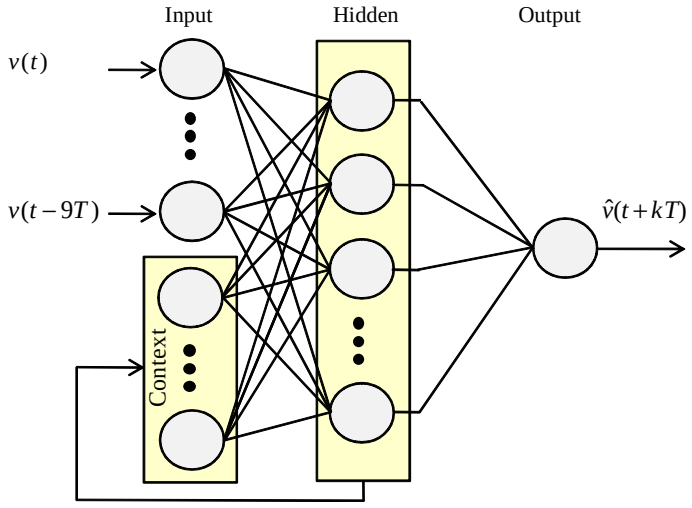

Figure 5.1: Wind speed prediction system in extremely short-term using CVNN

Table 5.1: Auto-correlation value of wind sped of learning data

Step time [s]	1	2	3	4	5
Correlation	0.690	0.498	0.381	0.303	0.251
Step time [s]	6	7	8	9	10
Correlation	0.219	0.191	0.181	0.165	0.154
Step time [s]	11	12	13	14	15
Correlation	0.133	0.126	0.118	0.104	0.092

trial and error approach. The sigmoid function $f(x)$ of the CVNN is as follows:

$$f(x) = \tanh(x) \qquad [-1 < f(x) < 1\ ] \tag{5.1}$$

where x is the net value. The learning of the CVNN is conducted by using the complex-valued BP. Then the initial value of weights is set from -0.1 to 0.1 randomly.

Figure 5.3 shows the transition of root mean square error, $RMSE$ [m/s] while the CVNN was learning. And then the transition of $RMSE$ while the RVNN is learning is also indicated in the same figure as a comparison object. The parameters of the RVNN is shown in Table 5.3 and Table 5.4 which are decided as the same scale as the CVNN. There are two method to decide the number of the hidden layer's neuron. The first is method the number of neuron is decided and indicated as RVNN-I so that the number of neuron of the RVNN just becomes double size compared with the CVNN. The second is

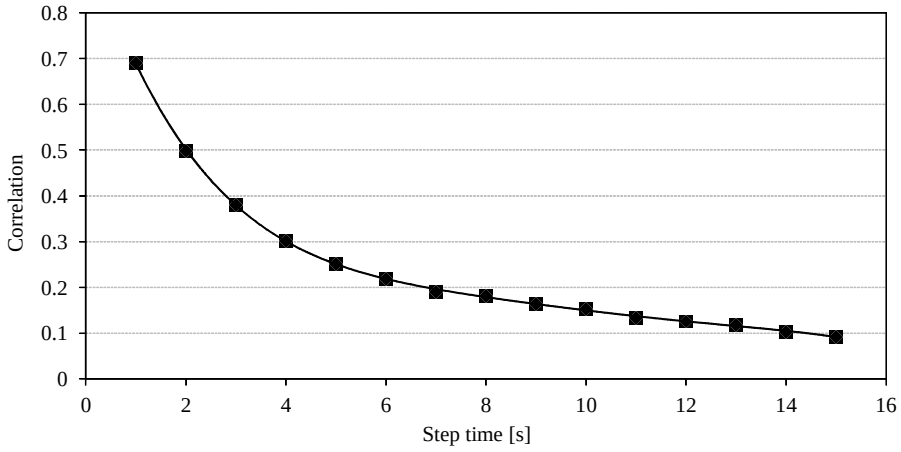

Figure 5.2: Auto-correlation value of wind speed of learning data

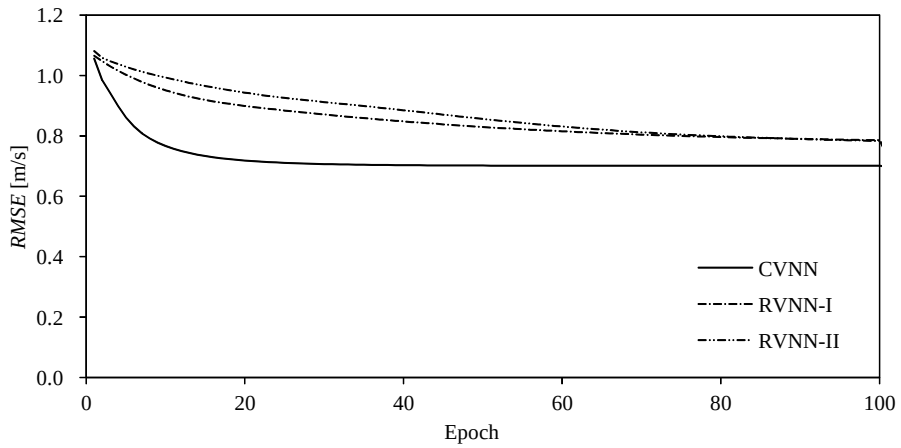

Figure 5.3: Transition of $RMSE$ during learning

method the number of neuron is decided and indicated as RVNN-II so that the number of connection becomes the same as that of the CVNN. The connection number of the CVNN is counted real part and imaginary part of connection as independent. From this result, it is confirmed that leaning error is convergent and the CVNN is used, which has been learned, for wind speed prediction.

5.2 Wind speed prediction results of extremely short-term

To confirm the usefulness of the proposed prediction system, the wind speed is predicted a second ahead by using the CVNN which have learned. Here, it is important to note that the wind speed data for evaluation (prediction) is not used as the

Table 5.2: Parameters of the CVNN

The number of neuron			Epoch	Coefficient
Input	Hidden	Output		
10	10	1	100	0.001

Table 5.3: Parameters of the RVNN-I

The number of neuron			Epoch	Coefficient
Input	Hidden	Output		
20	20	2	100	0.001

Table 5.4: Parameters of the RVNN-II

The number of neuron			Epoch	Coefficient
Input	Hidden	Output		
20	10	2	100	0.001

supervised data for learning the CVNN. At first, the CVNN have learned by using the first half of wind speed data of six hours (21,600 points data) that have been observed on April 7th as shown in Fig. 5.4. The other half of wind speed data (three hours) are used as a evaluation data for the CVNN. Figure 5.5(a) $\sim$ (c) show prediction result of wind speed a second ahead, while Fig. 5.5(a) indicates whole prediction result of three hours, Fig. 5.5(b) indicates prediction result of 30 minutes and Fig. 5.5(c) indicates prediction result of 180 seconds. From this result, predicted wind speed is agreement with lower wind speed region. Because wind speed data used for learning process has lower wind characteristics which is 1.6 m/s in average. Therefore, the CVNN have learned to adapt to low wind speed. Figure 5.6 (a) and (b) show wind speed prediction result for three hours by using RVNN-I and RVNN-II, respectively. In addition, Fig. 5.7 (a) and (b) show wind speed prediction result for first 180 seconds of three hours by using RVNN-I and RVNN-II, respectively. Table 5.5 shows prediction error of proposed prediction system and comparison system for both RVNN, and persistent model which is a conventional method and often used in short-term prediction [59, 60]. The prediction algorithm of persistent model is indicated below:

$$\hat{v}_{i+k} = v_i \tag{5.2}$$

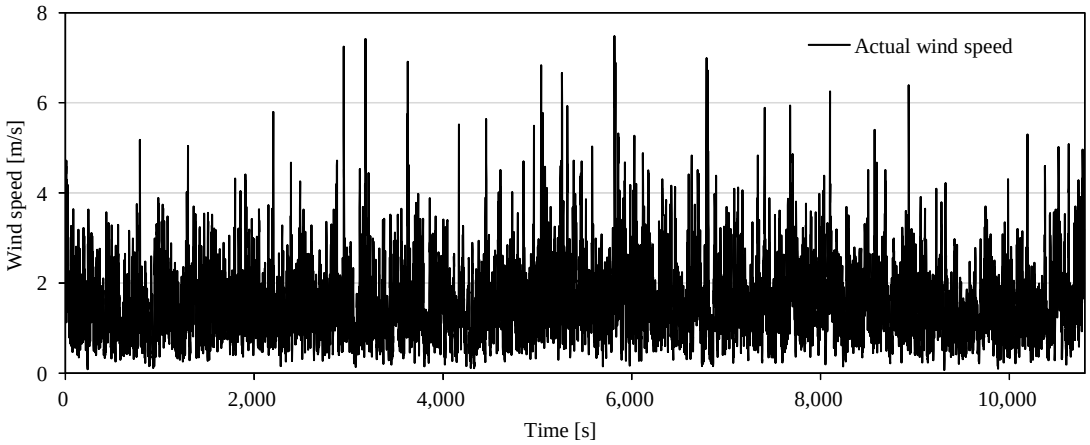

Figure 5.4: Wind speed data for learning (three hours, April 7th)

where k is the constant ($k = 1, 2, 3, ...$) and for example $k = 1$, v_{i+1} means one step ahead prediction. This equation means that wind speed at the present v_i becomes predicted wind speed v_{i+k} which is k step ahead. In Table 5.5, two kind of evaluation method is indicated which are mean average percentage error ($MAPE$) and root mean square error ($RMSE$). The definition of each evaluation function is as follows:

$$MAPE = \frac{1}{N}\sum_{i=0}^{N-1}\frac{|v_i - \hat{v}_i|}{v_i} \times 100 \tag{5.3}$$

$$RMSE = \sqrt{\frac{1}{N}\sum_{i=0}^{N-1}(v_i - \hat{v}_i)^2} \tag{5.4}$$

where v_i is the i-th actual wind speed, $\hat{v}_i$ is the i-th predicted wind speed, N is the number of prediction pattern. From Table 5.5, the proposed prediction system by using CVNN has good ability than the RVNN is shown. However, the results of persistent model is lower prediction error in $RMSE$ and maximum error evaluation. It is because of the definition of error equation in BP method (4.4), (4.8), and (4.9). These equations mean that CVNN learns difference $(v - \hat{v})$ between output $\hat{v}$ of NN and supervised data v even though the definition of error E is square function.

Moreover, wind speed prediction is conducted in different wind data on June 19th for evaluating prediction accuracy. Figure 5.8 and Fig. 5.9 show predicted wind speed and actual wind speed of simulation result in 410 seconds by using the CVNN and the RVNN, respectively. And Table 5.6 indicates prediction error in $MAPE$, $RMSE$, and maximum error. The proposed prediction system is confirmed has prediction ability

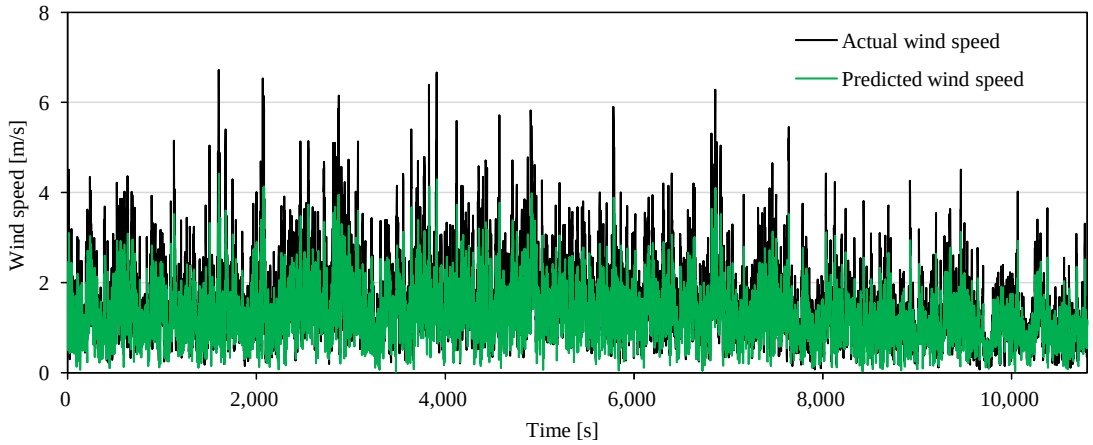

(a) Whole prediction result for three hours

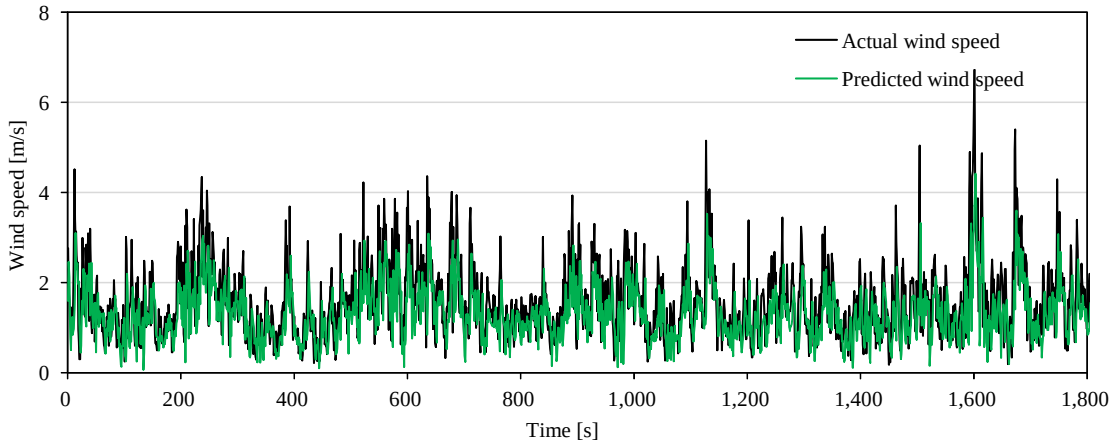

(b) Prediction result for first 30 minutes

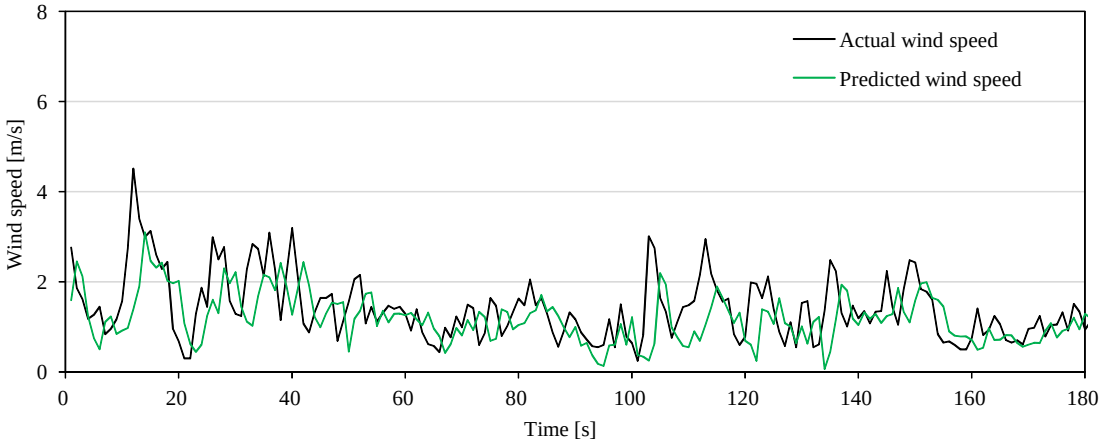

(c) Prediction result for first 180 seconds

Figure 5.5: Prediction results of wind speed a second ahead (April 7th): CVNN

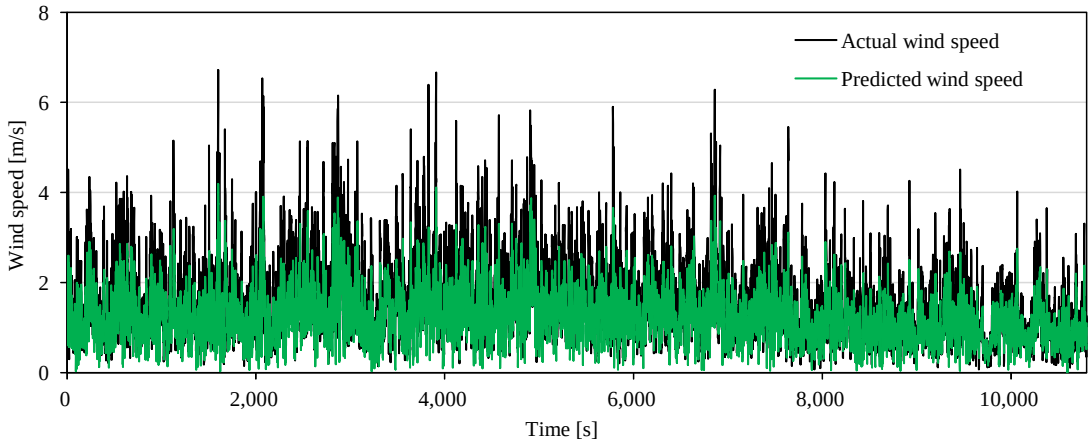

(a) RVNN-I

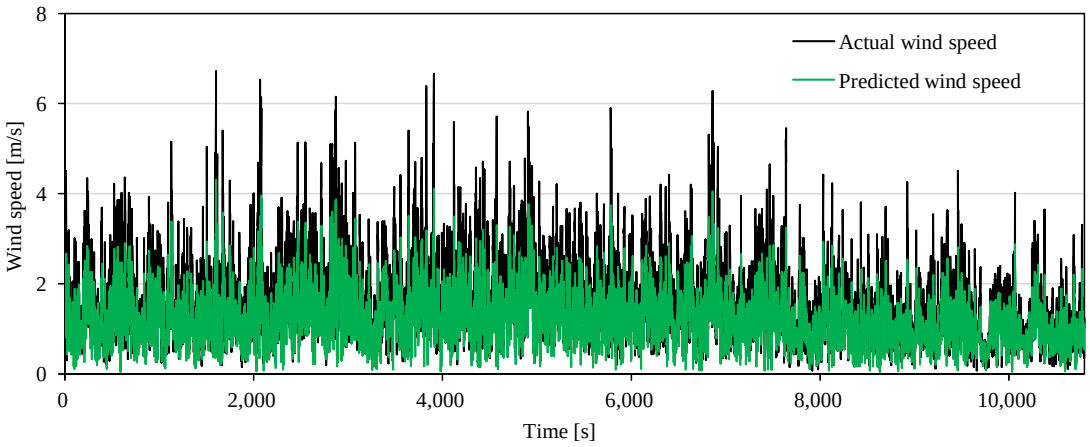

(b) RVNN-II

Figure 5.6: Prediction results of wind speed a second ahead (April 7th) whole prediction result for three hours

better than prediction system using RVNN. Besides, by comparing with persistent model, proposed system has advantage in $MAPE$ evaluation.

From those prediction result mentioned above, the prediction accuracy of the proposed system is confirmed has better ability compared with the RVNN. However, by comparing with persistent model, prediction accuracy in $MAPE$ is improved. As regarding $RMSE$ and maximum error, the improvement of prediction accuracy could not be seen. Therefore, the learning algorithm of NN needs to consider in order to improve not only average error but also maximum error.

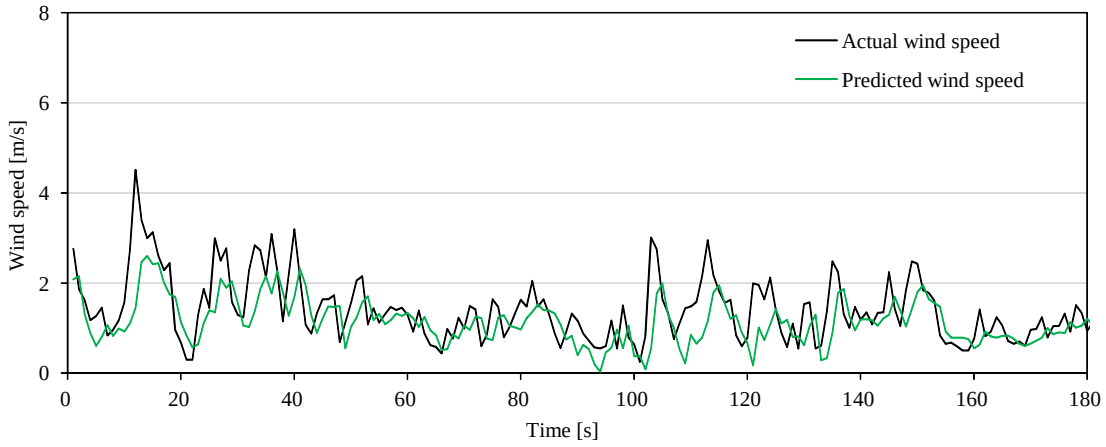

(a) RVNN-I

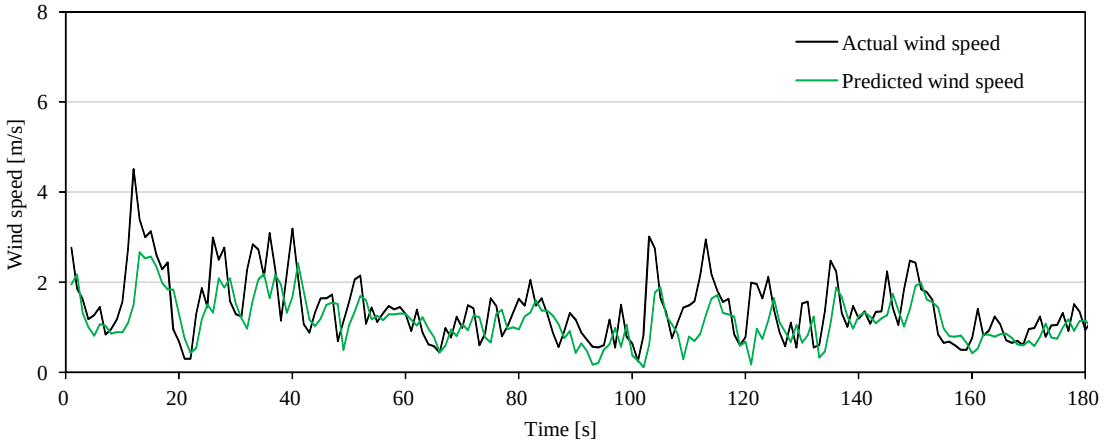

(b) RVNN-II

Figure 5.7: Prediction results of wind speed a second ahead (April 7th) prediction result for first 180 seconds of three hours

Table 5.5: Prediction error of simulation result (April 7th): Comparison proposed system CVNN with RVNN, and persistent model: Learning data is the first half of wind data on April 7th

	$MAPE$ [%]	$RMSE$ [m/s]	Maximum Error [m/s]
CVNN	33.81	0.67	5.15
RVNN-I	34.77	0.71	5.25
RVNN-II	34.57	0.70	5.34
Persistent model	35.17	0.64	4.95

Table 5.6: Prediction error of simulation result (June 19th): Comparison proposed system CVNN with RVNN, and persistent model: Learning data is the first half of wind data on April 7th

	$MAPE$ [%]	$RMSE$ [m/s]	Maximum Error [m/s]
CVNN	36.97	1.08	3.11
RVNN-I	40.21	1.20	3.33
RVNN-II	38.16	1.10	3.27
Persistent model	38.47	0.91	2.61

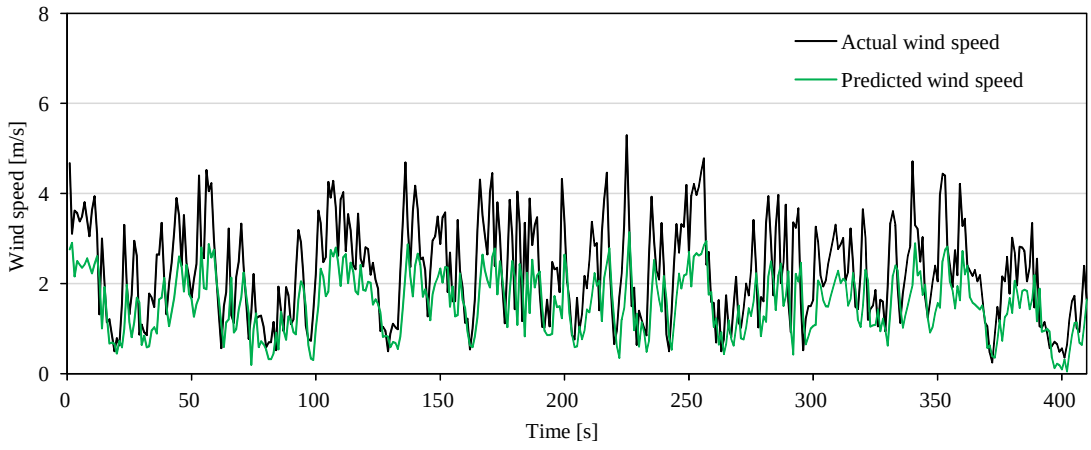

Figure 5.8: Prediction results of wind speed a second ahead (June 19th): CVNN

In next simulation, the first half of wind speed data on June 19th was used for learning the CVNN and the RVNN, respectively. And the last half of wind speed data

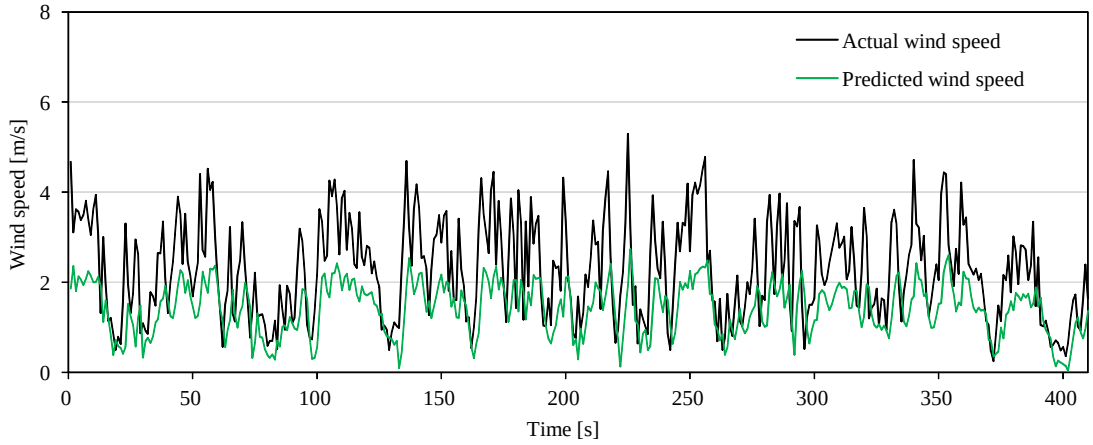

(a) RVNN-I

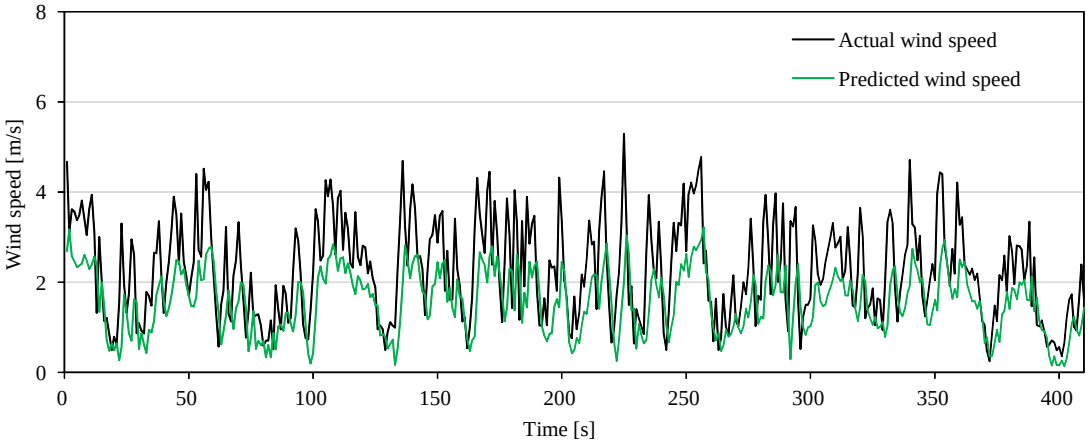

(b) RVNN-II

Figure 5.9: Prediction results of wind speed a second ahead (June 19th): RVNN

Table 5.7: Prediction error of simulation result (June 19th): Comparison proposed system CVNN with RVNN, and persistent model: Learning data is the first half of wind data on June 19th

	$MAPE$ [%]	$RMSE$ [m/s]	Maximum Error [m/s]
CVNN	38.33	0.84	3.02
RVNN-I	40.33	0.91	3.16
RVNN-II	38.41	0.87	3.04
Persistent model	38.47	0.91	2.61

Table 5.8: Prediction error of simulation result (Apr 7th): Comparison proposed system CVNN with RVNN, and persistent model: Learning data is the first half of wind data on June 19th

	$MAPE$ [%]	$RMSE$ [m/s]	Maximum Error [m/s]
CVNN	47.85	0.74	4.95
RVNN-I	59.74	0.85	5.78
RVNN-II	58.83	0.90	5.85
Persistent model	35.17	0.64	4.95

on June 19th and whole data on April 7th were used for evaluating the CVNN and the RVNN. Table 5.7 indicates the prediction error on June 19th, and Table 5.8 indicates the prediction error on April 7th.

Table 5.9 indicates the prediction error of wind direction that the learning data is the first half of wind data on April 7th, the evaluation data are the last half of wind data on April 7th and whole data on June 19th. Table 5.10 indicates the prediction error of wind direction that the learning data was the first half of wind data on June 19th, the evaluation data were the last half of wind data on June 19th and whole data on April 7th. From these tables, the prediction error of wind direction is the almost same in each prediction system, except for the result of April 7th in Table 5.10. The simulation result of April 7th in Table 5.10, the CVNN keep the prediction error of wind direction lower compared with other prediction system.

Table 5.9: Prediction error of simulation result (wind direction): Comparison proposed system CVNN with RVNN, and persistent model: Learning data is the first half of wind data on April 7th

	April 7th		June 19th	
	MAE [deg.]	Maximum [deg.]	MAE [deg.]	Maximum [deg.]
CVNN	31.92	179.83	29.39	176.47
RVNN-I	32.23	179.91	29.46	174.57
RVNN-II	32.05	179.45	29.37	162.65

Table 5.10: Prediction error of simulation result (wind direction): Comparison proposed system CVNN with RVNN, and persistent model: Learning data is the first half of wind data on June 19th

	June 19th		April 7th	
	MAE [deg.]	Maximum [deg.]	MAE [deg.]	Maximum [deg.]
CVNN	25.24	142.91	45.98	179.99
RVNN-I	24.08	168.80	90.64	179.99
RVNN-II	24.42	168.56	86.79	179.99

CHAPTER 6

Conclusions and Future Works

6.1 Conclusions

In this dissertation, a maximum power control system of a wind turbine by using predicted wind speed and a wind speed prediction system are mainly discussed.

There are many researches discuss about maximum power control of wind turbines by using a variety of hill climbing methods because of the large inertia of wind turbine. The preceding researches use current information such as wind speed, output voltage, generated electrical power, etc. Then, the time lag of control will occur by the influence of wind turbine inertia in environment with turbulence and it causes degradation of generated power. In order to extract maximum power from wind turbines, it is necessary that the rotational speed of wind turbines should be adjusted at optimal point in the real time but it is difficult. Therefore, a novel approach of maximum power control system for small wind turbines in wind variability environment by using predicted wind speed data is proposed. The features of the proposed control system are to use future information which is predicted wind speed and to set a reference trajectory of the rotational speed of the wind turbine based on both the predicted wind speed ahead of a few seconds and the mechanical time constant of the wind turbine. The effect of using the predicted data is that the controller can operate the wind turbine efficiently so that the rotational speed of the wind turbine catches up with the reference speed at maximum power point.

Until now, the wind speed prediction systems from 10 minutes to several hours ahead have been studied for applying to operation of power system and wind turbine control. Those prediction system are consisted by using a complex-valued neural net-

work (CVNN), a real-valued neural network (RVNN), or self-tuning fuzzy reasoning. And the effectiveness of those systems are confirmed. The prediction system consisting of the CVNN can take into account wind dynamics in two dimensional space by expressing wind data as a vector, which has both magnitude and direction, because the CVNN has a good ability for treating a complex-value. Due to that kind of the capability of the CVNN, improvement of prediction accuracy was seen comparing with a prediction system using the RVNN.

In order to confirm the validity of proposed control system and prediction system, the computer simulations are conducted. From simulation results of wind turbine control, the proposed control system is confirmed has better ability for generation efficiency compared with other comparison objects including conventional system. Then the improvement rate of generation efficiency reached about 12.6 % in case that predicted wind speed is obtained accurately without error. As regards the wind speed prediction system, the prediction system by using the CVNN has advantage of better prediction accuracy compared with the RVNN. For long-term prediction, the hierarchical typed CVNN and two dimensional wind data expressed by complex number to predict wind speed and direction by taking into account wind flow in two dimensional space is applied. For short-term prediction, the recurrent typed CVNN and observed series wind data expressed by complex number to predict wind speed and direction by taking into account wind flow and time series dynamics is applied. Simulation results demonstrate the validity of the proposed prediction systems. Then, the prediction system consisted of the CVNN is confirmed has better ability compared with that of the RVNN.

6.2 Future works

In terms of maximum power control system, the model of wind turbine is essential for proposed control system to set the reference trajectory of rotational speed to conduct experiment in real environment. It is because of the wind turbine has nonlinear characteristics, modeling method for nonlinear system is required. Here, a neural network can treat nonlinear data well and unknown system as regarding relation between input and output. Therefore, it is necessary to employ a neural network which is suitable for modeling wind turbine performance.

In addition, more accurate wind speed prediction system is desired. To introduce large scale wind turbines, wind speed prediction system is essential for running stably power systems at high quality level. In this dissertation, the wind speed prediction system by using the CVNN and multipoint data of MSM-GPV is proposed. Then, four points of MSM-GPV is used. According to Japan Meteorological Agency, treating data which is five to eight times for grid interval is needed to express wind flow in detail. It means that about 36 to 81 points of MSM-GPV data around prediction point are desired and will be implemented for next future.

As regards of short-term prediction, a novel learning algorithm and suitable learning data for nonlinear time series prediction such as wind speed needs to be considered. The present back propagation algorithm for learning a neural network has ability limitation for learning wind speed data. By trade-off problem between generalization performance and deep learning, it is also difficult for decision of the parameters of neural network. The CVNN realize stable learning compared with the RVNN, because the learning algorithm of the CVNN which is complex-valued back propagation has good ability for avoiding stuck in local minimum. Because a weight connection of the CVNN has real part and imaginary part component, even if the real part of weight is stuck the imaginary part of weight is usually not. Therefore, the problem of learning algorithm with suitable learning data will be the future task in the CVNN system.

◇ ◇ ◇ ◇ REFERENCES ◇ ◇ ◇ ◇

[1] Global Wind Energy Council: Global Wind Report Annual Market Update 2012, p. 8, Global Wind Energy Council, Belgium (2013)

[2] A. Grant, C. Johnstone, and N. Kelly: "Urban Wind Energy Conversion: The Potential of Ducted Turbines", Renewable Energy, Vol. 33, No. 6, pp. 1157–1163 (Jun. 2008)

[3] E. Dayan: "Wind Energy in Buildings: Power Generation From Wind in The Urban Environment - Where it is needed most", Refocus, Vol. 7, No. 2, pp. 33–34, 36, 38 (Mar./Apr. 2006)

[4] H. Tokuyama, Y. Nishizawa, and I. Ushiyama : "A Power Performance of a Micro Wind Turbine for Field Test on the Urban Site", J. of JWEA, Vol. 33, No. 1, pp. 101–105 (Jan. 2009) (In Japanese)

[5] J. Chen, J. Chen, and C. Gong: "Constant-Bandwidth Maximum Power Point Tracking Strategy For Variable-Speed Wind Turbines And Its Design Details", IEEE Trans. Ind. Electron., Vol. 60, No. 11, pp. 5050–5058 (Nov. 2013)

[6] Y. Sato, N. Yoshida, and R. Shimada: "Development of a City Type Compact Wind Power Generation System", IEEJ Trans., Vol. 125, No. 11, pp. 1016–1021 (Nov. 2005) (In Japanese)

[7] T. Senjyu, T. Hamano, N. Urasaki, K. Uezato, T. Funabashi, and H. Fujita: "Maximum Power Point Tracking Control for Wind Power Generating System Using Permanent Magnet Synchronous Generator", IEEJ Trans., Vol. 122, No. 12, pp. 1403–1409 (Dec. 2002) (In Japanese)

[8] S. Morimoto, T. Nakamura, and Y. Takeda: "Power Maximization Control of Variable Speed Wind Generation System Using Permanent Magnet Synchronous Generator", IEEJ Trans., Vol. 123, No. 12, pp. 1573–1579 (Dec. 2003) (In Japanese)

[9] T. Kawahito: "Maximizing Output Power of Wind Turbine Generator by Output Current Control", IEEJ Trans., Vol. 114, No. 3, pp. 283–289 (Mar. 1994) (In Japanese)

[10] G. Putrus, M. Narayana, M. Jovanovic, and P. S. Leung: "Maximum Power Point Tracking For Variable-Speed Fixed-Pitch Small Wind Turbines", Proc. CIRED 2009, pp. 542–545 Prague, Czech Republic (2009)

[11] T. Matsushima, S. Takagi, and S. Muroyama: "Characteristics of Highly Efficient Proper Type Small Wind Turbine With a Diffuser", Renewable Energy, Vol. 31, No. 9, pp. 1343–1354 (Jul. 2006)

[12] S. J. Watson, D. G. Infield, J. P. Barton, and S. J. Wylie: "Modeling of The Performance of a Building-Mounted Ducted Wind Turbine", J. of Physics: conf. ser., Vol. 75, No. 1, pp.012001(1-10) (Aug. 2007)

[13] Y. Ohya, T. Karasudani, A. Sakurai, K. Abe, and M. Inoue: "Development of a Shrouded Wind Turbine With a Flanged Diffuser", J. of Wind Eng. and Ind. Aerodynamics, Vol. 96, No. 5, pp. 524–539 (May 2008)

[14] A. Mirecki, X. Roboam, and F. Richardeau: "Architecture Complexity And Energy Efficiency of Small Wind Turbines", IEEE Trans. Ind. Electron., Vol. 54, No. 1, pp. 660–670 (Feb. 2007)

[15] J. Yaoqin, Y. Zhongqing, and C. Binggang: "A New Maximum Power Point Tracking Control Scheme For Wind Generation", Proc. PowerCon 2002, pp. 144–148, Kunming, China (2002)

[16] T. Tanaka, T. Toumiya, and T. Suzuki: "Output Control by Hill-Climbing Method For a Small Scale Wind Power Generating System", Renewable Energy, Vol. 12, No. 4, pp. 387–400 (Dec. 1997)

[17] E. Koutroulis and K. Kalaitzakis: "Design of a Maximum Power Tracking System For Wind-Energy-Conversion Applications", IEEE Trans. Ind. Electron., Vol. 53, No. 2, pp. 486–494 (Apr. 2006)

[18] S. M. R. Kazmi, H. Goto, H. Guo, and O. Ichinokura: "A Novel Algorithm For Fast And Efficient Speed-Sensorless Maximum Power Point Tracking in Wind Energy Conversion Systems", IEEE Trans. Ind. Electron., Vol. 58, No. 1, pp. 29–36 (Jan. 2011)

[19] K. Kim, T. L. Van, D. Lee, S. Song, and E. Kim: "Maximum Output Power Tracking Control in Variable-Speed Wind Turbine Systems Considering Rotor Inertial Power", IEEE Trans. Ind. Electron., Vol. 60, No. 8, pp. 3207–3217 (Aug. 2013)

[20] J. Chen, J. Chen, and C. Gong: "New Overall Power Control Strategy For Variable-Speed Fixed-Pitch Wind Turbines Within The Whole Wind Velocity Range", IEEE Trans. Ind. Electron., Vol. 60, No. 7, pp. 2652–2660 (Jul. 2013)

[21] T. Kitajima, T. Yasuno, and H. Sori: "Study on Output Prediction System of Wind Power Generation Using Complex-Valued Neural Network With Multipoint GPV Data", IEEJ Trans., Vol. 8, No. 1, pp. 33–39 (Jan. 2013)

[22] H. Sori and T. Yasuno: "Several-Hours-Ahead Wind Speed Prediction System Using Hierarchical Neural Network", J. of Signal Process., Vol. 12, No. 6, pp.507–514 (Nov. 2008)

[23] N. Fujimura, T. Yasuno, R. Yakushiji, K. Takigawa, K. Kawasaki: "Simple Wind Power Prediction System Using Self-Tuning Fuzzy Reasoning And Error Persistent Model", IEEJ Trans., Vol. 129, No. 5, pp.614–620 (May 2009) (In Japanese)

[24] E. Muljadi and C. P. Butterfield: "Pitch-Controlled Variable-Speed Wind Turbine Generation", IEEE Trans. Ind. Appl., Vol. 37, No. 1, pp. 240–246 (Jan./Feb. 2001)

[25] V. Valtchev, A. V. D. Bossche, J. Ghijselen, and J. Melkebeek: "Autonomous Renewable Energy Conversion System", Renewable Energy, Vol. 19, No. 1-2, pp. 259–275 (Jan. 2000)

[26] Izumi Ushiyama: Wind Energy, p. 116, Ohmsha, Japan (2005) (In Japanese)

[27] K. Lo, Y. Chen, and Y. Chang: "MPPT Battery Charger for Stand-Alone Wind Power System", IEEE Trans. Power Electron., Vol. 26, No. 6, pp. 1631–1638 (Jun.. 2011)

[28] T. Suzuki, T. Kamano, M. Fushimi, and H. Harada: "Windmill Simulator", Trans. SICE, Vol. 24, No. 9, pp. 960–966 (Sep. 1988) (In Japanese)

[29] K. Sasaki and T. Matsuzaka: "Dynamic Characteristics of a Wind Energy Conversion System and its Simulation", The Bulletin of Hachinohe Institute of Technology, Vol. 2, pp. 33–44 (Feb. 1983) (In Japanese)

[30] K. Z. Ostergaard, J. Stoustrup, and P. Brath: "Linear Parameter Varying Control of Wind Turbines Covering Both Partial Load And Full Load Conditions", Int. J. Robust Nonlinear Control, Vol. 19, No. 1, pp. 92–116 (Jan. 2009)

[31] R. Spee, S. Bhowmik, and J. H. R. Enslin: "Novel Control Strategies for Variable-Speed Doubly Fed Wind Power Generation Systems", Renewable Energy, Vol. 6, No. 8, pp. 907–915 (Nov. 1995)

[32] D. Q. Dang, Y. Wang, and W. Cai: "Offset-Free Predictive Control for Variable Speed Wind Turbines", IEEE Trans. Sustain. Energy, Vol. 4, No. 1, pp. 2–10 (Jan. 2013)

[33] A. M. De Broe, S. Drouilhet, and V. Gevorgian: "A Peak Power Tracker For Small Wind Turbines in Battery Charging Applications", IEEE Trans. Energy Convers., Vol. 14, No. 4, pp. 1630–1635 (Dec. 1999)

[34] G. E. P. Box and M. E. Muller: "A Note on The Generation of Random Normal Deviates", Ann. Math. Statistics, Vol. 29, No. 2, pp. 610–611 (Jun. 1958)

[35] Tomihiro Takano: "Natural Energy Power and Energy Storing Technology", IEEJ Trans., vol. 126, No. 9, pp. 857–860 (Sep. 2006) (In Japanese)

[36] Hiroshi Asano: "How to Integrate Variable Power Source into a Power Grid", IEEJ Trans., vol. 132, No. 4, pp. 297–300 (Apr. 2012) (In Japanese)

[37] M. Tsuchiya, T. Ishihara, Y. Fukumoto, H. Sukegawa, and K. Okubo: "The Wind Observation on Pacific Ocean for the Offshore Wind Farm", Proc. of National Symposium on Wind Engineering 19th, pp. 121–126 (2006) (In Japanese)

[38] K. Oishi and Y. Fukumoto: "R & D on Offshore Wind Power Generation System in Japan", IEEJ Trans., Vol. 129, No. 7, pp. 851–854 (2009) (In Japanese)

[39] A. Hashimoto, R. Kanougi, N. Hayasaki, A. Yamaguchi, F. Kajihara, and C. Arakawa: "Inter-comparison of the Meso Scale Meteorological Models for Wind Power Prediction", JAWE, vol. 35, No. 1, pp. 17–26 (Jan. 2010) (In Japanese)

[40] T. Iizaka, T. Kato, T. Kobayashi, T. Saito, H. Hayashi, and H. Hirakuchi: "Status of Power Output Forecast of Wind Power Generation", Proc. of Technical Meeting on Metabolism Society and Environmental Systems IEEJ, pp.13-18, Tokyo, Japan (2011) (In Japanese)

[41] K. Taniguchi, K. Ichiyanagi, K. Yukita, and Y. Goto: "Study on Forecast of Time Series of Wind Velocity for Wind Power Generation by Using Wide Meteorological Data", IEEJ Trans., vol. 128, No. 2, pp.416–422, (Feb. 2008) (In Japanese)

[42] S. Oke, S. Higashiyawa, Y. Suda, and H. Takikawa: "Any-Place Forecasting Method of Nationwide Time-Series Wind Speed Using Classified Forecast Models based on Wind Conditions", IEEJ Trans., vol.129, No. 5, pp.598–604 (May 2009) (In Japanese)

[43] S. Oke, Y. Ito, Y. Kemmoku, H. Takikawa, and T. Sakakibara: "Introduction of Atmospheric Pressure to Wind Speed Forecast with Artificial Neural Network", J. of JSES, Vol. 32, No. 5, pp.39–44 (2006) (In Japanese)

[44] S. Koumura, Y. Matsuda, Y. Sekine, Y. Shidama, and H. Yamaura: "Local Weather Prediction System by Neural Networks", Technical Report of IEICE, Vol. 94, No. 182, pp. 25–32 (2006) (In Japanese)

[45] A. Yona, T. Senjyu, N. Urasaki, and T. Funabashi: "Application of Recurrent Neural Network to 3-Hours-Ahead Generating Power Forecasting for Wind Power Generators", IEEJ Trans., vol. 129, No. 5, pp.591–597 (May 2009) (In Japanese)

[46] T. Senjyu, A. Yona, N. Urasaki, and T. Funabashi: "Application of Recurrent Neural Network to Long-Term-Ahead Generating Power Forecasting for Wind Power Generator", IEEE PSCE2006, pp. 1260–1265 (2006)

[47] S. Kakuta and G. Wu: "A Study of Forecasting Precision Enhancement of Short-term Wind Power Generation by use of NN Method", IEEJ Trans., vol. 129, No. 9, pp.1091–1097 (Sep. 2009) (In Japanese)

[48] S.L. Goh, M. Chen, D.H. Popovic, K. Aihara, D. Obradovic, and D.P. Mandic: "Complex-valued forecasting of wind profile", Renewable Energy, Vol. 31, No. 11, pp. 1733–1750 (Sep. 2006)

[49] S. Salcedo-Saanz, A.M. Perez-Bellido, E.G. Ortiz-Garcia, A. Portilla-Figueras, L. Prieto, and D. Paredes: Hybridizing the Fifth Generation Mesoscale Model with Artificial Neural Networks for Short-Term Wind Speed Prediction, Renewable Energy, Vol. 34, No. 6, pp. 1451–1457 (Jun. 2009)

[50] T. Nitta and T. Furuya : "A complex back-propagation learning", IPSJ, Vol.32, No. 10, pp.1319–1329 (1991) (In Japanese)

[51] T. Nitta and T. Furuya: "Characteristics of Learning in the Complex Back-propagation Learning Algorithm", IPSJ, vol. 34, No. 1, pp. 29–37 (1993) (In Japanese)

[52] A. Hirose : Complex-Valued Neural Networks: Theories and Applications, World Scientific Publishing Co. (2003)

[53] M. Kinouchi and M. Hagiwara: "Learning Temporal Sequences by Complex Neurons With Local Feedback", IEEJ Trans., Vol. 116, No. 7, pp. 748–754 (1996) (In Japanese)

[54] T. Iizaka, R. Jintsugawa, H. Kondo, Y. Nakanishi, Y. Fukuyama, and H. Mori: "A Wind Power Forecasting Method and Its Confidence Interval Estimation", IEEJ Trans., vol. 131, No. 10, pp. 1672–1678 (Oct. 2011) (In Japanese)

[55] J. L. Elman: "Finding Structure in Time", Cognitive Science, Vol. 14, pp. 179–211 (1990)

[56] A. Hirose and H. Onishi: "Proposal of Relative-Minimization Learning for Behavior Stabilization of Complex-Valued Recurrent Neural Networks", Neurocomputing, Vol. 24, pp. 163–171 (1999)

[57] J. Shima, M. Nishida, S. Kikuchi, H. Saito, and M. Nakanishi: "Learning Time Series by Complex-valued Neural Network with Short-term Memory", Technical Report of IEICE, Vol. 45, pp. 65–70 (2001) (In Japanese)

[58] H. Asoh: “Learning of Temporal Sequence Processing by Neural Networks”, IEEJ Trans., Vol. 110, No. 3 pp. 112–118 (Mar. 1990) (In Japanese)

[59] N. Hayasaki, I. Aoki, R. Tanikawa, and H. Fukuda: “Wind Power Forecasting System for the Control Area of Power Grid in Japan”, Proc. of The 13th National Symposium on Power and Energy Symposium, No. 8-9, Sapporo, Japan (Jun. 2008) (In Japanese)

[60] S. Kadokura, A. Hashimoto, Y. Hattori, S. Sugimoto, K. Wada, H. Hirakuchi, N. Tanaka, and T. Nanahara: “Development of the Prediction System for Wind Power Generation over a Wind Farm”, CRIEPI Research Report, No. V08065, (Jun. 2009) (In Japanese)

Publications

【Main Papers】

1. Takahiro Kitajima, Takashi Yasuno, Hitoshi Sori : Study on Output Prediction System of Wind Power Generation Using Complex-valued Neural Network with Multipoint GPV Data, IEEJ Transaction, Vol.8, No.1, pp.33–39, January 2013

2. Takahiro Kitajima, Takashi Yasuno : Maximum Power Control System for Small Wind Turbine Using Predicted Wind Speed, IEEJ Transaction, Vol.10, No.1, January 2015

【Sub Papers】

1. Takahiro Kitajima, Takashi Yasuno, Prediction System of Wind Speed and Direction using Complex-valued Neural Network, 2010 RISP International Workshop on Nonlinear Circuits, Communication and Signal Processing, pp. 636–639, Hawaii, USA, March, 2010

2. Takahiro Kitajima, Takashi Yasuno, Output Prediction of Wind Power Generation System Using Complex-valued Neural Network, SICE Annual Conference 2010, pp. 3610–3613, Taipei, Taiwan, August, 2010

3. Hitoshi Sori, Takashi Yasuno, Takahiro Kitajima, Simultaneous Prediction System of Wind Speed and Direction Using Complex-valued Neural Network, 32nd Wind Energy Utilization Symposium, pp. 287–288, Tokyo, Japan, November, 2010 (In Japanese)

4. Takahiro Kitajima, Takashi Yasuno, Prediction System of Wind Speed and Direction Using Complex-valued Neural Network with Multipoint GPV Data, 2011 RISP International Workshop on Nonlinear Circuits, Communication and Signal Processing , pp. 95–98, Tianjin, China, March, 2011

5. Takahiro Kitajima, Takashi Yasuno, Output Control of Wind Power Generation System Based on Predictive Control, 2012 RISP International Workshop on Nonlinear Circuits, Communication and Signal Processing, pp. 29–32, Hawaii, USA, March, 2012

6. Naoya Ikeda, Takashi Yasuno, Takahiro Kitajima, Wind Speed Prediction Method Using Complex-valued Neural Network Based on Wind Speed Frequency Spectrum, 2012 RISP International Workshop on Nonlinear Circuits, Communication and Signal Processing, pp. 760–763, Hawaii, USA, March, 2012

7. Hitoshi Sori, Takashi Yasuno, Takahiro Kitajima, Several-Hours-Ahead Wind Speed Prediction System Using Self-Organizing Map and Hierarchical Neural Network, 34th Wind Energy Utilization Symposium, pp. 453–456, Tokyo, Japan, November, 2012 (In Japanese)

8. Takahiro Kitajima, Takashi Yasuno, Maximum Power Control for Wind Power Generation With Predicted Wind Speed, 2013 RISP International Workshop on Nonlinear Circuits, Communication and Signal Processing, pp. 285–288, Hawaii, USA, March, 2013

9. Takahiro Kitajima, Takashi Yasuno, Naoya Ikeda, Wind Speed Prediction System Using Complex-valued Neural Network and Frequency Component of Wind Speed, IEICE Technical Report, vol. 113, No. 14, pp. 35–40, July, 2013 (In Japanese)

10. Takahiro Kitajima, Takashi Yasuno, Evaluation of Predictive Maximum Power Control of Wind Power Generation for Wind Speed Prediction Error, SICE Annual Conference 2013, pp. 742–745, Nagoya, Japan, September, 2013

【Conference Papers】

1. Takahiro Kitajima, Hitoshi Sori, Takashi Yasuno, Accuracy Estimation of Wind Speed Prediction System Using Hierarchical Neural Network, SJCIEE, p. 36, September, 2008

2. Takahiro Kitajima, Takashi Yasuno, Wind Speed Prediction System using Complex-valued Neural Network, Proc. of Electronics, Information and System Conference Electronics, Information and System Society IEEJ, pp. 1491–1492, September, 2009

3. Takahiro Kitajima, Takashi Yasuno, Wind Speed Prediction Using Hierarchical Neural Network Based on Frequency Information of Wind Speed, SJCIEE, p. 40, September, 2009

4. Takahiro Kitajima, Takashi Yasuno, Investigation of Useful Input for Prediction System of Wind Speed and Direction Using Complex-valued Elman's Neural Network, SJCIEE, p. 238, September, 2010

5. Takahiro Kitajima, Takashi Yasuno, Naoto Fujimura, Output Prediction System for Wind Power Generation Using Complex-valued Elman's Neural Network, SICE Shikoku, No. 212, November, 2010

6. Takahiro Kitajima, Takashi Yasuno, Study on Wind Speed Prediction System Using Complex-valued Neural Network with Multipoint Numerical Weather Prediction Data, SJCIEE, p. 276, September, 2011

7. Naoya Ikeda, Takashi Yasuno, Takahiro Kitajima, Wind Speed Prediction System Using Complex-valued Neural Network Under Frequency Analysis of Wind Speed, SJCIEE, p. 277, September, 2011

8. Takahiro Kitajima, Takashi Yasuno, Naoya Ikeda, Basic Investigation of Output Predictive Control System for Micro Wind Power Generator, SICE Shikoku, No. SO1-16, November, 2011

9. Takahiro Kitajima, Takashi Yasuno, Study on Maximum Power Output Control of Wind Power Generator Using Predicted Wind Speed Information, SJCIEE, p. 113, September, 2012

10. Naoya Ikeda, Takashi Yasuno, Takahiro Kitajima, Consideration of Normalization Method for Wind Speed Prediction System Using Complex-valued Neural Network, SJCIEE, p. 341, September, 2012

11. Takahiro Kitajima, Takashi Yasuno, Maximum Power Control Method for Micro Wind Power Generator Using Mechanical Time Constant and Predicted Wind Speed, National Convention of IEEJ, p. 493, March, 2013

12. Takahiro Kitajima, Takashi Yasuno, Extremely Short Term Wind Speed Prediction System Using Elman Type Neural Network, SJCIEE, p. 287, September, 2013

Acknowledgments

First of all, I would like to express the deepest appreciation to Prof. Takashi Yasuno. He gave me valuable advises through meaningful discussions while I was a member of Yasuno Laboratory for six years. Without his guidance and persistent help, this dissertation would not have been possible.

Special thanks to Prof. Naoyuki Shimomura and Prof. Masaki Hashizume who reviewed my thesis in advance and provided me insightful comments and suggestions at the defense presentation. I also owe my deepest gratitude to teachers in Department of Electrical and Electronic Engineering, The University of Tokushima, especially the teachers of electrical energy course. They support and gave me useful knowledges and comments while I was a student from bachelor' course to doctor's course in terms of lectures, public presentations, and so on.

Associate Prof. Hitoshi Sori in Tsuyama National College of Technology and Dr. Naoto Fujimura in Shikoku Research Institute Inc. made significant contributions to my research works. Thanks to Dr. Dwi Arman Prasetya and Dr. Yong Zhang who were doctoral student members in Yasuno laboratory, we had a grateful time for discussion about research works and talking a lot of topics. I also would like to thank technician Akinobu Kuwahara and students of Yasuno laboratory in 2008-2014. In addition, I would like to express the greatest appreciation to Senior Lecturer Anuar Bin Mohamed Kassim in Department of Mechatronics, Faculty of Electrical Engineering, Universiti Teknikal Malaysia Melaka for checking carefully English sentences of this dissertation.

I am deeply grateful to Nichia scholarship and Yume scholarship from The University of Tokushima for their financial support.

Finally, I would like to express my gratitude to all people who support me. I wish them the best of luck in their endeavors.

March 2014